Vibroacoustic behaviour of sandwich structures with spatially distributed resonators

Von der Fakultät Bau- und Umweltingenieurwissenschaften der Universität Stuttgart zur Erlangung der Würde eines Doktor-Ingenieurs (Dr.-Ing.) genehmigte Abhandlung

Vorgelegt von

Steffen Hettler

aus Leonberg

Hauptberichter : apl. Prof. Dr. rer. nat. habil. W. Maysenhölder

1. Mitberichter : Prof. Dr. David Thompson

2. Mitberichter : Univ. Prof. Dr.-Ing. Philip Leistner

Tag der mündlichen Prüfung: 30.01.2013

Lehrstuhl für Bauphysik der Universität Stuttgart

Fraunhofer Institut für Bauphysik, Stuttgart

2013

Acknowledgement

I would like to thank my supervisors Dr. Waldemar Maysenhölder, Dr. Philip Leistner, both Fraunhofer Institute of Building Physics, Stuttgart and Dr. David Thompson, ISVR University of Southampton, for the competent supervision, aiding and abetting and for showing the necessary patience.
I am very grateful to all colleagues at the Fraunhofer Institute of Building Physics who made my time at the institute very enjoyable and particularly valuable. It was a pleasure working with you.
A special thank to the ISVR in Southampton for organising the EDSVS Marie Curie fellowship program that allowed me to partly carry out this project in Southampton and Lyon.

Thank you to Chih-Mei for always being next to me throughout this very special time.
Finally, I wish to acknowledge and thank my family who has supported me throughout my entire education and made all this possible. Thank you very much, I am very grateful.

This project was financially supported by the Doctoral Scholarship Programme of the German Federal Environmental Foundation. Furthermore, this work was accepted as a research training project within the EU-funded European Doctorate in Sound and Vibration Studies Programme (EDSVS).

Contents

List of Figures

Symbols and Notation

Throughout this work SI units have been used.

General symbols

f	frequency [Hz]	t	time
l	length	v	velocity
w	transverse displacement	v_1,v_2	panel velocity
$\hat{w}$	amplitude of displacement	ω	angular frequency $(\omega = 2\pi f)$
x, y	co-ordinates	d	cavity thickness
$\mathbf{f}$	force vector	$\mathbf{q}$	generalized modal amplitude vector
$\mathbf{v}$	velocity vector	$\mathbf{Q}$	generalized modal force vector
$\mathbf{M}$	mass matrix	$\mathbf{S_c}$	coupling spring stiffness matrix
$\mathbf{K}$	stiffness matrix	$\mathbf{\Phi}, \mathbf{\Psi}$	mode shape matrices

Material symbols

h	uniform panel thickness	s	complex spring stiffness
m	mass	s_c	complex cavity spring stiffness
k	spring stiffness per unit area	ρ	mass density
E	Young's modulus	η	damping loss factor
B	bending stiffness	η_p	structural damping loss factor
D	complex panel bending stiffness	ν	Poisson's ratio

Acoustical symbols

c_0	speed of sound in air	f_c	coincidence frequency
k_0	wavenumber in air	ρ_0	air density
p	sound pressure	p_i	incident plane wave pressure
p_0	plane wave sound pressure at normal incidence	$\hat{p_0}$	plane wave sound pressure amplitude
		p_r	reflected plane wave pressure
p_1	pressure load incident panel	$\hat{p_1}$	constant incident pressure
p_2	pressure load radiating panel	v_i	incident sound velocity
P_i	incident sound power	v_r	reflected sound velocity
P_{rad}	radiated sound power	$\hat{A}$, $\hat{B}$	complex pressure amplitudes
R	sound reduction index	τ	sound transmission coefficient
ξ, φ	radiation angle	σ	radiation efficiency
θ, ϕ	angle of sound incidence		

Mass-spring model symbols

s''	complex spring stiffness per unit area	F	force per unit area
s_c''	complex cavity spring stiffness per unit area	m''	mass per unit area

Beam model symbols

F	force per unit width	$\hat{F}$	amplitude of force
m''	mass per unit area	m'	mass per unit width
P	pressure force	I_i	sound intensity
k_x, k_y	wavenumber on x,y-axis	k_b	free bending wavenumber
s'	complex spring stiffness per unit width		
s''	complex spring stiffness per unit area		
s_c'	complex cavity spring stiffness per unit width		
s_c''	complex cavity spring stiffness per unit area		

for beam mode

q_n	generalized modal amplitude	Q_n	generalized force
M_n	modal mass	K_n	modal stiffness
k_n	modal wavenumber	σ_n	modal radiation efficiency
Φ_n, Φ_m	mode shape function of beam mode		

$\mathbf{q}_n$	generalized modal amplitude vector	$\mathbf{M}_n$	mass matrix
$\mathbf{Q}_n$	generalized modal force vector	$\mathbf{K}_n$	stiffness matrix

Plate model symbols

A	area of panel	a, b	panel dimensions
F	Force	$\hat{F}$	Force amplitude
m''	mass per unit area	P	pressure force
k_x, k_y	wavenumber on x,y-axis	k_b	free bending wavenumber
k_p	wavenumber of oblique incident wave		
s''	complex spring stiffness per unit area		
s_c''	complex cavity spring stiffness per unit area		

for panel mode

q_{nm}	generalized modal amplitude	Q_{nm}	generalized force
M_{nm}	modal mass	K_{nm}	modal stiffness
k_{nm}	modal wavenumber	σ_{nm}	modal radiation efficiency
Φ_{nm}, Φ_{rq}	mode shape function of panel mode		

$\mathbf{q}_{nm}$	generalized modal amplitude vector	$\mathbf{M}_{nm}$	mass matrix
$\mathbf{Q}_{nm}$	generalized modal force vector	$\mathbf{K}_{nm}$	stiffness matrix

Abstract

Lightweight constructions are based on multi-layer structures. Typical lightweight structures are also commonly known as sandwich structures which can be designed to have satisfactory sound insulation at high frequencies but do not perform well at low frequencies. The objective of this thesis is to investigate the implementation of internal resonators to improve the sound insulation of sandwich constructions at low frequencies with least possible mass increase. The research is carried out using double panel lightweight partitions. The benefits of double panel partitions are combined with the frequency dependent effect of distributed internal resonators.

As internal resonant system, for this investigation internal vibration absorbers are implemented into the cavity of a double panel partition. With the focus on low frequencies, the interaction of the internal vibration absorbers with the modal behaviour of the panels is of particular interest. Based on the modal expansion method beam and plate models are derived. These analytical models allow the calculation of the sound transmission loss for both normal and oblique sound incidence. A tuning approach is derived using a simplified mass-spring model. This approach enabled the design of internal vibration absorbers for specific acoustical conditions. A significant increase in the sound reduction index at low frequencies was achieved by tuning the effect of the internal vibration absorbers to the structural resonance of the host double panel structure.

The increase in the sound reduction index is experimentally verified in a semi-anechoic chamber. For this purpose, the influence of the internal vibration absorbers on the vibroacoustic characteristic of a double panel structure is determined by comparing the measured radiated sound power of the host structure with and without absorbers.

This study successfully applied internal resonators to finite lightweight double panel structures for increasing the sound reduction at the MAM-resonance. Since modal formulations allowed the investigation of mass efficient resonator distributions, the frequency dependent increase in the sound reduction was achieved without a significant mass penalty.

Zusammenfassung

Leichtbaukonstruktionen sind gewöhnlich mehrschichtig aufgebaut, beispielsweise als zweischaliges Sandwichbauteil. Der zunehmende Einsatz solcher Leichtbauanwendungen aus ökonomischen und ökologischen Gründen erschwert einen hochwertigen Schallschutz, insbesondere bei tiefen Frequenzen. Unter der Nutzung der Vorteile von mehrschaligen Plattenstrukturen zielt diese Dissertation auf eine effiziente gewichtsminimierte Anwendung interner Resonatoren. Damit kann eine frequenzabhängige Verbesserung der Schalldämmung bei tiefen Frequenzen erreicht werden. Für die durchgeführten Untersuchungen wurde eine doppelwandige Leichtbaukonstruktion mit Hohlraum zwischen den Schalen als Trägerkonstruktion herangezogen.

Schwerpunkt dieser Arbeit ist die Untersuchung von internen Schwingungsabsorbern, welche in den Hohlraum eingebracht werden. Aufgrund der erwünschten Verbesserung der Schalldämmung bei tiefen Frequenzen ist ein Hauptaugenmerk dem modalen Verhalten der Grundstruktur gewidmet. In diesem Zusammenhang untersucht die Arbeit die Wirkung von an definierten Punkten eingebrachten internen Schwingungsabsorbern. Basierend auf der Methode der modalen Entwicklung wurde ein Balken- und ein Plattenmodell erstellt. Diese beiden Rechenmodelle ermöglichen es, den Zusammenhang der Positionierung der internen Resonatoren in Abhängigkeit von den Schwingungsmoden der Platten zu analysieren. Weiterhin wurde mit einem Feder-Masse-Modell ein Werkzeug zur Abstimmung der internen Resonatoren geschaffen. Zur Verifizierung des Einflusses der internen Schwingungsabsorber wurden Messungen in einem Halbfreifeldraum durchgeführt. Dabei wurde der Einfluss der Schwingungsabsorber auf die Grundstruktur anhand der abgestrahlten Schallleistung ermittelt.

Die Untersuchungen haben gezeigt, dass durch den Einsatz interner Resonatoren eine deutliche frequenzabhängige Verbesserung der Schalldämmung erreicht werden kann. Dabei handelt es sich um ein internes Absorbersystem, dessen Masse bei einer späteren industriellen Umsetzung in ein federndes Material eingebracht werden kann.

Introduction

Recent concerns about global warming, carbon dioxide emissions and energy consumption draw the focus on one common solution, the use of lightweight constructions. In this context, lightweight materials as partitions in civil, automotive, shipbuilding and aerospace engineering raised considerable interest in their capacity for acoustic insulation. Innovative lightweight constructions can provide high sound transmission loss and functionality. Therefore, acoustical comfort can be achieved taking the requirements due to environmental issues into account.

It is well known that lightweight structures tend to vibrate more easily and radiate more sound. In many fields of mechanical engineering design, absorbing or damping materials are applied to minimize noise emission at the expense of significant weight penalties. But these noise control solutions have only small effects on low-frequency noise problems. So far, researchers have paid less attention to low-frequency noise despite the fact that it has become a major problem in residential areas. With the increasing demand for lightweight constructions, the low-frequency noise becomes an even more urgent issue. Many outdoor sources emit considerable low-frequency noise, which is less effectively reduced by partitions and other protective structures. In order to solve problems of noise control in industry and transportation, it is often necessary to considerably increase the transmission loss of panels in a narrow frequency band. This problem becomes particularly important when discrete low-frequency components dominate the spectrum of noise that needs to be suppressed. Therefore, noise-optimized structures can be achieved by applying noise reduction

concepts that allow for lightweight design and higher functionality with respect to the intended application and operational conditions. This frequency dependent application is known as smart material technology. Innovative smart materials comprise frequency dependent adaptive properties to change the vibroacoustic characteristic of the structure by reducing structural vibrations or the efficiency of radiation. These structural modifications can be achieved by passive or active components.

Based on the smart material technology, the objective of this thesis is to investigate multifunctional lightweight structures with distributed resonant systems. The structures under investigation combine the benefits of multi-layer sandwich constructions with the frequency dependent effect of locally distributed internal resonators. Sandwich constructions with internal layers of resilient materials already provide sufficient sound transmission loss properties at higher frequencies. However, at low frequencies the sound transmission loss characteristic deteriorates significantly due to structural resonances.

This thesis introduces the implementation of vibration absorbers into the partition following the technique of embedded masses. Recent research on sound and vibration has shown interest in wave transmission in infinite structures with embedded masses. These structures comprise rigid masses coated by resilient materials which bears a similarity to a mechanical vibration absorber. In order to improve the sound reduction of lightweight structures at low frequencies, the idea of internal resonators combines the technique of embedded masses with the properties of vibration absorbers. For mechanical systems, low frequency resonance vibrations are often reduced by vibration absorbers.

In this thesis, the vibroacoustic behaviour of lightweight structures with internal resonators is described by three analytical models and verified experimentally. Since the aim of this thesis is to improve the sound transmission loss characteristic of lightweight structures at low frequencies with least possible mass increase, the modal behavior of the structure is taken into account. This thesis evaluates the performance of finite lightweight structures with internal resonators by the resulting sound transmission loss.

Structure of the thesis

Due to the expected influence of the modal behaviour of the host structure to the performance of internal resonators, this thesis is focused on the development of analytical tools to describe the effect of internal vibration absorbers. Accordingly, the complex interaction between the internal vibration absorbers and the host structure has been analysed comprehensively. As the project of internal vibration absorbers is still at an early stage, the experimental efforts are kept on a small scale. This thesis is structured as follows:

1. **Review of sound transmission:** This chapter reviews the important studies on the calculation of the sound transmission loss. During the last century, the fundamental principles of sound transmission through single and double partitions have been comprehensively investigated. Particular interest is given to published theoretical models on sound transmission through double panel partitions.

2. **Internal resonant systems:** This chapter discusses relevant literature on the idea of internal resonant elements . Recent research on sound transmission through partitions has contributed new innovative concepts to smart material solutions. These materials use narrow band effects for a frequency dependent improvement of the sound transmission properties. Applications using embedded masses in resilient materials are

discussed in conjunction with the concept of internal resonators.

3. **Mass-spring model:** In this chapter, the idea of internal resonators is introduced and described using a mass-spring model. This simplified model provides an initial insight into the general principles of implemented vibration absorbers. The equation of motion is formulated in matrix form.

4. **One-dimensional beam model:** It is expected that efficient positions for the internal vibration absorbers under investigation are dependent on structural modes of the host structure. In order to understand this interaction between the internal vibration absorbers and the panels of the structure, first, a one-dimensional beam model was derived. This chapter presents the derivation of the equations of motion using the modal expansion method. The beam model provides sound transmission loss formulations for normal and oblique sound incidence.

5. **Two-dimensional plate model:** Accounting for the second dimension, the beam-model was extended to the two-dimensional plate model. This plate model gives strong assistance in designing lightweight constructions with internal vibration absorbers. Prior to the production of samples it provides an estimation of the sound transmission loss for finite double panel structures with implemented vibration absorbers. Extending the beam model, equations for the calculation of the sound transmission loss for normal and oblique sound incidence are given.

6. **Parameter study:** Based on the mass-spring model, this chapter presents a tuning approach that reveals the parameters of the internal vibration absorbers for selected frequencies. For the structural resonance of a double panel partition, the dynamic interaction of the internal vibration absorbers with the host structure is visualized using a finite element analysis. When the internal vibration absorbers are tuned to the structural resonance of a double panel partition aspects of symmetry are discussed. The influence of the internal vibration absorbers

on the sound transmission loss of the host structure was computed for all three analytical models. Results for normal and oblique sound incidence are presented. For finite panels the effect of internal vibration absorbers with different numbers and locations was calculated using the two-dimensional plate model of chapter 5. At the end of this chapter, the application of wideband vibration absorbers to the concept of internal resonators is discussed.

7. **Measurement:** In this chapter a final measurement is presented for a simplified sample. The measurement illustrates the influence of the internal vibration absorbers on the host structure. For this purpose, the radiated sound power was measured for a double panel construction with and without implemented internal absorbers. The internal vibration absorbers were tuned to have their resonance at the Mass-Air-Mass resonance (MAM) of the double panel host structure.

8. **Summary and Outlook:** This chapter summarizes the main impacts of internal vibration absorbers to the sound transmission of lightweight constructions. Conclusions are drawn for the potential of internal vibration absorbers as integral part of innovative lightweight solutions. Finally, suggestions for further studies on the concept of internal resonators and in particular internal vibration absorbers are given.

Contributions of the research

The contribution of this thesis lies in the first comprehensive study on internal vibration absorbers as internal low-frequency resonator within double panel partitions. In order to improve the sound transmission loss of lightweight constructions, internal vibration absorbers are designed to reduce sound transmission at low frequencies. Therefore, this thesis considers finite structures taking the modal influence into account. The principles of internal vibration absorbers and their effect on lightweight constructions were investigated by three analytical models. These models provide significant assistance to subsequent parameter studies and specific proposals for industrial applications.

As part of the project on internal resonators, this thesis provides :

- Analytical tools for the design of internal vibration absorbers and the estimation of their effect on the sound transmission loss of double panel lightweight partitions.
- Numerical parameter studies.
- Initial experimental verification demonstrating the effect of internal vibration absorbers.

Chapter 1

Review of sound transmission

Sound transmission loss is the reduction in noise level due to propagation of a sound wave through an object or medium. Some media transmit sound better than others, an effect which is quantified by the sound transmission loss. The investigation of the fundamental principles of sound transmission through partitions was the subject of research for many years. By understanding this physical problem, various ways for the prediction of sound transmission loss were published. The research on sound transmission revealed the sound transmission characteristics of single and double panel partitions, which is schematically presented in Figure 1.1.

1.1 Single panel partitions

At low frequencies, the sound transmission loss of an infinite single panel is described by the "mass law" where the transmission loss of the panel depends upon the frequency of the sound and the mass per unit area of the partition. Analytical models for the prediction of sound transmission loss were developed under certain idealized conditions. Most of these models assumed that the panels are infinitely extended and the incident sound field on the panel is a plane wave or random incidence. In 1942, Cremer [1] demonstrated the existence of the important "coincidence" effect in the overall sound transmission loss of single panel partitions (Figu-

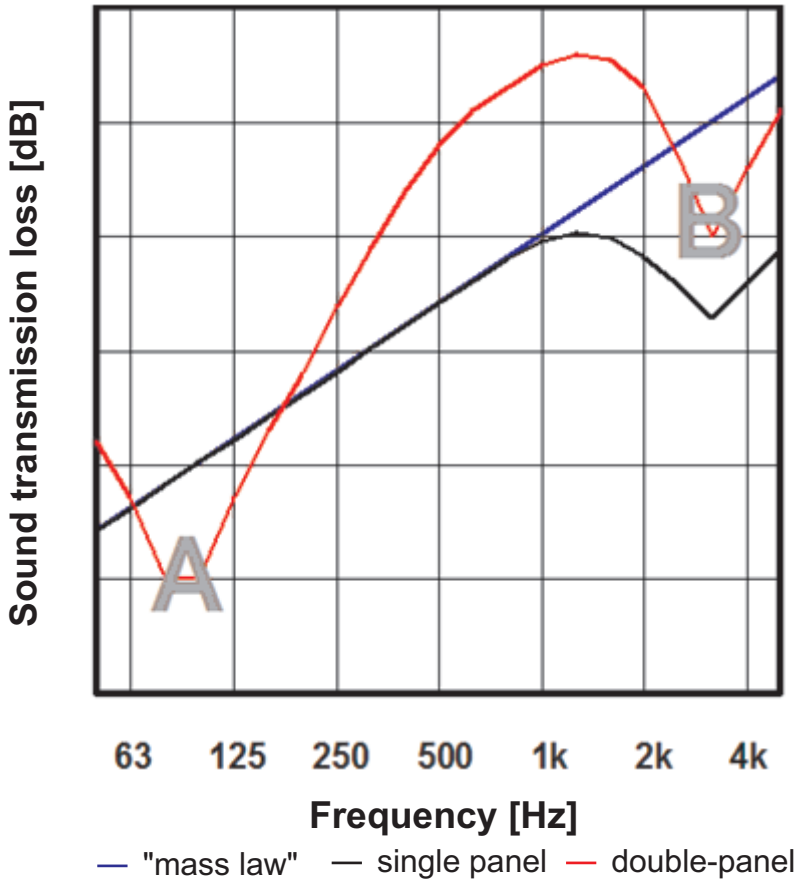

Figure 1.1: Sketch of sound transmission loss over frequency. A: double panel resonance; B: coincidence effect

re 1.1). At the coincidence frequency, the bending wavelength of the panel and the acoustic trace wavelength in air are equal. This relation is illustrated in Figure 1.2. Below the coincidence frequency, the transverse bending wavelength of the panel is smaller than the wavelength of an acoustic wave in air at the same frequency. In this case, the sound transmission loss of a panel is described by the mass law that corresponds to an increase of 6 dB/octave for single angle of incidence [2]. Above the coincidence frequency the bending wave is longer than the acoustic wavelength. Therefore, above the coincidence transmission sound is less efficiently transmitted. The sound transmission loss increases again. .

Continuing the study on infinite single panel partitions, London [3] inves-

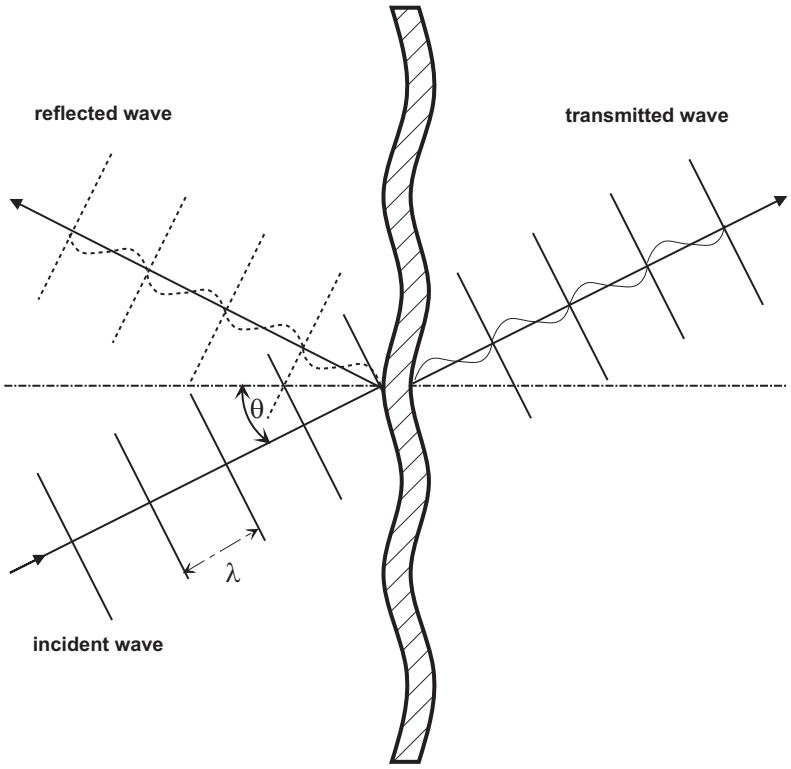

Figure 1.2: Sound transmission through an infinite thin panel for oblique plane wave incidence.

tigated the transmission loss of a single panel partition in a diffuse field. A further fundamental work on sound transmission loss of a single panel was published by Sewell [4], who obtained a complete solution for finite panels using a modal approach. This approach applies the modal expansion method, where the contribution of each mode is taken into account over the frequency band considered.

The formulations presented in this thesis on a finite structure with internal resonators are entirely described by such a modal approach.

1.2 Double panel partitions

Double panel partitions and sandwich structures are typical lightweight structures with multiple layers. Double panel partitions are primarily used in buildings while the much thinner sandwich constructions are commonly used for industrial applications.

Common double panel partitions used in buildings contain air or mineral wool in the cavity. Unfortunately, the sound transmission loss is not just the sum of the results for two leaves when used in isolation. For this reason, the sound transmission loss of double panel partitions is much more complex than that of single panel partitions. At low frequencies the air or the absorbent in the cavity acts as a spring and dynamically couples the two leaves transferring vibrational energy from one layer to the other. This energy transfer causes a significant deterioration of the sound transmission loss at the so called Mass-Air-Mass resonance (MAM) or double panel resonance (Figure 1.1). Besides the MAM-resonance, which mainly depends on the mass of the panels and the distance between the panels, the sound transmission loss of the double panel partition is significantly controlled by the properties of the absorbent and the frame with its structural connections.

In 1949 Beranek and Work [5] studied the transmission of sound through a simple double panel partition without structural connections. They dealt only with normal incidence and did not consider any damping terms. Beranek and Work modelled the interaction between different layers using an impedance approach which allows for the analysis of a large number of possible panel constructions at normal sound incidence. As for the research on single panel partitions, London [6] studied the transmission loss of a double wall in a diffuse sound field. For infinite double panel partitions London introduced a ray approach for the cavity without absorbent. He described the sound transmission within the cavity by forward and reverse travelling waves between the two leaves. By integration over the in-

cidence angle, the average transmission loss for a diffuse sound field was calculated. Based on the formulations of Beranek and London, Mulholland *et al.* [7] studied the transmission loss of double panel partitions with absorbent in the cavity. The absorption was assumed to take place on the surfaces of the panels. Therefore, the sound absorption in the cavity was introduced by an extra term in the sound transmission formulation by attributing an absorption coefficient to the inner surfaces of the panels. As London's multiple-reflection theory model is restricted to the case where no absorbing material is contained within the cavity, Cummings and Mulholland [8] modified London's model to finite-sized double partitions at arbitrary angles of incidence with sound absorption located on the edge of the cavity. For the first time, this approach accounts for the modal in-plane sound field of the cavity depending on cavity wave number, wave direction and the impedance at the edges of the cavity.

This research on arbitrary angles of sound incidence established two classical methods for predicting the transmission loss of a panel at diffuse sound incidence. The first is the diffuse field method [9], also known as Paris formula. By this formulation the transmission coefficient of the panel is derived as function of frequency and angle of incidence and an integration over angle is performed. The second classical method is the so called mode coupling method, presented by White and Powell [10]. This approach derives the transmission loss of a finite rectangular double panel partition by considering the dominant coupling of the room modes in the transmission and reception room. The modal coupling between the rooms is related to the structural and acoustical characteristic of the partition.

In a next step, the sound transmission through double panel partitions was investigated by Price and Crocker [11] who applied statistical energy analysis (SEA) to the research on sound transmission loss. The statistical energy analysis uses resonant coupling for the description of a complicated system by dividing the system into subsystems which correspond to its uncoupled modes. In the case of a double panel partition, the model

consists of five coupled resonant systems: room-panel-cavity-panel-room. Price and Crocker first studied the transmission through double panel partitions only with absorption placed at the edges of the cavity [12]. This method gives simple expressions for reverberant sound fields but uses coupling loss factors on a rather empirical basis. In the last decades, this basic application of SEA for the prediction of the sound transmission loss of double panel partitions was improved by a number of authors [13–16].

The effect of cavity absorption was considered in different models. Gösele [17] proposed a simplified method to predict the sound transmission loss through double panel partitions without structure-borne connections. In Gösele's analysis it is necessary to have a prior knowledge of the transmission loss of the face panels. The sound absorbing material is considered as a spring with stiffness depending on the specific flow resistance. Approximate formulas are obtained for the transmission loss above and below the coincidence frequency. Fahy [2] simulated the effect of cavity absorption by using a complex wave number which is highly related to the flow resistivity. Later Fahy [18] extended his model by three principal parameters characterizing the acoustic properties of the absorptive material. These are the flow resistivity, the porosity of the absorptive material and a structure factor. Although resonant transmission between the adjacent rooms was not considered in Fahy's models, the advantage of these models is the illustration of the lowest structural panel mode in the sound transmission loss characteristic.

Taking multi-dimensional wave propagation in the porous material into account, Bolton *et al.* [19] presented a theoretical model based on the theory proposed by Biot [20]. Formulations introduced by Biot and subsequently Allard *et al.* [21] describe the wave propagation in infinite elastic porous materials by stress-strain relations in the porous layer. For the wave propagation in elastic porous cavity materials Bolton *et al.* integrated this stress-strain principle into the prediction of transmission loss of double panel constructions at arbitrary angles of incidence.

So far, the cavity absorptive material was assumed to be one simple poro-elastic material. If the double panel construction is considered as a layered system of three arbitrary layers, the formulations governed by the stress-strain relations lead to the theories of infinite layered medias. The contributions of Skelton and James [22] on isotropic and anisotropic infinite layered media suggested the dynamic stiffness matrix approach for multi-layered medias. Maysenhölder and James extended this approach to additional layer types including porous media modelled according to Biot's theory [20]. The method was implemented into a software tool called LAYERS [23].

Several further publications were focused on specific aspects of multiple layer structures. The work of Au and Byrne [24], used the transfer impedance method for the analysis of lagging structures comprising flexible and impervious layers, such as rubber and orthotropic profiled panels. The model of Au and Byrne was modified for double panel partitions by Ver [25]. The influence of the boundary conditions to the sound transmission loss was the subject of several studies [26,27]. Recently, the increasing numerical resources of personal computers brought the numerical finite element (FE) analysis [28] and boundary element (BE) analysis [28] to the investigation of sound transmission through single and double panel partitions. The FE and BE techniques were used to analyse the effect of room dimensions on the resonant sound insulation of partitions at low frequencies [29–31].

Following the research on single panel partitions, the research on sound transmission through double panel partitions revealed various approaches for the calculation of the sound transmission loss characteristic. For normal and diffuse sound field incidence research on sound transmission through double panel partitions achieved a high level of accuracy. A comprehensive understanding for aspects of cavity absorption and modal influences was established.

Nowadays, besides the research on an accurate estimation of sound transmission through double panel partitions, an increasing number of research projects are devoted to the frequency areas with a particular high sound transmission. In order to achieve a higher sound reduction for example at the MAM-resonance or the coincidence frequency, innovative solutions from material science are applied to double panel partitions. In the following, this study discusses the application of vibration absorbers in the cavity of finite double panel partitions.

Chapter 2

Internal resonant systems

2.1 Introduction

The sound transmission loss of double panel partitions can be described by three physical phenomena; the deterioration at the MAM-resonance, the coincidence effect, and the increase at middle and higher frequencies (Figure 1.1). In comparison to single panel partitions, at frequencies above the MAM-resonance, the use of double panel partitions achieves large improvements in sound insulation for a wide frequency range. At frequency bands centered at the coincidence frequency, the sound transmission loss is low due to flexural modes in resonance. For diffuse sound incidence, these modes have the same wavelength as the acoustical incident waves. As these flexural modes are in resonance, the transmission of sound can be reduced by increasing the internal damping of the panels [18]. Therefore, the most common approach for mitigating coincidence dips is using constrained layer damping [32].

Comprehensive understanding of the coincidence frequency is available in the corresponding acoustic literature. The coincidence frequency is defined by the material parameters of the panel. For a panel with mass per unit area m'', thickness h, Young's modulus E and Poisson's ratio ν the

coincidence is calculated by

$$f_c = \frac{c_0^2}{2\pi}\sqrt{\frac{12m''(1-\nu^2)}{Eh^3}} \tag{2.1}$$

where c_0 is the speed of sound in air.

Hence, increasing a plate's elastic modulus speeds up flexural waves and lowers the plate's coincidence frequency. Increasing a plate's density increases its mass, slowing down flexural waves, and raises the plate's coincidence frequency. Therefore, if increasing the structural damping is not possible, the partitions can be designed by shifting the coincidence frequency out of the frequency range of interest. Stiffening a plate lowers its coincidence frequency and allows it to radiate sound at lower frequencies. Conversely, mass loading a plate raises its coincidence frequency [33].

Hence, considering the coincidence frequency as a manageable issue for both single and double panel partitions, the use of double panel partitions results in a significant improvement of the sound transmission loss above the MAM-resonance. However, the sound transmission loss of double panel partitions still decreases rapidly at low frequencies around the MAM-resonance. This deterioration occurs in the low frequency range that already has poor sound insulation. Therefore this drop in sound insulation may be perceived as more important than the improvement in high frequencies. Consequently, the benefits of double panel partitions for the sound transmission loss at high frequencies are achieved on the expense of low sound insulation at low frequencies.

The increasing use of double panel partitions, or multi layer structures, requires innovative solutions allowing for a higher sound insulation at low frequencies. With strict limitations on mass and size, the necessary increase of sound insulation can perhaps be achieved by the application of resonant systems. For this purpose, the cavity between the two panels of a double panel partition offers a great opportunity for the application

of internal resonant systems. In 1985, the issue of low sound transmission loss at low frequencies and the use of resonant system was subject of a pilot study. Enger and Vigran [34] indicated the possibilities of using the air gap of a double panel partition for the implementation of resonant systems, but no detailed analysis was presented. Enger and Vigran achieved sound attenuation by effective shunting of the stiffness of the air cavity by a low impedance resonant system. By this means, several concepts of resonant systems can be considered to be implemented into the cavity of multi-layer structures. Taking successful techniques of adjacent sound and vibration areas into account, the most promising techniques are: from room acoustics, the use of Helmholtz resonators, from material science, the research on photonic band gaps and from the area of structural vibration engineering, the well known vibration absorbers.

2.2 Helmholtz resonator

Based on the physical principle of Enger and Vigran, the use of tuned Helmholtz resonators to improve the sound transmission loss of double panel partitions was published by different authors. Mason and Fahy [35] investigated the potential effectiveness of Helmholtz resonators coupled to the air cavity enclosed between the two leaves of the partition. Prydz *et al.* [36] presented two different methods to analyze the transmission loss of a multi-layer panel with internal Helmholtz resonators. One of the methods is based on the pressure ratio approach of Beranek and Work [5] and the other uses a transfer matrix approach [37]. So far, only infinite structures were the subject of these approaches.

For a finite double panel partition with an air-cavity, Mao and Pietrzko [38] presented an analytical model of fully coupled structural-acoustic Helmholtz-resonators. The governing equations of the system were obtained by a modal coupling method taking the acoustical field within the cavity into account. Additionally, the optimal parameters of the Helmholtz resonators

maximizing the improvement of the sound transmission loss were discussed in detail. The results show that tuned acoustic resonators applied to a double panel structure can provide large increase in the transmission loss at a selected frequency range. In particular, substantial improvements may be obtained around the MAM-resonance.

In general, an efficient use of Helmholtz resonators requires double panel constructions with air-cavity. Nevertheless, in order to combine the benefits of absorptive materials and Helmholtz resonators, Prydz *et al.* [36] attached an additional absorptive layer into the cavity.

Another concept of combining different noise reducing measures was presented by Estève and Johnson [39]. For the interior noise control of a cylinder, Estève and Johnson suggested the combined use of passive distributed vibration absorbers and Helmholtz resonators.

Recent material research follows the idea of inherent acoustical solutions. By this means, acoustical elements are already included into materials during the production process. In this context, an interesting material was presented by Ladner *et al.* [40] called innovative metallic hollow sphere absorptive material. The acoustic dissipation is achieved by viscothermal effect inside hollow spheres and micro-porosities. It is considered as a high absorptive material that incorporates Helmholtz resonators. The Helmholtz-resonator consists of the hollow sphere as resonator volume and the micro porosities as neck. Presented results show an increased sound reduction at frequencies above 1 kHz. Moving this increase to lower frequencies will be restricted by the required space for the hollow spheres.

A similar solution was presented by Iwao *et al.* [41,42] for the automotive industry. Due to internal material modifications, a sound insulation panel is used as engine shield which simultaneously provides the contradictory requirements of sound insulation and ventilation.

2.3 Resonant sonic materials

Recently, investigations on innovative materials that provide an increased sound transmission loss without increasing the total mass brought attention to the concept of "classical wave spectral gap", in particular the "photonic band gap". This concept was originally introduced in the area of electromagnetic wave sciences. Due to periodic structures in photonic crystals the propagation of electromagnetic waves is affected which leads to the effect of forbidden frequency bands where electromagnetic waves cannot propagate through the structure [43]. This physical phenomenon is called the "photonic band gap".

In theory, by the extension to studies of elastic waves the principle of spectral band gaps can achieve total sound attenuation in a certain frequency range. Within this frequency range the elastic wave gap forbids vibrations to propagate. With respect to photonic crystals, the necessary periodic modulation within the structure can be implemented by localized resonances. At the University of Hong Kong [44] a group of physicists proposed a local resonance band gap mechanism by a "locally resonant sonic material". For this purpose, composites containing cubic arrays of silicon-rubber coated lead spheres immersed in an epoxy matrix were designed. First investigations of this locally resonant sonic material showed a significant reduction of the sound transmission at frequencies between 250 Hz and 500 Hz. A subsequent publication presented measurements of the locally resonant sonic material in an impedance tube which confirmed the reduction in sound transmission [45]. However, whether this material can be applied to achieve a significant improvement of the sound transmission loss in the low frequency range is not yet indicated.

In order to predict the performance of such a locally resonant material, Maysenhölder modelled a structure with embedded resonant systems as an idealised thin plate with periodically arranged inhomogeneities [46]. He used a theoretical description for the sound transmission loss of peri-

odically inhomogeneous thin plates [47]. The formulations of this theory were implemented in the computer code HYPERAKUS [48]. Maysenhölder presented first results calculated with HYPERAKUS, but it was found that the numerical requirements were rather high and exceeded the capacity limits of available computer systems.

In principle, resonant sonic materials can be modelled by mechanical mass-spring systems [49]. When Maysenhölder presented his study on locally resonant materials modelled as periodically inhomogeneous thin plates, he also provided a simplified model based on harmonic oscillators [46]. Considering the lead core as the mass and the silicone as the spring of an oscillating system mounted on a simply supported plate representing the epoxy matrix, the main features of the sound transmission characteristic were demonstrated by this model. In a subsequent study, Maysenhölder presented an advanced formulation of the harmonic oscillator [50], in which both spring constant and mass of the harmonic oscillator were described by complex functions of frequency. The idea of using a complex mass formulation for composite structures was originally introduced by the investigation of sound absorbing materials made of basic rubberlike material with heavy inclusions using a complex density notation [51, 52]. The extension to structural acoustics by Maysenhölder allowed for a convenient description of locally resonant materials when internal resonant systems are enclosed in a rigid frame. Xiao *et al.* [53] published a parameter study carried out using a thin epoxy plate containing a periodic square array of lead discs hemmed around by rubber. Numerical results proved the existence of full band gaps where flexural vibration is prevented. Special interest was given to the width of the first full band gap which turned out to be highly dependent on the radius ratio of lead disc to rubber cladding and the filling fraction.

Multiple mass inclusions added to the poro-elastic layer of standard acoustic blankets were subject of measurements presented by Kidner *et al.* [54]. At low frequencies around 100 Hz, an increase of the insertion loss by 15

dB was achieved due to the randomly distributed mass inclusions. Therefore, the idea of resonant sonic materials can be considered as an innovative engineering application which has been studied theoretically for a couple of years. Recently, a first practical implementation used the idea of distributed mass inclusions as new passive noise control device to reduce aircraft interior noise [55].

Besides the research on resonant sonic materials above, Weith and Petersson investigated the wave propagation throughout beams and plates with embedded rubber coated steel balls [56, 57]. It is well known that added masses and springs on structures reduce the vibrational response to an external force at an arbitrary location [32]. For selected positions, the attached masses and springs act as secondary forces which eliminate the vibration response for certain frequency bands, also known as stop-bands. Weith and Petersson investigated the effect of added resonant inserts by so called periodic microstructure composites. First, steel balls were embedded into the neutral layer of homogeneous beams [56,58] and plates [57,59] and the expected stop-bands were obtained. In a second step, the steel balls were exchanged by rubber coated steel balls, therefore they were now resonant. Thus, by implementation of rubber coated steel balls Weith and Petersson discovered that the stop- and pass-band behaviour vanished but attenuation was achieved by the resonance effects of the now resonant inserts. Weith and Petersson showed the general potential of internal resonant systems by evaluating transfer functions of periodic microstructure composite beams and plates.

Both the research on resonant sonic material and on periodic microstructure composites revealed promising results. However, presented results are restricted to infinite structures or high frequencies. This thesis will extend the research on internal resonant systems to the issue of sound transmission through finite structures and low frequencies. Especially the research on infinite structures can be hardly transferred into real applications. In 2002, based on the results presented by Maysenhölder [46] the

author carried out measurements on finite double panel partitions in a sound transmission laboratory. The measurements were conducted according to the standard DIN EN ISO 140-3. Although the results of Maysenhölder [46] showed for infinite structures a clear resonant effect, this expected effect due to the internal absorbers was not detected by the measurements. As a consequence, the experiments on finite structures following the work of Maysenhölder were continued by the author in a impedance tube for plane wave incidence [60]. It was concluded, that the implementation of resonant systems requires a more complex understanding of the entire structure, taking the modal behaviour into account.

2.4 Vibration absorber

The resonant sonic materials above can be considered as a mechanical internal vibration absorber system, where the entire mass is attached to the resilient material.

Since the vibration absorber has been described by Ormondroyd and Den Hartog [61], it was widely used for structural vibration and noise control, e.g. in automobiles, buildings, airplanes or to protect sensitive equipment from adverse vibrations. The idealised vibration absorber consists of a rigid mass attached to one end of a spring which has constant stiffness. Depending on the application, the vibration absorber is also frequently called a vibration neutralizer [62]. The classical vibration absorber is used to control a troublesome resonance frequency of the host structure. The term vibration neutralizer is referred to the purpose of suppressing the vibration due to a troublesome forcing frequency. Therefore, the classical purpose of a vibration absorber is required when applying it to partitions for broadband excitation and this term is used throughout this thesis.

For many years, intensive research has been conducted on beam structures with added masses and springs. Additional masses and springs attached to the beam structure at certain location may reduce the response to an external force at an arbitrary location. Ordinary applications involve a vibration absorber to control vibration of resonant structures at the point where it is attached. Recent applications applied vibration absorbers to control sound radiation from vibrating structures by changing the global structural response [62,63]. Vibration absorbers attached on beams and plates can be used for structural acoustic optimization with various intentions. Primarily, the radiated acoustic power, due to structural vibration, is minimized by reducing the structural response. Another approach determines optimized surface velocity profiles when the structure has minimum acoustic radiation. The desired velocity profiles are realized by using vibration absorbers.

Efimtsov and Lazarev [64,65] described the sound transmission loss of panels with attached vibration absorbers and other resonant elements. For single [64] and double panel partitions [65] various applications of mounted resonant elements were presented. The different applications were discussed by their physical behaviour, caused by structural and acoustical excitation. Presented results showed that the use of resonant elements can increase the transmission loss of sound insulating structures and reduce the acoustic radiation in the low-frequency range, where conventional structures do not provide the required efficiency of sound insulation. Specific applications concerning aerospace structures were presented using mounted vibration absorbers to reduce the sound transmission into acoustic volumes bounded by cylindrical shells [66,67].

This project extends these studies by implementing vibration absorbers in the intervening cavity of double panel partitions. In order to improve the sound transmission loss of lightweight constructions in the low frequency region, various resonant elements are implemented into the cavity of double panel partitions. Gösele [68] suggested in his study the use of "acoustical leeches". Following the idea of Gösele, this study was devoted to derive a theoretical description of double panel partition with internal vibration absorbers. Regarding the research on distributed vibration absorbers for global structural control solutions, this work paid attention to the location of the vibration absorbers. By this means, the modal behaviour of both panels was taken into account.

In conclusion, this study has the objective to achieve an increased sound transmission loss at the MAM-resonance by implementing vibration absorbers into the cavity of double panel partitions. It is intended to achieve this increase with least possible mass penalty. Special interest is given to an absorber system similar to "resonant sonic material", where the absorber mass is coated by a resilient material.

Chapter 3

Mass-spring model

The implementation of vibration absorbers into the intervening cavity of a double panel partition enables various configurations. With respect to the general description of a vibration absorber as a mechanical mass-spring system, double panel partitions with differently attached internal vibration absorbers can be illustrated by a simple mass-spring model. In addition, regarding the main purpose of the application of internal vibration absorbers to sound transmission at low frequencies, this simple mass-spring approach provides a first understanding of the general physical principles of the structures under investigation.

3.1 Host double panel partition

The host structure of this project was a lightweight double panel construction without structural connections and a cavity filled only with air. Therefore, it was described by the mass-spring model as shown in Figure 3.1. The panels and the air gap were considered as a coupled mechanical acoustical system.

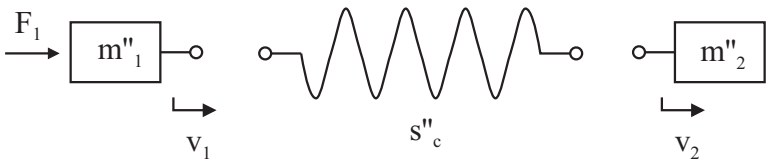

Figure 3.1: Mass-spring model of a double panel partition.

The two panels of the double panel partition are assumed to be lumped masses with the mass per unit area m_1'' and m_2''. These two masses are connected by a translational spring representing the cavity layer between the panels. The cavity spring is assumed to be massless and have constant stiffness k. For an air cavity this spring stiffness per unit area k is given by

$$k = \frac{c_0^2 \rho_0}{d} \tag{3.1}$$

where c_0 is the velocity of air, ρ_0 is the density of air and d stands for the thickness of the air cavity. The damping loss factor η is introduced by using the complex stiffness for the cavity spring $s_c'' = k(1 + i\eta)$.

Applying force equilibrium conditions the equations of motion for the two panels of the double panel partition due to a harmonic input force per unit area F_1 at circular frequency ω can be written as

$$\begin{aligned} i\omega m_1'' v_1 + \frac{1}{i\omega} s_c''(v_1 - v_2) &= F_1 \\ i\omega m_2'' v_2 + \frac{1}{i\omega} s_c''(v_2 - v_1) &= 0 \end{aligned} \tag{3.2}$$

where v_1 and v_2 are the velocities of the two panels. These equations can be simplified to

$$\left(i\omega \begin{bmatrix} m_1'' & 0 \\ 0 & m_2'' \end{bmatrix} + \frac{1}{i\omega} \begin{bmatrix} s_c'' & -s_c'' \\ -s_c'' & s_c'' \end{bmatrix} \right) \begin{pmatrix} v_1 \\ v_2 \end{pmatrix} = \begin{pmatrix} F_1 \\ 0 \end{pmatrix}. \tag{3.3}$$

Introducing mass matrix and stiffness matrix notation the equation of mo-

tion of the double panel partition is described by

$$\frac{1}{i\omega}\left(-\omega^2\mathbf{M}+\mathbf{K}\right)\mathbf{v}=\mathbf{f} \tag{3.4}$$

where the mass matrix $\mathbf{M}$ and the stiffness matrix $\mathbf{K}$ are given by

$$\mathbf{M}=\begin{bmatrix} m_1'' & 0 \\ 0 & m_2'' \end{bmatrix}, \mathbf{K}=\begin{bmatrix} s_c'' & -s_c'' \\ -s_c'' & s_c'' \end{bmatrix},$$

and the velocity vector $\mathbf{v}$ and force vector $\mathbf{f}$ are

$$\mathbf{v}=\begin{bmatrix} v_1 \\ v_2 \end{bmatrix}, \mathbf{f}=\begin{bmatrix} F_1 \\ 0 \end{bmatrix}.$$

For the double panel partition the motion of the incident panel due to the harmonic input force F_1 is transmitted to the radiating panel through the cavity spring. For the mass-spring model (Figure 3.1), the panel on the left hand side with mass per unit area m_1'' and the adjacent incident force is called the incident panel and the panel on the right hand side with mass per unit area m_2'' is called the radiating panel. In principle, the sound transmission of the double panel structure is controlled by the structural response and the corresponding sound radiation which is caused by the motion of the radiating panel. In order to achieve a better understanding of the structural characteristics of the internal vibration absorbers, attention was given initially to the structural response without taking the acoustical sound radiation into account. For a double panel structure the structural response can be obtained by the transfer impedance, which is defined by the ratio of the incident input force to the generated velocity of the radiating panel. Figure 3.2 shows the transfer impedance F_1/v_2 of a double panel structure with two 1 mm thick steel panels with the mass per unit area m''= 7.8 kg/m^2. Damping of the panels and of the cavity spring was assumed to be small with $\eta = 0.01$. For an air cavity of 3 mm the MAM-resonance appears at 555 Hz. This air cavity is chosen initially

here in order that the mass law region can be observed clearly below the MAM-resonance.

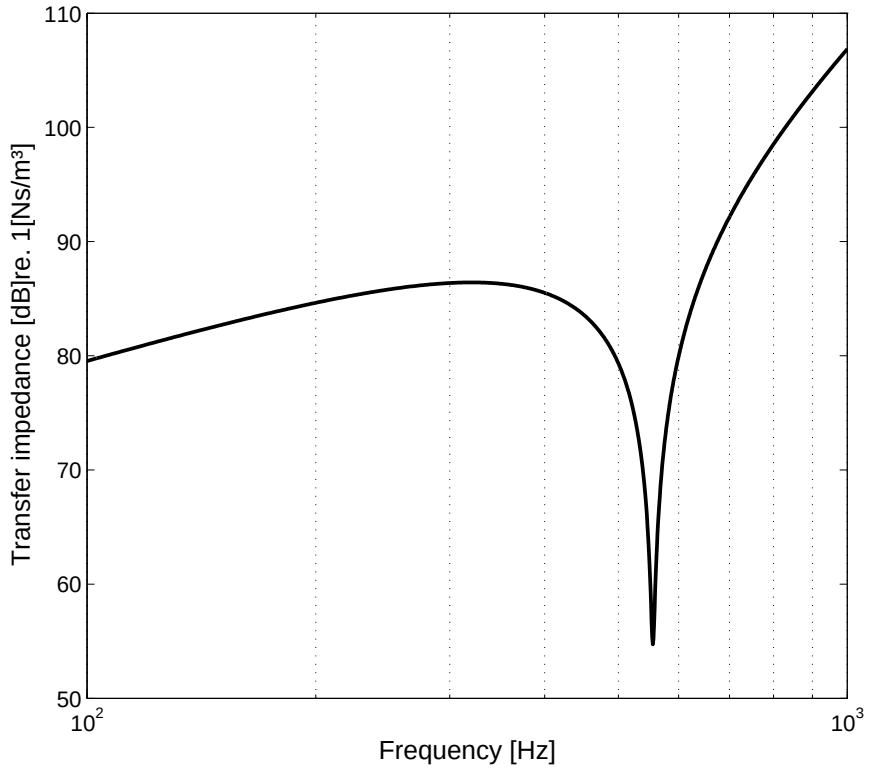

Figure 3.2: Transfer impedance of the double panel partition.

3.1.1 Fluid loads

The analysis of the sound transmission loss of a double panel partition has to take the fluid loadings on both sides of the partition into account [2]. As far as typical applications of double panel partitions are concerned, the double panel partition is surrounded by air. If a plane wave impinges on the incident panel, it induces vibrations of the incident panel, reflected waves, and transmission through the structure, as shown in Figure 3.3.

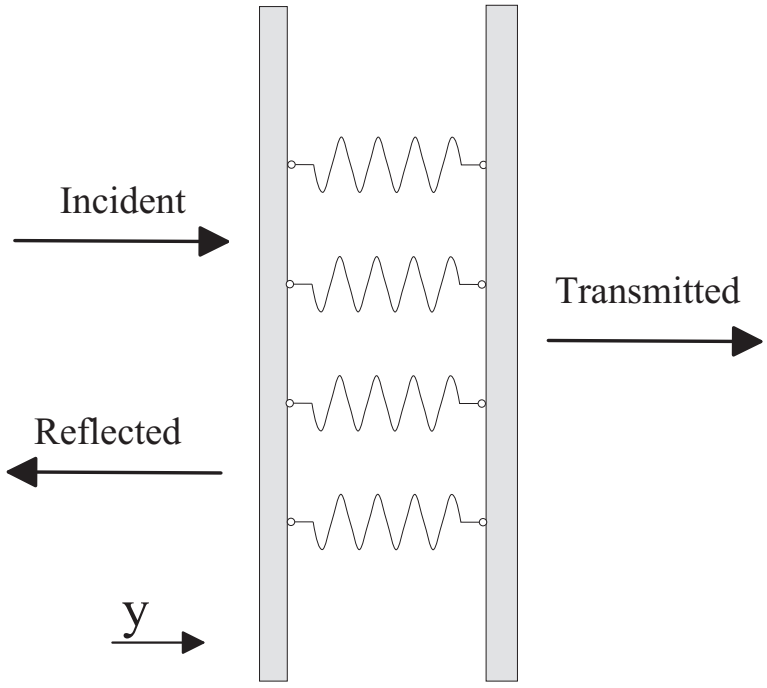

Figure 3.3: Normal incidence sound transmission through a double panel partition.

Thus, for a plane wave incident upon the partition the incident pressure field for normal incidence is written as

$$p_0 = \hat{A}e^{i(\omega t - k_0 y)} \tag{3.5}$$

where for the speed of sound in air c_0 the wavenumber $k_0 = \frac{\omega}{c_0}$.

The sound pressure reflected from the partition is written as

$$p_r = \hat{B} e^{i(\omega t + k_0 y)}. \tag{3.6}$$

$\hat{A}$ and $\hat{B}$ are the complex pressure amplitudes of the plane waves. The total pressure field at the surface of the incident panel at $y = 0$ is given by the incident and the reflected pressure.

$$p_1 = p_0 + p_r = (\hat{A} + \hat{B}) e^{i\omega t} \tag{3.7}$$

Using the continuity condition of the velocity at the surface of the incident panel, the displacement of the partition is linked to the pressure fields and corresponding particle velocities by

$$v_1 = v_i + v_r = \frac{(\hat{A} - \hat{B})}{\rho_0 c_0} e^{i\omega t} \tag{3.8}$$

which yields the pressure acting on the incident panel

$$p_1 = p_0 + p_r = (2\hat{A} - \rho_0 c_0 v_1) e^{i\omega t}. \tag{3.9}$$

Furthermore, the pressure load at the radiating panel is given by

$$p_2 = -(\rho_0 c_0 v_2) e^{i\omega t}. \tag{3.10}$$

Therefore, when taking into account the reflection at the source panel and the fluid load at the radiating panel, the mass matrix and the force vector of the mass-spring model above (Equation 3.4) are modified as follows

$$\mathbf{M} = \begin{bmatrix} m_1'' - i\frac{\rho_0 c_0}{\omega} & 0 \\ 0 & m_2'' - i\frac{\rho_0 c_0}{\omega} \end{bmatrix}, \quad \mathbf{f} = \begin{bmatrix} 2p_0 \\ 0 \end{bmatrix}. \tag{3.11}$$

Using the same parameters as for the previous calculation of the transfer impedance of the double panel structure (Figure 3.2), the comparison of

the transfer impedance with and without fluid loads is shown in Figure 3.4.

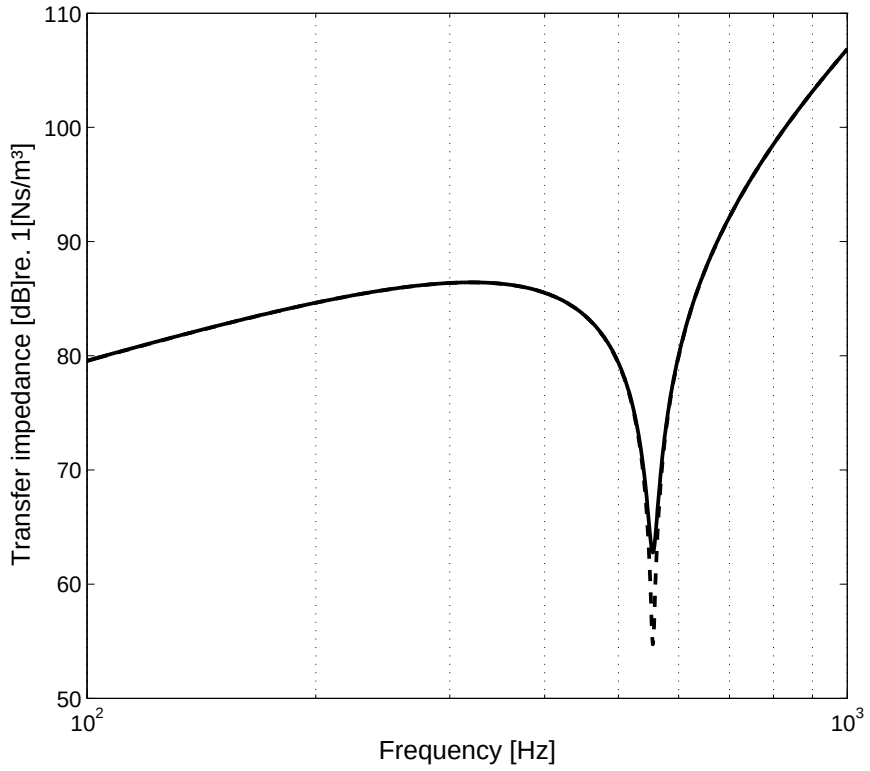

Figure 3.4: Transfer impedance of the double panel partition with and without fluid loads. (- -) without fluid load; (—) with fluid load

At both sides the fluid loads are acting with the specific acoustic impedance of air $\rho_0 c_0$ against the motion of the panels. In comparison with the mass-spring model (Figure 3.1) without fluid loads, the introduction of the fluid loads leads to a reduced velocity v_2 of the radiating panel. This reduced motion means also an increased transfer impedance. This effect is shown in Figure 3.4. Due to the applied dB scale only the significant reduction at the MAM-resonance is evident. The reduction at the MAM-resonance is significantly high, since a double panel partition has very low impedance at this structural resonance.

3.1.2 Sound reduction index

The sound transmission coefficient τ describes the ratio of the transmitted sound power P_{rad} to the incident sound power P_i.

$$\tau = \frac{P_{rad}}{P_i} \tag{3.12}$$

The sound transmission loss of partitions is defined by the sound reduction index R

$$R = 10 \log_{10} \frac{1}{\tau} \tag{3.13}$$

or

$$R = 10 \log_{10} \frac{P_i}{P_{rad}}. \tag{3.14}$$

For normal sound incidence of a plane sound wave with pressure amplitude p_0 the incident sound power per unit area is given by

$$P_i = \frac{|p_0|^2}{2\rho_0 c_0}. \tag{3.15}$$

If the velocity of the radiating panel is determined by the mass-spring model, the radiated power of the structure per unit area is expressed using the complex velocity v_2 as

$$P_{rad} = \frac{1}{2} \sigma \rho_0 c_0 \, |v_2|^2 \tag{3.16}$$

where a unit radiation efficiency σ can be assumed due to the assumption of plane waves. Hence the sound reduction index is given by

$$R = 10 \log_{10} \left(\left| \frac{p_0}{\rho_0 c_0 v_2} \right|^2 \right) = 10 \log_{10} \left(\left| \frac{Z_{12}}{2\rho_0 c_0} \right|^2 \right) \tag{3.17}$$

where $Z_{12} = \dfrac{F_1}{v_2} = \dfrac{2p_0}{v_2}$ is the transfer impedance.

The sound transmission characteristic for the previous host double pa-

nel partition with 1 *mm* steel panels and 3 *mm* air cavity is presented in Figure 3.5. As stated in section 3.1.1, the sound transmission loss is calculated throughout this study for a double panel structure with surrounding air fluid loads. The result of the mass-spring model is compared with the mass law of a single panel with the total mass of the host structure.

For the double panel partition the mass law for normal sound incidence is written for the frequency f as [33]

$$R \simeq 20 \log_{10}((m_1'' + m_2'')f) - 42. \tag{3.18}$$

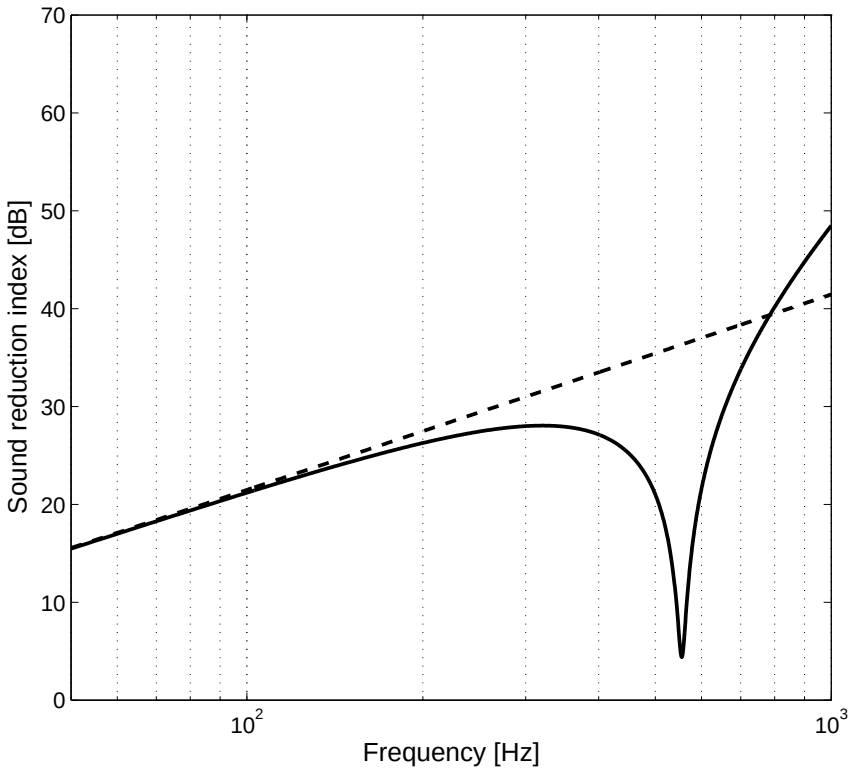

Figure 3.5: Sound reduction index of the double panel partition calculated by the mass-spring model. (- -) mass law; (—) mass-spring model

3.2 One-sided vibration absorber

Considering the classical mass-spring attachment of vibration absorbers to panels, in the case of a double panel partition the internal vibration absorbers can be attached to either of the two panels or to both panels. Therefore, in the latter assembly two one-sided vibration absorbers can be attached to either panels of the double panel partition as shown in Figure 3.6. The absorber masses are denoted by m''_{r1} and m''_{r2} and the complex absorber stiffnesses by s''_1 and s''_2.

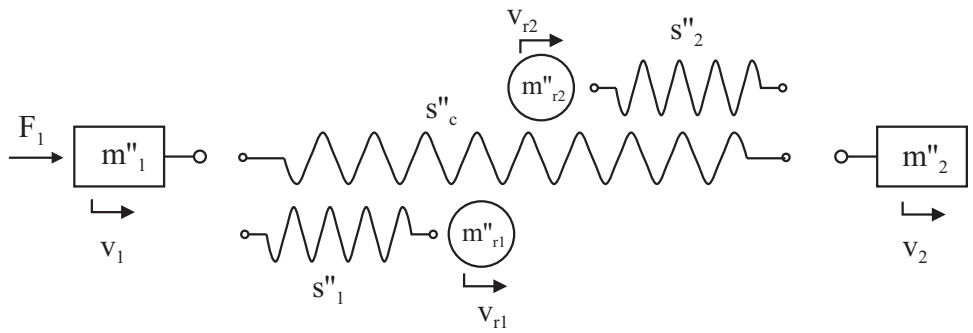

Figure 3.6: Mass-spring model of a double panel partition with two one-sided vibration absorbers.

This configuration of a double panel partition with internal vibration absorbers can again be described by the previous matrix formulation.

$$\frac{1}{i\omega}\left(-\omega^2\mathbf{M}+\mathbf{K}\right)\mathbf{v}=\mathbf{f} \tag{3.19}$$

Taking the internal vibration absorbers into account, the mass matrix and stiffness matrix are written as

$$\mathbf{M}=\begin{bmatrix} m''_1-i\frac{\rho_0 c_0}{\omega} & 0 & 0 & 0 \\ 0 & m''_{r1} & 0 & 0 \\ 0 & 0 & m''_{r2} & 0 \\ 0 & 0 & 0 & m''_2-i\frac{\rho_0 c_0}{\omega} \end{bmatrix}, \mathbf{K}=\begin{bmatrix} s''_c+s''_1 & -s''_1 & 0 & -s''_c \\ -s''_1 & s''_1 & 0 & 0 \\ 0 & 0 & s''_2 & -s''_2 \\ -s''_c & 0 & -s''_2 & s''_c+s''_2 \end{bmatrix},$$

and the velocity vector $\mathbf{v}$ and force vector $\mathbf{f}$ are

$$\mathbf{v} = \begin{bmatrix} v_1 \\ v_{r1} \\ v_{r2} \\ v_2 \end{bmatrix}, \mathbf{f} = \begin{bmatrix} 2p_0 \\ 0 \\ 0 \\ 0 \end{bmatrix}.$$

The corresponding transfer impedance for the double panel partition with 1 mm steel panels when the internal vibration absorbers have equal absorbers masses of 0.5 kg/m^2 is shown in Figure 3.7. The resonances of the internal vibration absorbers were set to 200 Hz and 300 Hz. The vibration absorbers were lightly damped as was the host structure, with η=0.01.

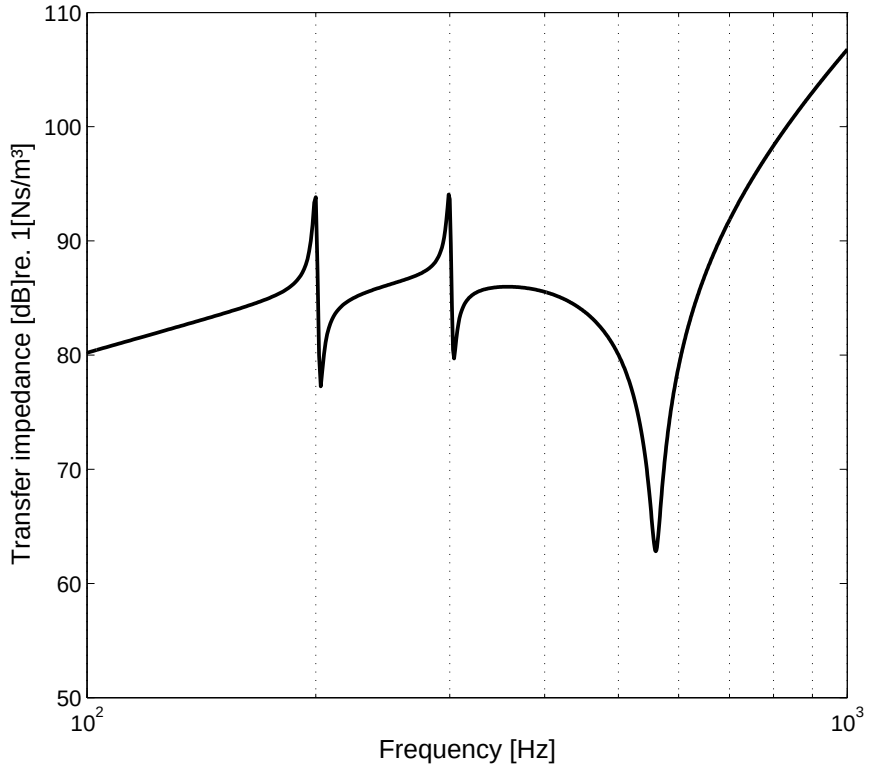

Figure 3.7: Transfer impedance of the double panel partition with two one-sided vibration absorbers.

The transfer impedance reveals the expected characteristic of a vibration absorber with a peak at the resonance frequency of the blocked mass-spring system followed by a dip. In fact, since the internal vibration absorbers were not tuned to a resonance of the host structure, the obtained transfer impedance presents the typical characteristic of a vibration neutralizer which is designed for a specific troublesome frequency, see section 2.4.

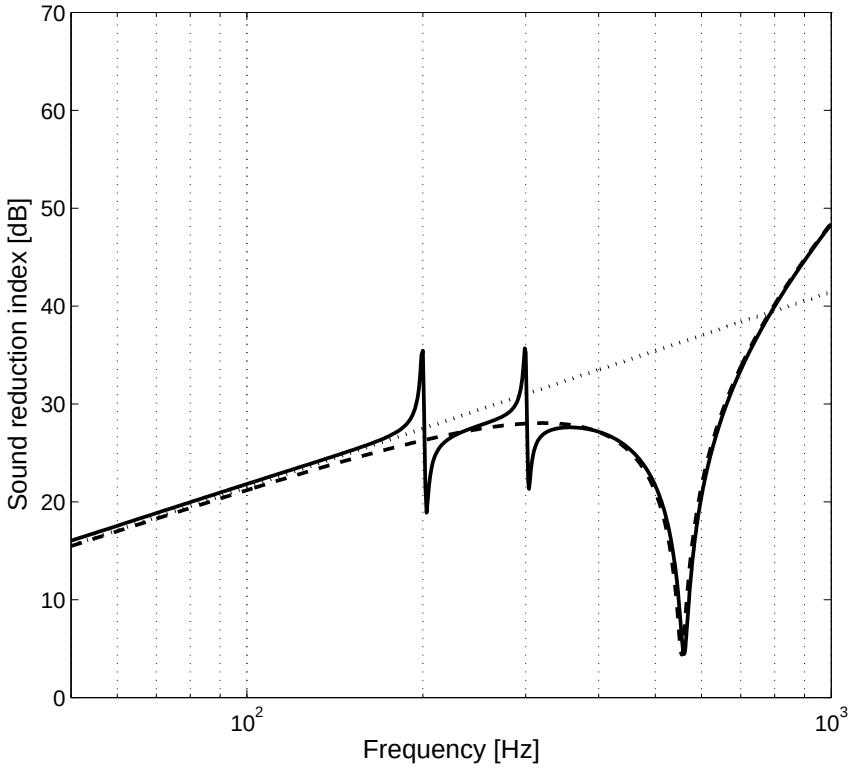

Figure 3.8: Sound reduction index of the double panel partition with two attached one-sided vibration absorbers, calculated by the mass-spring model. $(\cdots)$ mass law; (- -) mass-spring model without absorbers; (—) mass-spring model with absorbers

Using a vibration neutralizer increases the sound reduction index of a

structure at a specific frequency in order to enhance the structure for suppressing a specific sound source with a troublesome frequency that corresponds with the frequency of the neutralizer resonance. The peak of the increased sound transmission loss is accompanied by a deterioration of the sound transmission loss. However, the deterioration can be controlled to appear at a frequency where the sound source is not harmful. Therefore, no high sound reduction characteristic of the structure is required.

For the two internal vibration absorbers with the resonance frequencies at 200 Hz and 300 Hz Figure 3.8 shows the corresponding sound reduction index calculated according to the formulations of section 3.1.2.

3.3 Two-sided vibration absorber

The mass-spring formulations above can be used for the study of internal two-sided vibration absorbers. Regarding the idea of embedded masses, the configuration of a two-sided vibration absorber consists of an absorber mass that is attached to both panels of the double panel partition by two springs. Hence, the two panels are dynamically coupled by the cavity spring and the two-sided vibration absorber. This is shown in Figure 3.9 where the absorber mass is denoted by m_r'' and the complex absorber stiffnesses by s_1'' and s_2''.

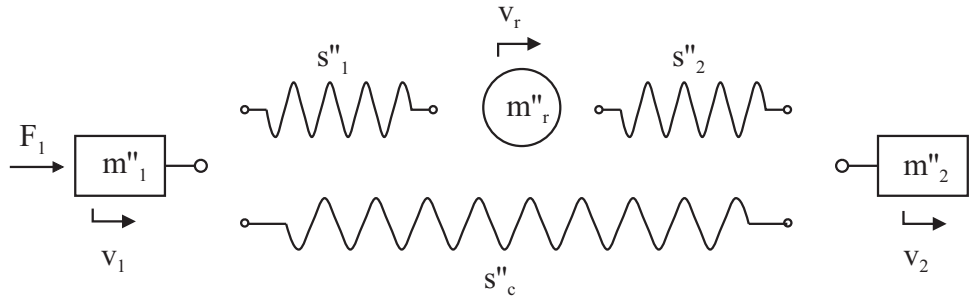

Figure 3.9: Mass-spring model of a double panel partition with two-sided vibration absorber.

Applying the previous mass-spring analysis

$$\frac{1}{i\omega}\left(-\omega^2\mathbf{M}+\mathbf{K}\right)\mathbf{v}=\mathbf{f} \tag{3.20}$$

the mass matrix and stiffness matrix for this configuration are as follows

$$\mathbf{M}=\begin{bmatrix} m_1''-i\frac{\rho_0 c_0}{\omega} & 0 & 0 \\ 0 & m_r'' & 0 \\ 0 & 0 & m_2''-i\frac{\rho_0 c_0}{\omega} \end{bmatrix}, \mathbf{K}=\begin{bmatrix} s_c''+s_1'' & -s_1'' & -s_c'' \\ -s_1'' & s_1''+s_2'' & -s_2'' \\ -s_c'' & -s_2'' & s_2''+s_c'' \end{bmatrix},$$

and the vectors are given by

$$\mathbf{v}=\begin{bmatrix} v_1 \\ v_r \\ v_2 \end{bmatrix}, \mathbf{f}=\begin{bmatrix} 2p_0 \\ 0 \\ 0 \end{bmatrix}.$$

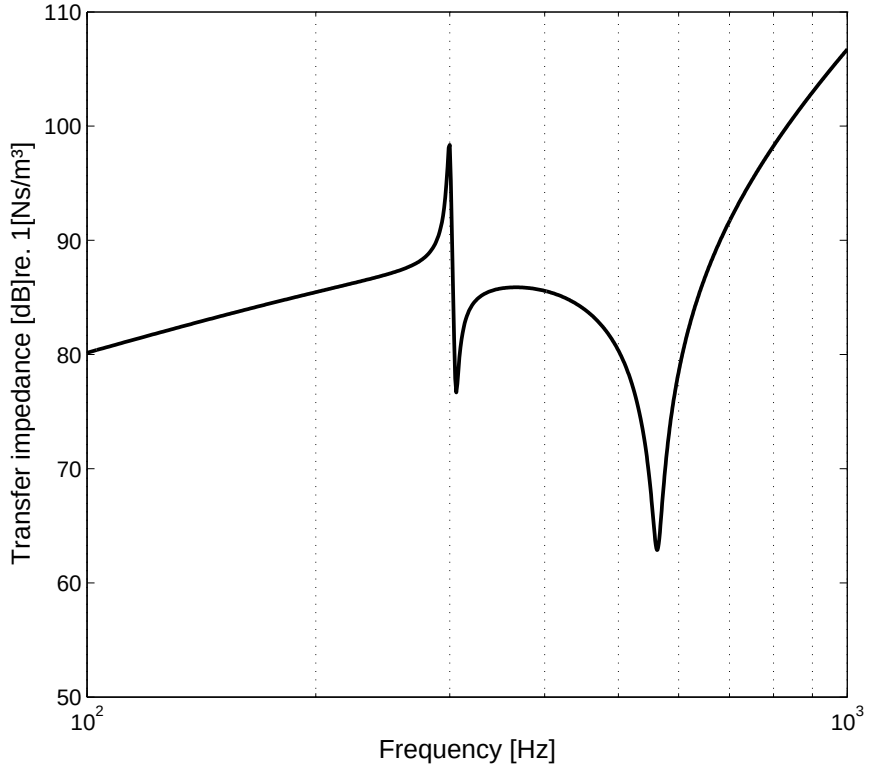

Figure 3.10: Transfer impedance of the double panel partition with two-sided vibration absorber.

Figure 3.10 shows the transfer impedance for the previously calculated double panel partition with 1 mm steel panels with a mass per unit area m''= 7.8 kg/m^2 (Figure 3.2) and attached lightly damped two-sided vibration absorber (η=0.01). The vibration absorber has an absorber mass of 1 kg/m^2 and is tuned to give the absorber resonance at 300 Hz. The corresponding sound transmission characteristic is presented in Figure 3.11. In conclusion, the implementation of internal vibration absorbers as one-sided or two-sided absorber systems can achieve a considerable reduction of the sound transmission at specific frequencies although with the penalty of an increase at other frequencies.

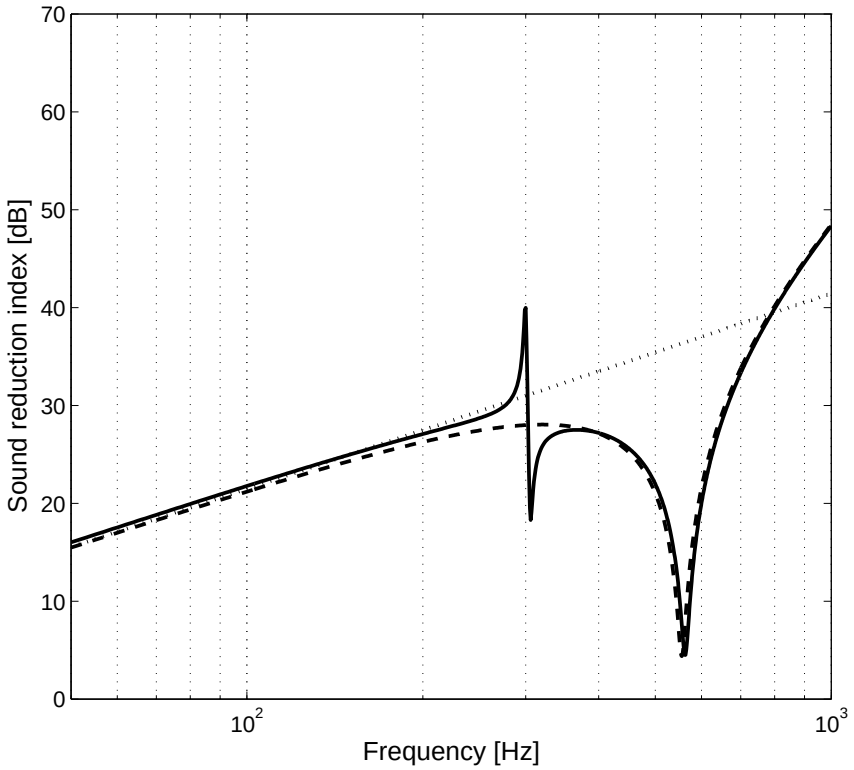

Figure 3.11: Sound reduction index of the double panel partition with two-sided vibration absorber, calculated by the mass-spring model. (· · ·) mass law; (- -) mass-spring model without absorbers; (—) mass-spring model with absorbers

Chapter 4

Beam model

This project applies the concept of internal vibration absorbers to finite double panel partitions with special interest in the number and location of the vibration absorbers. At low frequencies it is assumed that the internal vibration absorbers are affected by the modal behaviour of the two panels. However, the simple mass-spring model of the previous chapter considered the panels as lumped masses without flexural characteristics. Therefore, for the analysis of the transverse displacement of the double panel partitions with internal vibration absorbers, a one dimensional beam model has been derived. Based on the modal expansion method [32], the beam model is entirely modal considering the contribution of each mode over the frequency band of interest. By this means, the effect of internal vibration absorbers on the structure can be determined for different locations and numbers.

All the partitions in this study are finite and rectangular, baffled by an infinite and rigid baffle. The panels are modelled with simply supported boundaries using the Kirchhoff plate theory. For the purpose of this project, it was sufficient to confine the considerations to the motion of the panels in flexure only.

The beam model follows Cremer's model of floating floors [69, 70]. This

model consists of two elastic panels with a resilient layer in between. The panels are represented by uniform simply supported beams in bending connected by a layer of distributed uncoupled springs. The motion of the incident panel is transferred to the second panel through the mechanical springs. This fundamental assumption of the beam model is valid well below the first transverse acoustic resonance of the cavity [71].

4.1 Host double panel partition

The host double panel partition of this project is modelled by the beam model using two simply supported beams of length l and infinite width. The beam model for the double panel partition is shown in Figure 4.1 for an incident pressure load p_1.

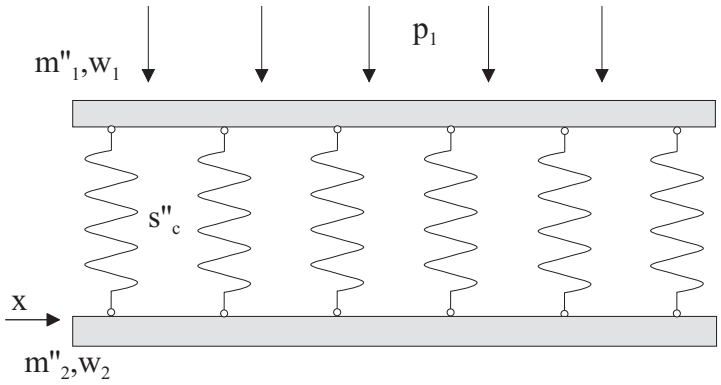

Figure 4.1: Beam model of a double panel partition.

As for the mass-spring model, first, formulations for this beam model were derived assuming a continuous cavity spring. Furthermore, formulations were derived for the cavity being represented by discrete springs. These discrete springs are considered to be equally distributed along the length of the beams.

4.1.1 Continuous cavity spring

For an isotropic thin plate, the equation of motion according to Kirchhoff's plate theory is given for the transverse displacement $w(x, y, t)$ by

$$D\nabla^4 w(x, y, t) + \rho h \frac{\partial^2 w(x, y, t)}{\partial t^2} = p_1(x, y, t) \tag{4.1}$$

with uniform thickness h, and density ρ. The complex plate bending stiffness D accounting for the structural damping η_p is given by

$$D = \frac{Eh^3}{12(1-\nu^2)}(1 + i\eta_p) \tag{4.2}$$

where ν is the Poisson's ratio and E is the Young's modulus.

For the beam model the Kirchhoff formulation is modified for a uniform thin elastic beam as follows

$$D\nabla^4 w(x, t) + \rho h \frac{\partial^2 w(x, t)}{\partial t^2} = p_1(x, t). \tag{4.3}$$

Considering harmonic motion with time dependence $e^{i\omega t}$, the transverse displacement of a beam can be written as

$$w(x, t) = \hat{w} e^{i\omega t}. \tag{4.4}$$

Substituting this formulation into Equation 4.3 and omitting the time dependence $e^{i\omega t}$ the equation of motion for a uniform thin elastic beam is given by

$$D\nabla^4 w(x) - \omega^2 m'' w(x) = p_1(x) \tag{4.5}$$

where m'' is the mass per unit area and $w(x)$ is the transverse displacement along the beam.

For a constant incident pressure $\hat{p}_1$ along the beam $p_1(x) = \hat{p}_1$. Applying the bending wave formulation of Equation 4.5 to the beam model descrip-

tion of the double panel partition shown in Figure 4.1, the equations of motion of the host double panel partition can be written as

$$\begin{aligned} D_1\nabla^4 w_1(x) - \omega^2 m_1'' w_1(x) + s_c''(w_1(x) - w_2(x)) &= \hat{p}_1 \\ D_2\nabla^4 w_2(x) - \omega^2 m_2'' w_2(x) + s_c''(w_2(x) - w_1(x)) &= 0 \end{aligned} \tag{4.6}$$

where s_c'' is the complex spring stiffness of the continuous resilient cavity layer. The mass per unit area m'' and the transverse displacement $w(x)$ of the two beams are represented by the subscripts (1) and (2).

The modal expansion method describes an alternative formulation for the transverse displacement. The contribution of each mode is taken into account over the entire frequency band considered. By the modal expansion method the forced response $w(x,t)$ of a beam is given by the product of the modal amplitudes and eigenvectors, which satisfy the boundary conditions.

$$w(x,t) = \sum_{n=1}^{\infty} q_n(t)\Phi_n(x) \tag{4.7}$$

The generalized coordinates q_n are frequently known as modal amplitudes and the eigenvectors $\Phi_n(x)$ are also called mode shape functions. The mode shape functions of vibration for a simply supported beam are known to be [72]

$$\Phi_n(x) = \sin\frac{n\pi}{l}x. \tag{4.8}$$

Therefore, for a constant incident pressure load the response of the host double panel partition (Equation 4.6) is derived in the form of the following equations, which include for each individual beam the complete infinite set of sinusoidal modes. These modes are not necessarily representing the modes of the coupled double panel system but are a convenient set of basis functions that satisfy the boundary conditions.

$$
\begin{aligned}
&D_1 \nabla^4 \sum_{n=1}^{\infty} q_{1,n} \Phi_{1,n}(x) - \omega^2 m_1'' \sum_{n=1}^{\infty} q_{1,n} \Phi_{1,n}(x) \\
&\quad + s_c'' \left(\sum_{n=1}^{\infty} q_{1,n} \Phi_{1,n}(x) - \sum_{n=1}^{\infty} q_{2,n} \Phi_{2,n}(x) \right) = \hat{p}_1 \\
&D_2 \nabla^4 \sum_{n=1}^{\infty} q_{2,n} \Phi_{2,n}(x) - \omega^2 m_2'' \sum_{n=1}^{\infty} q_{2,n} \Phi_{2,n}(x) \\
&\quad + s_c'' \left(\sum_{n=1}^{\infty} q_{2,n} \Phi_{2,n}(x) - \sum_{n=1}^{\infty} q_{1,n} \Phi_{1,n}(x) \right) = 0
\end{aligned} \tag{4.9}
$$

For the double panel partitions of this project, it is assumed that both beams have identical length and boundary conditions. Thus, for the analysis only the mode shape function Φ_n was required.

$$
\Phi_{1,n} = \Phi_{2,n} = \Phi_n \tag{4.10}
$$

After substitution of the mode shape function for a simply supported beam (Equation 4.8) the partial differentiation $\nabla^4 = \dfrac{\partial^4}{\partial x^4}$ leads to

$$
\begin{aligned}
&D_1 \sum_{n=1}^{\infty} k_n^4 q_{1,n} \Phi_n(x) - \omega^2 m_1'' \sum_{n=1}^{\infty} q_{1,n} \Phi_n(x) \\
&\quad + s_c'' \left(\sum_{n=1}^{\infty} q_{1,n} \Phi_n(x) - \sum_{n=1}^{\infty} q_{2,n} \Phi_n(x) \right) = \hat{p}_1 \\
&D_2 \sum_{n=1}^{\infty} k_n^4 q_{2,n} \Phi_n(x) - \omega^2 m_2'' \sum_{n=1}^{\infty} q_{2,n} \Phi_n(x) \\
&\quad + s_c'' \left(\sum_{n=1}^{\infty} q_{2,n} \Phi_n(x) - \sum_{n=1}^{\infty} q_{1,n} \Phi_n(x) \right) = 0
\end{aligned} \tag{4.11}
$$

with the modal wavenumber $k_n = \dfrac{n\pi}{l}$.

In order to describe these equations of motion by the matrix formulation that was already used for the mass-spring model, Equation 4.11 is multi-

plied with the modal shape function for the m-th mode

$$\Phi_m(x) = \sin \frac{m\pi}{l} x \tag{4.12}$$

and integrated over the length l.

$$\begin{aligned}
&\int_0^l D_1 \sum_{n=1}^{\infty} k_n^4 q_{1,n} \Phi_n(x) \Phi_m(x)\, \mathrm{dx} - \int_0^l \omega^2 m_1'' \sum_{n=1}^{\infty} q_{1,n} \Phi_n(x) \Phi_m(x)\, \mathrm{dx} \\
&\quad + s_c'' \left(\int_0^l \sum_{n=1}^{\infty} q_{1,n} \Phi_n(x) \Phi_m(x)\, \mathrm{dx} - \int_0^l \sum_{n=1}^{\infty} q_{2,n} \Phi_n(x) \Phi_m(x)\, \mathrm{dx} \right) = \int_0^l \hat{p}_1 \Phi_m(x)\, \mathrm{dx} \\
&\int_0^l D_2 \sum_{n=1}^{\infty} k_n^4 q_{2,n} \Phi_n(x) \Phi_m(x)\, \mathrm{dx} - \int_0^l \omega^2 m_2'' \sum_{n=1}^{\infty} q_{2,n} \Phi_n(x) \Phi_m(x)\, \mathrm{dx} \\
&\quad + s_c'' \left(\int_0^l \sum_{n=1}^{\infty} q_{2,n} \Phi_n(x) \Phi_m(x)\, \mathrm{dx} - \int_0^l \sum_{n=1}^{\infty} q_{1,n} \Phi_n(x) \Phi_m(x)\, \mathrm{dx} \right) = 0
\end{aligned} \tag{4.13}$$

Using the orthogonality relationship

$$\int_0^l \Phi_n(x) \Phi_m(x)\, \mathrm{dx} = \begin{cases} 0 & n \neq m \\ \frac{l}{2} & n = m \end{cases} \tag{4.14}$$

the equations of motion of the host double panel partition (Equation 4.13) can be written as

$$\begin{aligned}
&D_1 k_n^4 \frac{l}{2} q_{1,n} - \omega^2 m_1'' \frac{l}{2} q_{1,n} + s_c'' \frac{l}{2} (q_{1,n} - q_{2,n}) = \frac{\hat{p}_1 l}{n\pi} (1 - \cos n\pi) \\
&D_2 k_n^4 \frac{l}{2} q_{2,n} - \omega^2 m_2'' \frac{l}{2} q_{2,n} + s_c'' \frac{l}{2} (q_{2,n} - q_{1,n}) = 0.
\end{aligned} \tag{4.15}$$

If generalized coordinates are used, the vibrational motion of a beam due to the n-th mode is illustrated in Figure 4.2 below.

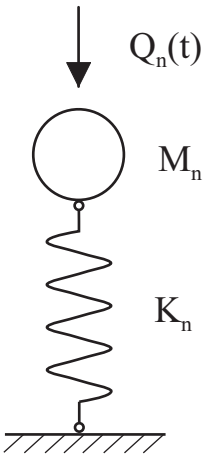

Figure 4.2: Motion of individual beam by generalized coordinates.

This modal mass-spring system for the n-th mode of an individual beam is described by

$$-\omega^2 M_n q_n + K_n q_n = Q_n. \tag{4.16}$$

Therefore, the previous simplification of Equation 4.13 revealed the modal mass M_n and the modal stiffness K_n.

$$\begin{array}{rcl} M_n & = & m'' \frac{l}{2} \\ K_n & = & D k_n^4 \frac{l}{2} \end{array} \tag{4.17}$$

Based on Equation 4.15, for the n-th mode the beam model of the double panel partition with continuous cavity spring is described by the intended matrix formulation as

$$\left(-\omega^2 \mathbf{M}_n + \mathbf{K}_n\right) \mathbf{q}_n = \mathbf{Q}_n \tag{4.18}$$

where the mass matrix $\mathbf{M}_n$ and the stiffness matrix $\mathbf{K}_n$ are given by

$$\mathbf{M}_n = \frac{l}{2} \begin{bmatrix} m_1'' & 0 \\ 0 & m_2'' \end{bmatrix}, \mathbf{K}_n = \frac{l}{2} \begin{bmatrix} D_1 k_n^4 + s_c'' & -s_c'' \\ -s_c'' & D_2 k_n^4 + s_c'' \end{bmatrix}$$

and the generalized amplitude vector $\mathbf{q}_n$ and force vector $\mathbf{Q}_n$ are

$$\mathbf{q}_n = \begin{bmatrix} q_{1,n} \\ q_{2,n} \end{bmatrix}, \mathbf{Q}_n = \begin{bmatrix} \frac{\hat{p}_1 l}{n\pi}(1 - \cos n\pi) \\ 0 \end{bmatrix}.$$

Since the generalized force Q_n was obtained as

$$Q_n = \frac{\hat{p}_1 l}{n\pi}(1 - \cos n\pi), \tag{4.19}$$

it can be considered separately for even and odd modes.

$$Q_n = \begin{cases} \frac{2\hat{p}_1 l}{n\pi} & n = odd \\ 0 & n = even \end{cases} \tag{4.20}$$

Thus, for the constant pressure load $\hat{p}_1$ along the beam only the odd modes contribute to the motion of the structure.

If generalized amplitudes are determined for a mode n by solving Equation 4.18, the motion of the panels of the double panel host structure can be determined by Equation 4.7. Dependent on the dimensions of the structure and the frequency range of interest the summation in Equation 4.7 needs to be performed for a certain number of modes N. An estimation for this number of modes contributing to the motion of the structure for a frequency range defined by a maximum frequency ω_{max} is obtained by [72]

$$N = \frac{k_b l}{\pi} \tag{4.21}$$

where the maximum bending wave number of a beam is given by

$$k_b = \sqrt[4]{\frac{\omega_{max}^2 m''}{D}}.$$

As a matter of fact, the higher the number of modes used for the calculation, the more accurate is the result for higher frequencies. For the host dou-

ble panel partition (see page 62) used throughout the project with 1 m long steel panels that have a mass per unit are of 7.8 kg/m^2 Equation 4.21 yields the number of 20 modes if frequencies up to 1000 Hz are under investigation. The frequency range up to 1000 Hz was during this project frequently used for calculations. On the other hand, the following results presented for this frequency range are calculated in general with more than 100 modes.

4.1.2 Fluid loads

The representation of the double panel partition by the one-dimensional beam model extends the previous mass-spring model by the flexible behaviour of the host structure. But the flexible response depends on the incident sound field. Therefore, the one-dimensional beam model accounts for a plane wave pressure load at normal and oblique incidence.

For a normally incident plane wave pressure load p_0 the incident pressure is constant along the beam having the amplitude $\hat{p}_0$, $p_0(x) = \hat{p}_0$. In this case, assuming the radiation efficiency $\sigma = 1$, for normal sound incidence the fluid loading on both sides of the partition is taken into account by the specific acoustic impedance at the surface of the panels as shown for the mass-spring model (Equation 3.11). Accounting for the fluid loads, for the n-th mode the mass matrix $\mathbf{M}_n$ and the generalized force vector $\mathbf{Q}_n$ in Equation 4.18 are written as

$$\mathbf{M}_n = \frac{l}{2}\begin{bmatrix} m_1'' - i\frac{\rho_0 c_0}{\omega} & 0 \\ 0 & m_2'' - i\frac{\rho_0 c_0}{\omega} \end{bmatrix} \qquad \mathbf{Q}_n = \begin{bmatrix} \frac{2\hat{p}_0 l}{n\pi}(1-\cos n\pi) \\ 0 \end{bmatrix}. \tag{4.22}$$

The oblique sound incidence of a plane wave on a beam structure is shown in Figure 4.3. The incident and reflected pressure fields for oblique incidence are given by

$$\begin{aligned} p_i &= \hat{A}e^{i(\omega t - k_x x - k_y y)} \\ p_r &= \hat{B}e^{i(\omega t - k_x x + k_y y)}. \end{aligned} \tag{4.23}$$

Therefore, the total incident pressure field at the surface of the incident panel at $y = 0$ is described as follows

$$p_1 = p_i + p_r = (\hat{A} + \hat{B})e^{i(\omega t - k_x x)}. \tag{4.24}$$

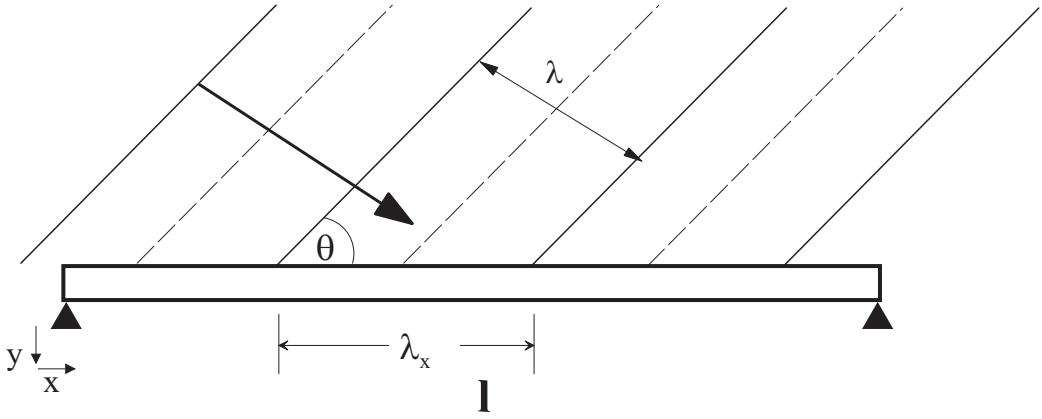

Figure 4.3: Sound field impinging on a beam at angle θ.

At $y = 0$ the velocity component normal to the partition can be written as

$$v_1 = v_i + v_r = \frac{(\hat{A} - \hat{B})\cos\theta}{\rho_0 c_0} e^{i(\omega t - k_x x)}. \tag{4.25}$$

For oblique sound incidence the pressure loads on either side of the double panel partition are as follows

$$\begin{aligned} p_1 &= (2\hat{A}e^{-ik_x x} - \frac{\rho_0 c_0}{\cos\theta} v_1) e^{i\omega t} \\ p_2 &= -\left(\frac{\rho_0 c_0 v_2}{\cos\theta}\right) e^{i\omega t}. \end{aligned} \tag{4.26}$$

By this means, based on Equation 4.6, the double panel partition is described for oblique sound incidence as

$$\begin{aligned} D_1 \nabla^4 w_1(x) - \omega^2 (m_1'' - i\tfrac{\rho_0 c_0}{\omega \cos\theta}) w_1(x) + s_c''(w_1(x) - w_2(x)) &= 2\hat{p}_0 e^{-ik_x x} \\ D_2 \nabla^4 w_2(x) - \omega^2 (m_2'' - i\tfrac{\rho_0 c_0}{\omega \cos\theta}) w_2(x) + s_c''(w_2(x) - w_1(x)) &= 0 \end{aligned} \tag{4.27}$$

where $\hat{p}_0$ is the complex pressure amplitude of the incident plane wave and $k_x = k_0 \sin\theta$ the so-called trace wave number. Applying the modal expansion approach on the pressure element in Equation 4.27 leads to the

modal incident pressure as follows

$$Q_n = 2 \int_0^l \hat{p}_0 e^{(-ik_x x)} \Phi_n(x) \, \mathrm{d}x. \tag{4.28}$$

Using the integral solution

$$\int e^{ax} \sin bx \, \mathrm{dx} = \frac{e^{ax}}{a^2 + b^2} (a \sin bx - b \cos bx) \tag{4.29}$$

substitution of $\Phi_n = \sin(\frac{n\pi}{l} x)$ and $k_x = k_0 \sin\theta$ yields

$$\int_0^l e^{(-ik_x x)} \Phi_n(x) \, \mathrm{dx} = \frac{l}{n\pi \left(1 - \left(\frac{k_x}{k_n}\right)^2\right)} \left(1 - (-1)^n e^{(-ik_x l)}\right). \tag{4.30}$$

Therefore, the modal incident pressure Q_n is written as

$$Q_n = 2\hat{p}_0 \frac{l}{n\pi \left(1 - \left(\frac{k_x}{k_n}\right)^2\right)} \left(1 - (-1)^n e^{(-ik_x l)}\right). \tag{4.31}$$

which is valid for $k_x \neq k_n$. In fact, for normal sound incidence Equation 4.31 yields the known formulation

$$Q_n = \frac{2\hat{p}_0 l}{n\pi} (1 - \cos n\pi). \tag{4.32}$$

The critical condition $k_x = k_n$ is only an issue for oblique sound incidence but for each individual mode at a different angle of incidence. In fact, in this study this critical condition was not observed for the calculations of the sound transmission loss at diffuse sound incidence using the beam model. The considered diffuse sound field was only described by angles of incidence with integer numbers and a spacing of one degree. Therefore, the very specific mode angle combination of the critical condition could hardly match with the considered angles of incidence.

For the double panel partition with continuous cavity spring and plane wave pressure load at oblique incidence the fluid loads at both sides of the partition are taken into account by the specific acoustic impedance of the fluids. For this reason, the mass matrix of Equation 4.18 is modified as follows

$$\mathbf{M}_n = \frac{l}{2}\begin{bmatrix} m_1'' - i\frac{\rho_0 c_0}{\omega\cos\theta} & 0 \\ 0 & m_2'' - i\frac{\rho_0 c_0}{\omega\cos\theta} \end{bmatrix}. \tag{4.33}$$

Further, the force vector $\mathbf{Q}_n$ is given by

$$\mathbf{Q}_n = \begin{bmatrix} Q_n \\ 0 \end{bmatrix}. \tag{4.34}$$

with the modal pressure force Q_n above (Equation 4.31).

4.1.3 Discrete cavity springs

If the resilient cavity layer is described by discrete springs, these springs have to be considered at discrete positions of the host structure. Therefore, a formulation of single point forces acting at discrete positions on the structure was required.

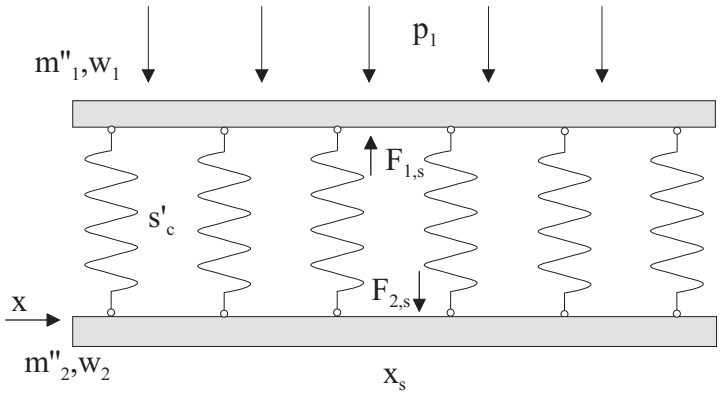

Figure 4.4: Beam model of a double panel partition with discrete cavity springs.

In general, a single harmonic point force at position x_s is described by

$$F(x_s, t) = \hat{F} e^{i\omega t} \delta(x - x_s). \tag{4.35}$$

If a spring is connecting the two simply supported beams of the beam model at position x_s, see Figure 4.4, the coupling forces acting on the beams are

$$F_{1,s} = F_s = -F_{2,s}. \tag{4.36}$$

The previous assumption that both beams have the same modal shape function

$$\Phi_{1,n} = \Phi_{2,n} = \Phi_n \tag{4.37}$$

leads to the corresponding coupling generalized forces of the n-th mode.

$$Q_{n_{1,s}} = Q_{n_s} = -Q_{n_{2,s}} \tag{4.38}$$

Applying the previous approach of multiplying with Φ_m (Equation 4.12) and integrating over the length l to Equation 4.35, the generalized force Q_{n_s} corresponding to the point force $F(x_s, t)$ is obtained as

$$Q_{n_s}(t) = \int_0^l F(x_s, t)\Phi_m(x)\,\mathrm{dx} = \hat{F} e^{i\omega t}\Phi_m(x_s). \tag{4.39}$$

Thus, the generalized coupling force acting on the beams is given by

$$Q_{n_s}(t) = s_c'(w_1(x_s) - w_2(x_s))e^{i\omega t}\Phi_m(x_s). \tag{4.40}$$

Using the modal expansion method for N modes with the transverse displacement $w(x, t) = \sum_{n=1}^{N} q_n(t)\Phi_n(x)$ yields

$$Q_{n_s}(t) = s_c' \left(\sum_{n=1}^{N} q_{1,n}(t)\Phi_n(x_s) - \sum_{n=1}^{N} q_{2,n}(t)\Phi_n(x_s) \right) \Phi_m(x_s). \tag{4.41}$$

This equation can be simplified to

$$Q_{n_s}(t) = s_c' \left(\sum_{n=1}^{N} \Phi_m(x_s)\Phi_n(x_s)(q_{1,n}(t) - q_{2,n}(t)) \right). \tag{4.42}$$

Supposing that J springs are distributed along the beams, the generalized force Q_n comprises the contributions of the forces applied due to the J discrete springs. According to Equation 4.39, the generalized force due to a number of J springs is obtained by

$$Q_n(t) = \sum_{j=1}^{J} \hat{F}_j e^{i\omega t} \Phi_m(x_j) \tag{4.43}$$

which yields for the generalized coupling force

$$Q_{n_s}(t) = s_c' \sum_{j=1}^{J} \left(\sum_{n=1}^{N} \Phi_m(x_j)\Phi_n(x_j)(q_{1,n}(t) - q_{2,n}(t)) \right). \tag{4.44}$$

If the time dependence $e^{i\omega t}$ is omitted, the equations of motion for the double panel partition with discrete cavity springs can be based on Equation 4.15. Therefore, by substitution of the cavity spring term Q_{n_s} the equations of motion can be written as

$$\begin{aligned} D_1 k_n^4 \frac{l}{2} q_{1,n} - \omega^2 m_1'' \frac{l}{2} q_{1,n} + s_c' \sum_{j=1}^{J} \left(\sum_{n=1}^{N} \Phi_m(x_j)\Phi_n(x_j)(q_{1,n}(t) - q_{2,n}(t)) \right) &= Q_n \\ D_2 k_n^4 \frac{l}{2} q_{2,n} - \omega^2 m_2'' \frac{l}{2} q_{2,n} + s_c' \sum_{j=1}^{J} \left(\sum_{n=1}^{N} \Phi_m(x_j)\Phi_n(x_j)(q_{2,n}(t) - q_{1,n}(t)) \right) &= 0. \end{aligned} \tag{4.45}$$

where $Q_n = \frac{\hat{p}_1 l}{n\pi}(1 - \cos n\pi)$, see Equation 4.19.

Using the matrix formulation of Equation 4.18 and regarding the fluid loads (section 4.1.2), the host double panel partition with J discrete cavity

springs is described for all angles of sound incidence by

$$\left(-\omega^2\mathbf{M}+\mathbf{K}\right)\mathbf{q}=\mathbf{Q} \tag{4.46}$$

with the mass matrix $\mathbf{M}=\begin{bmatrix}\mathbf{M_1}-i\frac{\rho_0 c_0 l}{2\omega\cos\theta} & 0\\ 0 & \mathbf{M_2}-i\frac{\rho_0 c_0 l}{2\omega\cos\theta}\end{bmatrix}$

where the $N\times N$ diagonal matrix $\mathbf{M_i}=\frac{l}{2}\begin{bmatrix} m''_{i,1} & & 0\\ & m''_{i,n} & \\ 0 & & \ddots\end{bmatrix}$,

with the stiffness matrix $\mathbf{K}=\begin{bmatrix}\mathbf{K_1}+s'_c\mathbf{\Phi}\mathbf{\Phi}^\mathbf{T} & -s'_c\mathbf{\Phi}\mathbf{\Phi}^\mathbf{T}\\ -s'_c\mathbf{\Phi}\mathbf{\Phi}^\mathbf{T} & \mathbf{K_2}+s'_c\mathbf{\Phi}\mathbf{\Phi}^\mathbf{T}\end{bmatrix}$

where the $N\times N$ diagonal matrix $\mathbf{K_i}=\frac{l}{2}\begin{bmatrix} D_i k_1^4 & & 0\\ & D_i k_n^4 & \\ 0 & & \ddots\end{bmatrix}$,

and with the $N\times J$ mode shape matrix $\mathbf{\Phi}=\begin{bmatrix}\Phi_{11} & \Phi_{12} & \Phi_{1j}\\ \Phi_{21} & \Phi_{22} & \cdots\\ \Phi_{n1} & \vdots & \ddots\end{bmatrix}$.

The vectors $\mathbf{q}=\begin{pmatrix}\mathbf{q_1}\\ \mathbf{q_2}\end{pmatrix}$, $\mathbf{Q}=\begin{pmatrix}\mathbf{Q}_n\\ \mathbf{0}\end{pmatrix}$ include the N length vectors for the generalized amplitudes $\mathbf{q_1}$, $\mathbf{q_2}$ and for the generalized pressure force $\mathbf{Q}_n$.

For the n-th mode the modal pressure force Q_n is given by

$$Q_n=2\hat{p}_0\frac{l}{n\pi\left(1-\left(\frac{k_x}{k_n}\right)^2\right)}\left(1-(-1)^n e^{(-ik_x l)}\right),$$

see Equation 4.31.

4.1.4 Sound reduction index

For the beam model, the velocity v_2 of the radiating panel differs along the length of the beam. Particularly at low frequencies the radiation is controlled by the characteristic of the panel modes.

The incident sound power per unit width of a plane wave for an arbitrary angle of incidence is given by the component of incident intensity normal to the partition as

$$I_i(\theta) = \frac{1}{2\rho_0 c_0} |p_0|^2 \cos\theta. \tag{4.47}$$

For the beam model with the structure represented by beams of length l, this leads to the incident sound power

$$P_i(\theta) = \frac{|p_0|^2 l}{2\rho_0 c_0} \cos\theta. \tag{4.48}$$

For the flexible double panel structure of this project the radiated sound power is defined by the transverse velocity as

$$P_{rad} = \frac{\sigma \rho_0 c_0}{2} \int_0^l |v_2(x)|^2 \, \mathrm{dx} \tag{4.49}$$

where σ is the radiation efficiency.

Substitution of the transverse velocity by the generalized coordinate q_2 of the beam model yields for the incident angle θ

$$P_{rad}(\theta) = \frac{\sigma \rho_0 c_0}{2} \int_0^l |\omega \sum_{n=1}^{N} q_{2,n}(\theta) \Phi_n(x)|^2 \, \mathrm{dx}. \tag{4.50}$$

Solving the integral by the orthogonality condition (Equation 4.14) yields

$$P_{rad}(\theta) = \frac{\rho_0 c_0 \omega^2 l}{4} \sum_{n=1}^{N} |q_{2,n}(\theta)|^2 \sigma_n \tag{4.51}$$

Since the main interest of this study was given to low frequencies, the presented analytical solution ignored the cross-modal contributions.

The formulations of the modal radiation efficiencies σ_n of a beam in flexure were published by Wallace [73].

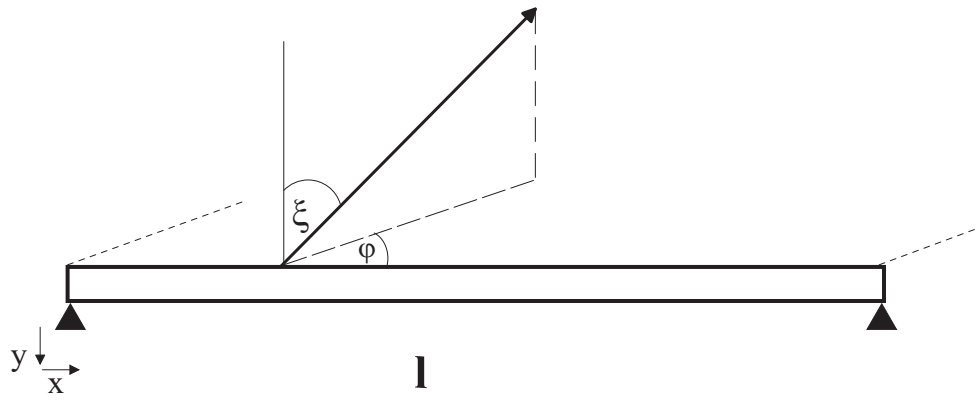

Figure 4.5: Sound radiation of a beam for radiation angles ξ and φ.

For a beam with length l the modal radiation efficiencies are given by

n = odd

$$\sigma_n = \frac{32k_0^2 l}{n^2\pi^4} \int_0^{\pi/2}\int_0^{\pi/2} \left[\frac{\cos\left(\frac{\alpha}{2}\right)\sin\left(\frac{\beta}{2}\right)}{\left(1-\left(\frac{\alpha}{n\pi}\right)^2\right)\beta}\right]^2 \sin\xi \mathrm{d}\xi \mathrm{d}\varphi \tag{4.52}$$

n = even

$$\sigma_n = \frac{32k_0^2 l}{n^2\pi^4} \int_0^{\pi/2}\int_0^{\pi/2} \left[\frac{\sin\left(\frac{\alpha}{2}\right)\sin\left(\frac{\beta}{2}\right)}{\left(1-\left(\frac{\alpha}{n\pi}\right)^2\right)\beta}\right]^2 \sin\xi \mathrm{d}\xi \mathrm{d}\varphi \tag{4.53}$$

where

$$\begin{aligned} \alpha &= k_0 l \sin\xi\cos\varphi \\ \beta &= k_0 sin\xi \sin\varphi. \end{aligned}$$

The sound reduction index is based on the sound transmission coefficient which is defined by ratio of the incident sound power to the radiated sound power, see subsection 3.1.2. Hence, the sound transmission coefficient for normal sound incidence is given by

$$\tau = \frac{\rho_0^2 c_0^2 \omega^2}{2|p_0^2|} \sum_{n=1}^{N} |q_{2,n}|^2 \sigma_n. \tag{4.54}$$

Accordingly, the sound transmission coefficient for oblique sound incidence with the incidence angle θ can be written as

$$\tau(\theta) = \frac{\rho_0^2 c_0^2 \omega^2}{2|p_0^2| cos\theta} \sum_{n=1}^{N} |q_{2,n}(\theta)|^2 \sigma_n. \tag{4.55}$$

Having derived the formulation for oblique sound incidence, the sound reduction index for an ideal diffuse incident sound field can be calculated by the diffuse sound transmission coefficient which is defined for a beam structure using the Paris formula [9] as follows

$$\tau_{diff} = \frac{\int_0^{\pi/2} \tau(\theta) \sin\theta \cos\theta \, \mathrm{d}\theta}{\int_0^{\pi/2} \sin\theta \cos\theta \, \mathrm{d}\theta} = 2 \int_0^{\pi/2} \tau(\theta) \cos\theta \sin\theta \, \mathrm{d}\theta. \tag{4.56}$$

For a double panel structure with length $l = 10\ m$ and continuous cavity spring Figure 4.6 shows the sound reduction index for normal sound incidence calculated by the beam model for $N = 1000$ modes. The double panel structure consists of two 1 mm steel panels with a mass per unit area of 7.8 kg/m^2. The air cavity is now and throughout the following study set to a more practical value of 20 mm. For this 20 mm air cavity the MAM-resonance appears at 215 Hz. Damping in the structure was assumed to be small. For the panels $\eta_p = 0.01$ and for the air cavity $\eta = 0.01$ were used as damping factors.

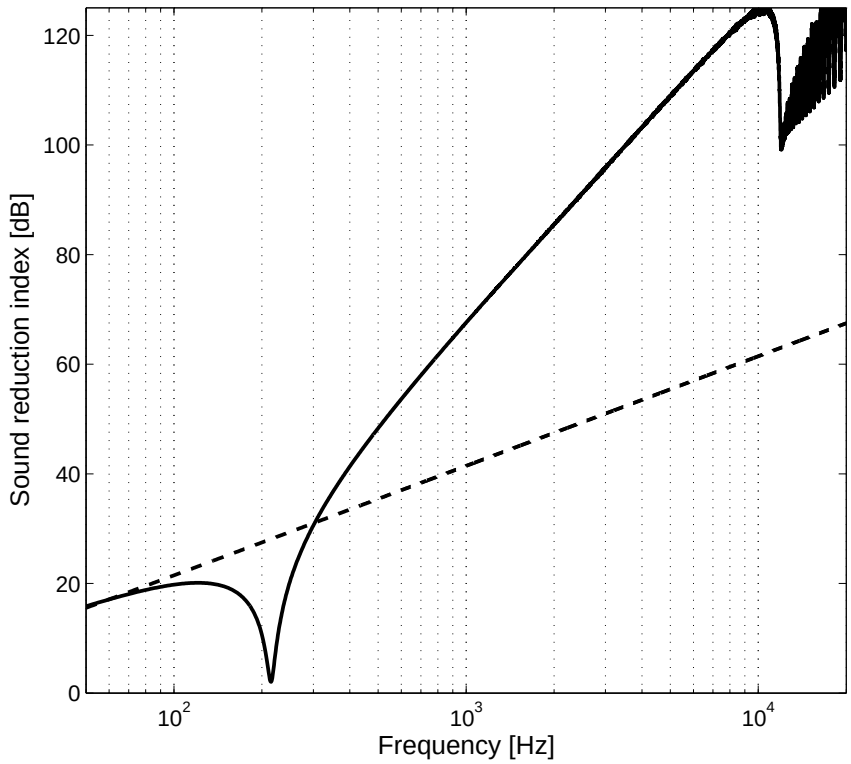

Figure 4.6: Sound reduction index of the host double panel partition with $l = 10\ m$ using the beam model for normal sound incidence. (- -) mass law; (—) beam model

Below the MAM-resonance the stiffness of the cavity spring causes the two panels to move as a single partition. Therefore, the sound reduction index follows the mass law with the total mass of the two panels. However, this is not true for small structures. At low frequencies short structures radiate less efficiently and have higher sound reduction. This is shown in Figure 4.7 using again 1000 modes for the beam model calculation. If the length is reduced to $l = 1\ m$, the sound reduction index of the double panel structure with two 1 mm steel panels reveals a different behaviour from the "mass law" below the MAM-resonance.

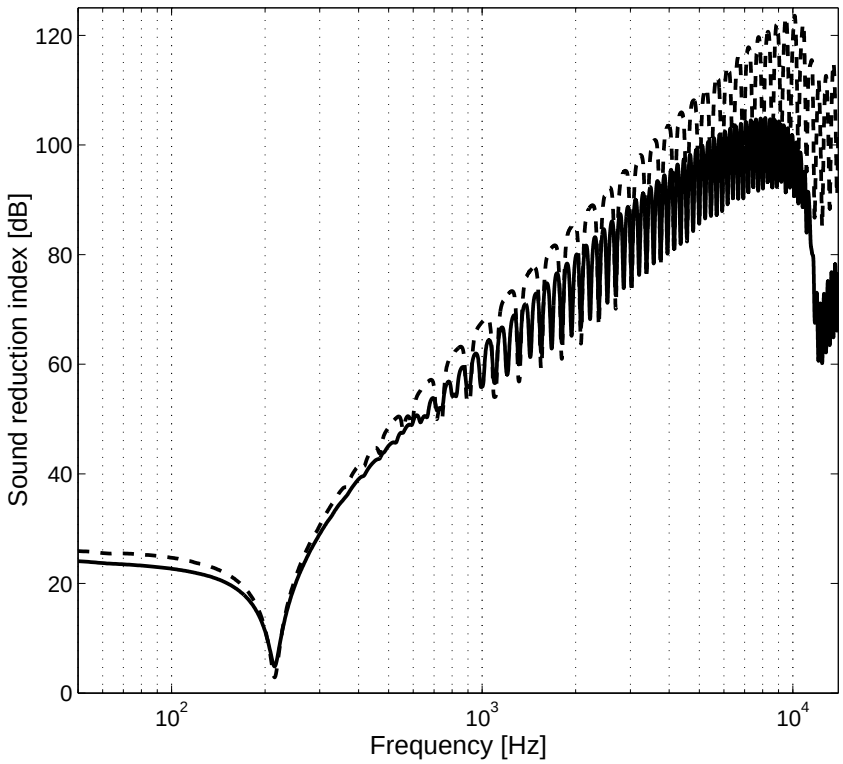

Figure 4.7: Sound reduction index of the host double panel partition with $l = 1\ m$ using the beam model. (- -) normal sound incidence; (—) diffuse sound incidence

Figure 4.7 shows a comparison of the sound reduction index for normal and diffuse sound incidence calculated by the beam model for the previous double panel structure with length $l = 1\ m$ and continuous cavity spring. It can be seen that with increasing frequency the sound reduction for diffuse field sound incidence is significantly lower than the sound reduction for normal sound incidence [18].

At the resonance frequencies of higher order modes, the sound reduction index is reduced below the dominating characteristic of the first fundamental mode which occurs at 2.5 Hz. Above 12000 Hz the critical frequen-

cy of the steel panels is evident. The obtained result for the diffuse sound reduction index presented in Figure 4.7 was considered as sufficient since it shows the main characteristic of the diffuse sound reduction.

In the following this project discusses the effect of internal vibration absorbers in relation to normal and diffuse field sound incidence using the beam model. The host partition was represented by the double panel structure with two 1 mm steel panels. Since the calculation of short structures requires considerably less modes, the presented results were calculated for the described host double panel partition with length $l = 1\ m$.

Host double panel partition

Incident steel panel m_1''	:	7.8 kg/m^2
Radiating steel panel m_2''	:	7.8 kg/m^2
Length l	:	1 m
Structural damping η_p	:	0.01
Air cavity	:	20 mm
MAM-resonance	:	215 Hz
Fundamental panel mode	:	2.5 Hz

4.2 One-sided vibration absorber

As for the previous mass-spring model, the beam model considers the internal vibration absorbers as classical mass-spring systems attached to the two beams. For the arrangement with one-sided vibration absorbers (section 3.2), the vibration absorbers are attached to the beams at individual positions. These positions can be chosen to be identical or different for both beams. For an incoming plane wave pressure load p_0 Figure 4.8 shows the host double panel partition with discrete one-sided vibration absorbers attached to the beams at opposite positions.

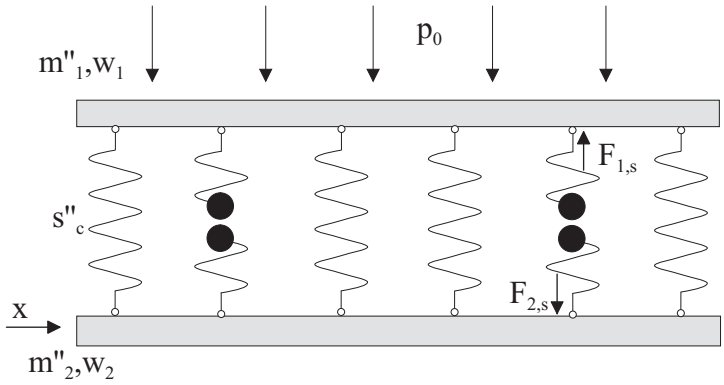

Figure 4.8: Double panel partition with continuous cavity spring and discrete one-sided vibration absorbers.

This project is aimed to apply the concept of internal vibration absorbers with least possible mass increase. Therefore, the following investigations analyse the efficiency of one-sided vibration absorbers by taking the number and positions of the internal absorber systems into account. With the beam model approach investigations on various distributions of attached vibration absorbers were intended. Nevertheless, in this section, vibration absorbers were first considered as a continuous system. In this case, the results obtained by the mass-spring model and the beam model should be identical. In the second step, the vibration absorbers were attached as discrete systems. The discrete absorbers were assumed to act in parallel to a continuous cavity spring.

4.2.1 Continuous vibration absorber

If the internal vibration absorbers are considered as a continuous system attached to either of the beams, for each beam the vibration absorber has constant properties.

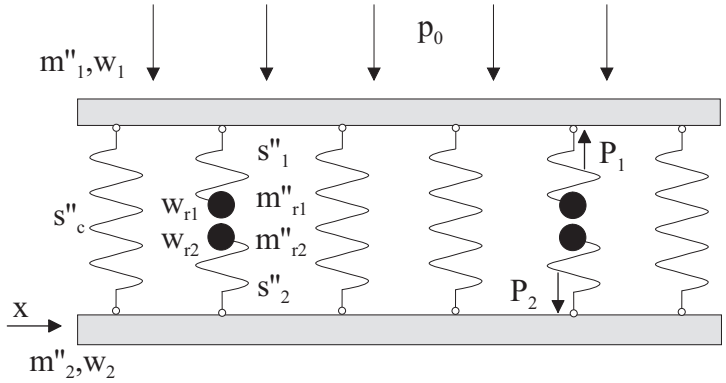

Figure 4.9: Beam model of a double panel partition with continuous cavity spring and continuous one-sided vibration absorber at incident plane wave pressure p_0.

With respect to the properties of the vibration absorber the angular resonance frequencies $\omega_{r1}^2 = \frac{s_1''}{m_{r1}''}$ and $\omega_{r2}^2 = \frac{s_2''}{m_{r2}''}$ are introduced.

The continuous one-sided vibration absorbers are implemented into the beam model by the additional pressure forces

$$\begin{aligned} P_1(x) &= s_1''(w_1(x) - w_{r1}(x)) &= \omega_{r1}^2 m_{r1}''(w_1(x) - w_{r1}(x)) \\ P_2(x) &= s_2''(w_2(x) - w_{r2}(x)) &= \omega_{r2}^2 m_{r2}''(w_2(x) - w_{r2}(x)). \end{aligned} \tag{4.57}$$

The absorber masses are moving with the transverse displacements w_{r1} and w_{r2}. Since an absorber mass is acting on the structure with the pressure force

$$P_r = -\omega^2 m_r'' w_r \tag{4.58}$$

the pressure forces of Equation 4.57 can be written by the angular resonance frequencies ω_{r1} and ω_{r2} as

$$\begin{aligned} P_1(x) &= \omega_{r1}^2 m_{r1}'' \frac{1}{1-\frac{\omega_{r1}^2}{\omega^2}} \\ P_2(x) &= \omega_{r2}^2 m_{r2}'' \frac{1}{1-\frac{\omega_{r2}^2}{\omega^2}}. \end{aligned} \tag{4.59}$$

These terms can therefore be added to the stiffness matrix.

Using generalized coordinates, the following analysis on the double panel partition with continuous internal vibration absorber is based on Equation 4.18. The double panel partition with continuous vibration absorber is described for the n-th mode by

$$\left(-\omega^2 \mathbf{M}_n + \mathbf{K}_n\right) \mathbf{q}_n = \mathbf{Q}_n. \tag{4.60}$$

In this case, the influence of vibration absorbers on the structure can be described by the stiffness matrix $\mathbf{K}_n$, which will not affect the mass matrix $\mathbf{M}_n$, the generalized amplitude vector $\mathbf{q}_n$ or the force vector $\mathbf{Q}_n$. Based on the matrix formulation of Equation 4.18 $\mathbf{M}_n$, $\mathbf{q}_n$ and $\mathbf{Q}_n$ were obtained for an arbitrary angle of incidence as follows

$$\mathbf{M}_n = \frac{l}{2} \begin{bmatrix} m_1'' - i\frac{\rho_0 c_0}{\omega \cos\theta} & 0 \\ 0 & m_2'' - i\frac{\rho_0 c_0}{\omega \cos\theta} \end{bmatrix}, \mathbf{q}_n = \begin{bmatrix} q_{1,n} \\ q_{2,n} \end{bmatrix}, \mathbf{Q}_n = \begin{bmatrix} Q_n \\ 0 \end{bmatrix}$$

in which

$$Q_n = 2\hat{p}_0 \frac{l}{n\pi \left(1 - \left(\frac{k_x}{k_n}\right)^2\right)} \left(1 - (-1)^n e^{(-ik_x l)}\right).$$

Accounting for the continuous vibration absorbers attached to either beam as shown in Figure 4.9, the stiffness matrix $\mathbf{K}_n$ in Equation 4.60 is given by

$$\mathbf{K}_n = \begin{bmatrix} D_1 k_n^4 \frac{l}{2} + s_c'' \frac{l}{2} + \frac{\omega_{r1}^2 m_{r1}''}{1-\frac{\omega_{r1}^2}{\omega^2}} & -s_c'' \frac{l}{2} \\ -s_c'' \frac{l}{2} & D_2 k_n^4 \frac{l}{2} + s_c'' \frac{l}{2} + \frac{\omega_{r2}^2 m_{r2}''}{1-\frac{\omega_{r2}^2}{\omega^2}} \end{bmatrix}.$$

Attached at both panels of the host double panel partition a continuous internal one-sided vibration absorber with the resonance frequency at 215 Hz leads to the sound reduction index as shown in Figure 4.10.

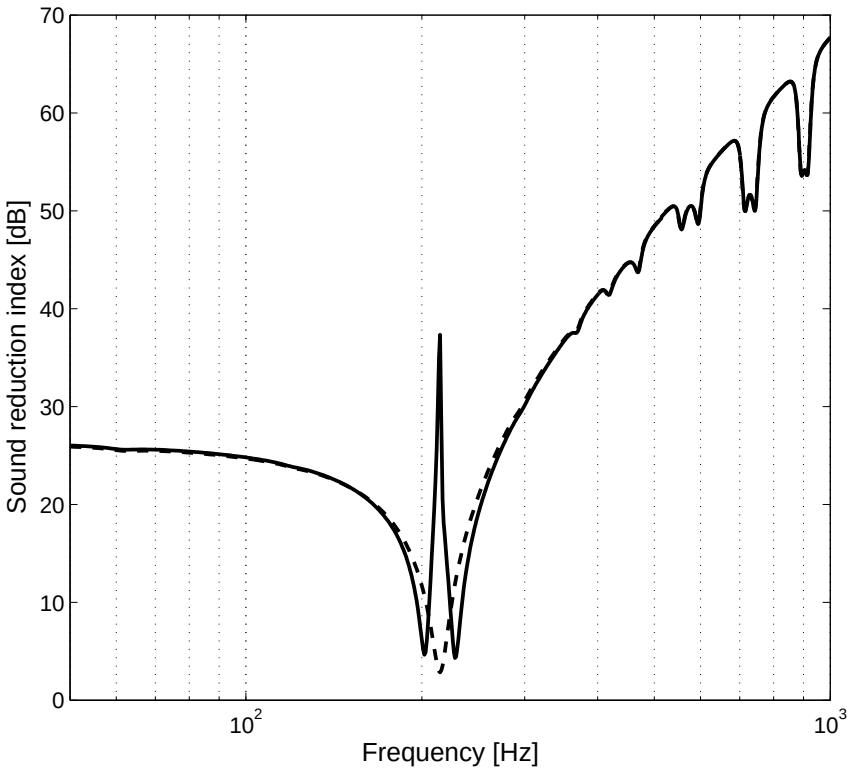

Figure 4.10: Sound reduction index of the host double panel partition with continuous one-sided vibration absorbers attached at both panels calculated by the beam model. (- -) without; (—) with absorber

The mass of one continuous one-sided vibration absorber per panel was $m_r = 0.5\,kg/\mathrm{m}^2$. Therefore, the total increase of the construction was $1\,kg/\mathrm{m}^2$ as in chapter 3. To the absorber springs a damping factor of η=0.01 was assigned.

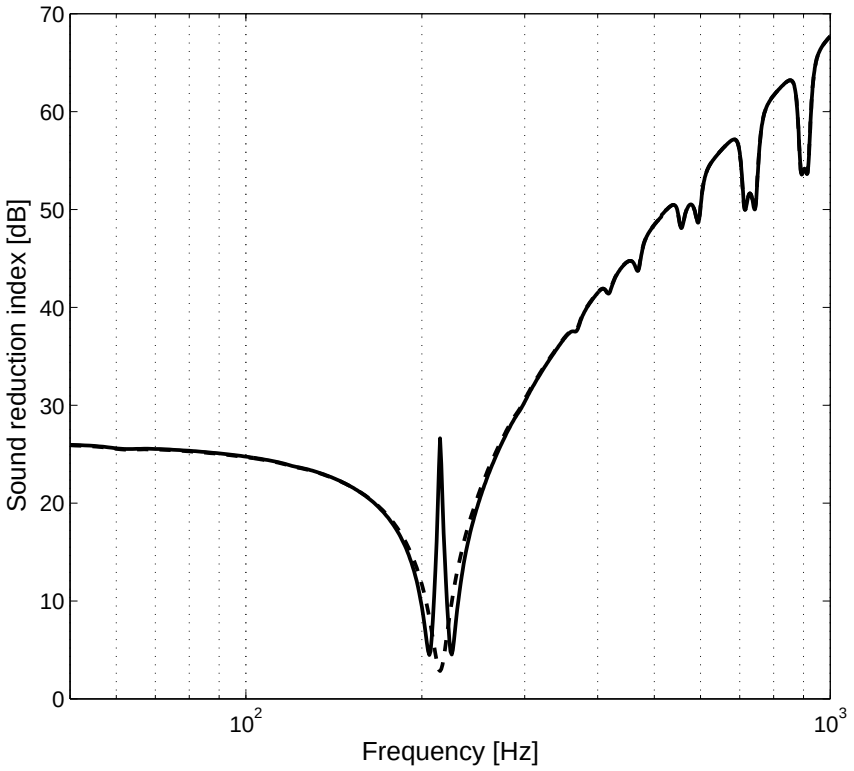

Figure 4.11: Sound reduction index of the host double panel partition with one continuous one-sided vibration absorber attached at one panel using the beam model. (- -) without; (—) with absorber

For one continuous one-sided vibration absorber with $m_r = 0.5\,kg/\mathrm{m}^2$ the sound transmission loss is shown in Figure 4.11. It can be seen, that for a single continuous one-sided vibration absorber a reduced absorber effect is obtained.

The same continuous one-sided vibration absorber fastened to either the incident or the radiating panel leads to an identical sound transmission loss of the construction.

4.2.2 Continuous cavity spring and discrete vibration absorbers

The idea of internal vibration absorbers is based on the principle of local resonances. A number of internal vibration absorbers are locally distributed within the cavity of the double panel partition. Thus, for a cavity filled with air or resilient material the additionally attached vibration absorbers are implemented into a continuous cavity spring at discrete positions. Therefore, a double panel partition with resilient cavity and locally distributed vibration absorbers can be described by the combination of the previous formulations for continuous and discrete cavity springs.

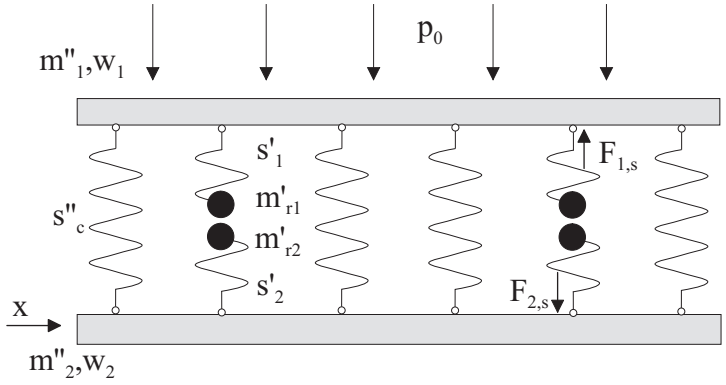

Figure 4.12: Beam model of a double panel partition with continuous cavity spring and discrete one-sided vibrations absorbers for an incoming plane wave pressure load.

For this purpose, the attached absorber systems are taken into account by their additional forces applied to the host structure as shown in Figure 4.12. If the matrix formulation for the classical double panel partition with continuous cavity spring (Equation 4.18) is extended by the additio-

nal terms for the discrete vibration absorbers, the double panel partition with continuous cavity spring and J locally distributed internal vibration absorbers is described using Equation 4.60 and the stiffness matrix as follows

$$\mathbf{K} = \begin{bmatrix} \mathbf{K_1} + \mathbf{S_c} + \frac{\omega_{r1}^2 m'_{r1}}{1-\frac{\omega_{r1}^2}{\omega^2}} \mathbf{\Phi}\mathbf{\Phi}^\mathbf{T} & -\mathbf{S_c} \\ -\mathbf{S_c} & \mathbf{K_2} + \mathbf{S_c} + \frac{\omega_{r2}^2 m'_{r2}}{1-\frac{\omega_{r2}^2}{\omega^2}} \mathbf{\Phi}\mathbf{\Phi}^\mathbf{T} \end{bmatrix},$$

with the $N \times N$ diagonal matrices

$$\mathbf{K_i} = \frac{l}{2} \begin{bmatrix} D_i k_1^4 & & 0 \\ & D_i k_n^4 & \\ 0 & & \ddots \end{bmatrix}, \mathbf{S_c} = \frac{l}{2} \begin{bmatrix} s_c'' & & 0 \\ & s_c'' & \\ 0 & & \ddots \end{bmatrix}$$

and with the $N \times J$ mode shape matrix $\mathbf{\Phi} = \begin{bmatrix} \Phi_{11} & \Phi_{12} & \Phi_{1j} \\ \Phi_{21} & \Phi_{22} & \cdots \\ \Phi_{n1} & \vdots & \ddots \end{bmatrix}$.

The terms for the discrete vibration absorbers are based on the analysis of Equation 4.46. Using the beam model, the following results present the sound reduction index of the host structure with attached one-sided vibration absorbers. The absorbers were designed with a constant damping factor η=0.01. If 9 absorbers with a resonance frequency at 215 Hz and a total mass of 0.5 kg/m are attached to one panel with an equal distribution, the sound reduction index of the host partition is obtained as shown in Figure 4.13.

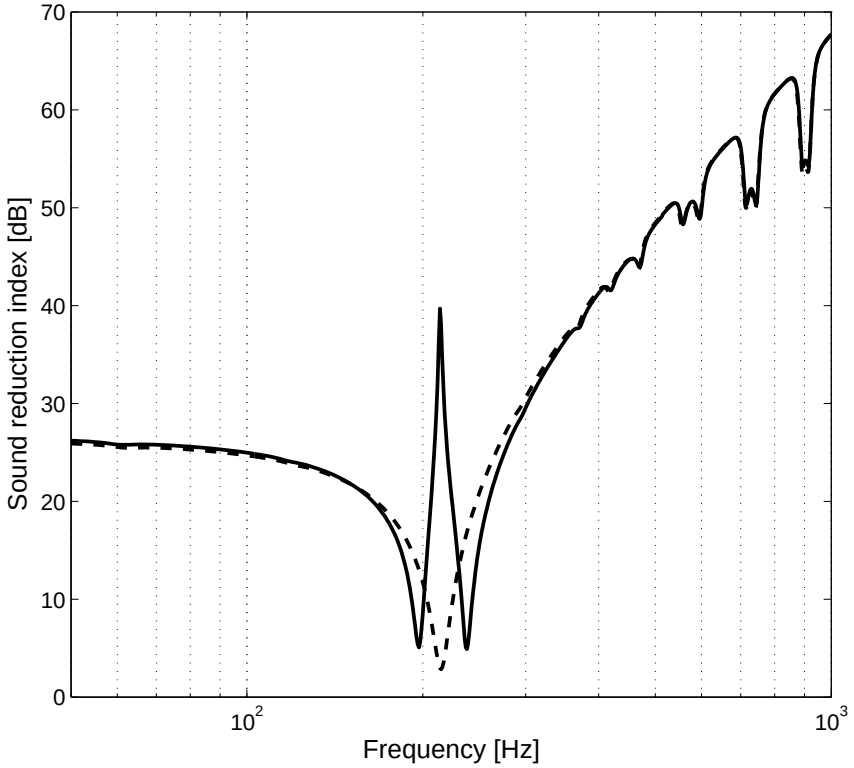

Figure 4.13: Sound reduction index of the double panel host partition with 9 one-sided vibration absorbers equally attached at one panel using the beam model for normal sound incidence. (- -) without; (—) with absorber

This result is identical for the absorbers attached to the incident or the radiating panel. For the number of 9 one-sided vibration absorbers per unit length, Figure 4.13 and Figure 4.10 show similar results.

Furthermore, one-sided vibration absorbers may be considered to have different tuning frequencies. For the resonance frequencies 200 Hz and 225 Hz the sound transmission loss was calculated for three general arrangements. For all three arrangements 18 internal absorbers with a total mass increase of 1 kg/m were implemented. First, 18 absorbers with the two different resonance frequencies were equally distributed at both pa-

nels. For the second and third arrangement at each panel only absorbers with equal resonance frequency were attached. Accordingly, 9 absorbers with the resonance frequency of 200 Hz were attached to the incident panel, 9 absorbers with the resonance frequency of 225 Hz were attached to the radiating panel and the other way around. All three configurations revealed the same sound reduction index as shown in Figure 4.14.

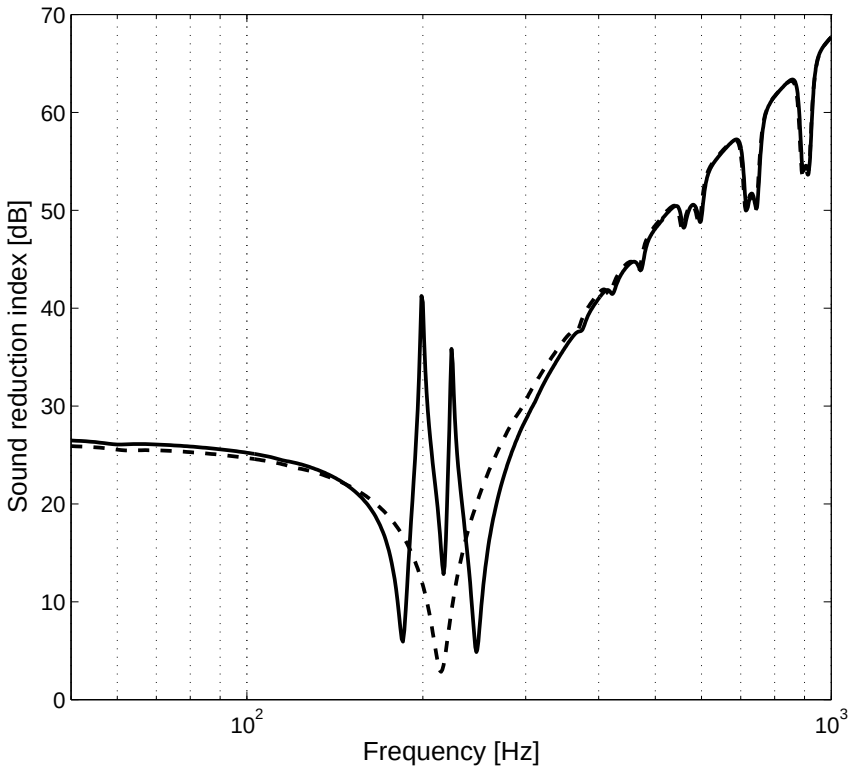

Figure 4.14: Sound reduction index of the host double panel partition with one-sided vibration absorbers with two resonance frequencies using the beam model for normal sound incidence. (- -) without; (—) with absorber

In conclusion, the implementation of internal vibration absorbers as one-sided absorber systems appears as a promising solution in order to increase the sound transmission loss of double panel partitions at low frequencies. Especially the possibility of various absorber distributions provide a

high degree of flexibility.

However, there are constructional issues to be taken into account when the double panel partition is assembled at the installation site. In particular, it seems to be rather difficult to ensure that the absorber systems are fastened exactly at the calculated positions on the panels. Furthermore, the intended resonance frequency of the internal vibration absorbers is highly dependent on a strong long term connection between the absorber spring and the structure. Therefore, the installation of the one-sided vibration absorbers is considered as a highly delicate issue and actually unpredictable.

For this reason, in this work the one-sided vibration absorber was not discussed in more detail. All the installation issues discussed above are not expected for the following internal two-sided vibration absorbers. The two-sided vibration absorber describes an innovative solution for multi-layer constructions without causing additional difficulties in installation. It can be easily implemented into the resilient cavity layer already at the factory. Thus, the position and resonance frequency of the internal vibration absorbers can be assured by an automated production process. By this means, for example the assembly of a partition at the installation site is not changed.

4.3 Two-sided vibration absorber

The double panel partition with two-sided vibration absorbers is characterized by the coupling forces connecting the absorber mass to the beam structures. Using the previous matrix formulation, the beam model considers these coupling forces by implementation into the stiffness matrix. Formulations were derived for both continuous and discrete internal two-sided vibration absorbers using the previous angular frequencies ω_{r1} and ω_{r2}, see section 4.2.

4.3.1 Continuous vibration absorber

Figure 4.15 shows the the host double panel partition with continuous cavity spring and continuous two-sided vibration absorbers for an incoming plane wave pressure load p_0.

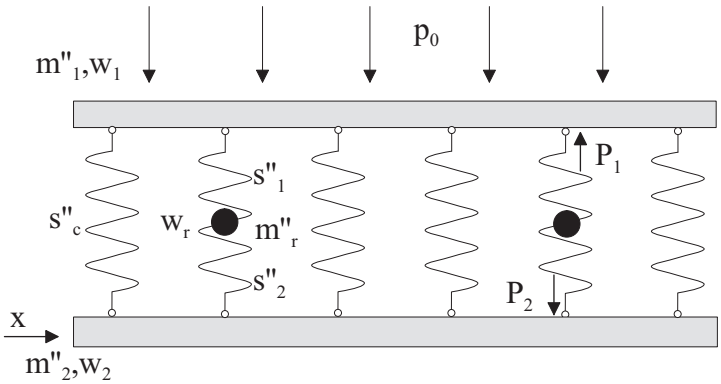

Figure 4.15: Beam model of a double panel partition with continuous cavity spring and continuous two-sided vibration absorber.

In the case of two-sided vibration absorbers, the absorber mass is connected to the beam structures by two springs. For a continuous absorber the coupling forces P_1 and P_2 are given by the spring stiffness of the two springs, the displacement of the beams and the motion of the absorber

mass w_r as follows

$$\begin{aligned} P_1 &= s_1'' \left(w_1(x) - w_r(x) \right) \\ P_2 &= s_2'' \left(w_r(x) - w_2(x) \right). \end{aligned} \tag{4.61}$$

The motion of the absorber mass w_r is related to the coupling forces by

$$P_1 - P_2 = -\omega^2 m_r'' w_r. \tag{4.62}$$

Thus, solving Equation 4.61 by substituting Equation 4.62 the motion of the absorber mass can be eliminated and the coupling forces are described solely by the displacements of the two beams.

$$\begin{aligned} P_1(x) &= R_1 w_1(x) - R_2 w_2(x) \\ P_2(x) &= R_2 w_1(x) - R_3 w_2(x). \end{aligned} \tag{4.63}$$

Using the angular frequencies ω_{r1} and ω_{r2}, the elimination of w_r yields the three coefficients

$$\begin{aligned} R_1 &= \frac{(\omega_{2_r}^2 - \omega^2) m_r''}{1 + \dfrac{\omega_{2_r}^2}{\omega_{1_r}^2} - \dfrac{\omega^2}{\omega_{1_r}^2}} \\ R_2 &= \frac{\omega_{2_r}^2 m_r''}{1 + \dfrac{\omega_{2_r}^2}{\omega_{1_r}^2} - \dfrac{\omega^2}{\omega_{1_r}^2}} \\ R_3 &= \frac{(\omega_{1_r}^2 - \omega^2) m_r''}{1 + \dfrac{\omega_{1_r}^2}{\omega_{2_r}^2} - \dfrac{\omega^2}{\omega_{2_r}^2}}. \end{aligned} \tag{4.64}$$

For the n-th mode, the double panel partition with continuous cavity spring and continuous two-sided vibration absorber is described by the matrix formulation of Equation 4.60 after substituting the following stiffness matrix.

$$\mathbf{K}_n = \begin{bmatrix} D_1 k_n^4 \frac{l}{2} + s_c'' \frac{l}{2} + R_1 & -s_c'' \frac{l}{2} - R_2 \\ -s_c'' \frac{l}{2} - R_2 & D_2 k_n^4 \frac{l}{2} + s_c'' \frac{l}{2} + R_3 \end{bmatrix}. \tag{4.65}$$

The terms for the continuous two-sided vibration absorbers are implemented into the stiffness matrix.

4.3.2 Continuous cavity spring and discrete vibration absorbers [74, 75]

The double panel partition with continuous cavity spring and two-sided vibration absorbers attached at discrete positions is shown in Figure 4.16

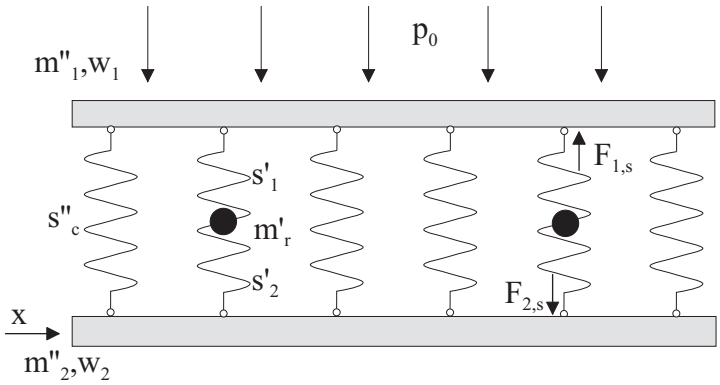

Figure 4.16: Beam model of a double panel partition with continuous cavity spring and discrete two-sided vibration absorbers.

If the vibration absorbers are attached at discrete positions, the locally acting coupling forces of the beam model are again described by three coef-

ficients

$$R_1 = \frac{(\omega_{2_r}^2 - \omega^2)m_r'}{1 + \frac{\omega_{2_r}^2}{\omega_{1_r}^2} - \frac{\omega^2}{\omega_{1_r}^2}}$$
$$R_2 = \frac{\omega_{2_r}^2 m_r'}{1 + \frac{\omega_{2_r}^2}{\omega_{1_r}^2} - \frac{\omega^2}{\omega_{1_r}^2}}$$
$$R_3 = \frac{(\omega_{1_r}^2 - \omega^2)m_r'}{1 + \frac{\omega_{1_r}^2}{\omega_{2_r}^2} - \frac{\omega^2}{\omega_{2_r}^2}}. \tag{4.66}$$

The comprehensive analysis on the double panel host structure and various configurations of internal vibration absorbers above, revealed fundamental matrix formulations for the beam model. The analytical integration of the vibration absorbers was achieved by the corresponding modifications of the stiffness matrix. By this means, based on Equation 4.46 the double panel partition with J discrete two-sided vibration absorbers is described by

$$\left(-\omega^2\mathbf{M} + \mathbf{K}\right)\mathbf{q} = \mathbf{Q} \tag{4.67}$$

where the stiffness matrix is given by

$$\mathbf{K} = \begin{bmatrix} \mathbf{K_1} + \mathbf{S_c} + R_1\mathbf{\Phi}\mathbf{\Phi}^\mathbf{T} & -\mathbf{S_c} - R_2\mathbf{\Phi}\mathbf{\Phi}^\mathbf{T} \\ -\mathbf{S_c} - R_2\mathbf{\Phi}\mathbf{\Phi}^\mathbf{T} & \mathbf{K_2} + \mathbf{S_c} + R_3\mathbf{\Phi}\mathbf{\Phi}^\mathbf{T} \end{bmatrix},$$

with the $N \times N$ diagonal matrices

$$\mathbf{K_i} = \frac{l}{2}\begin{bmatrix} D_i k_1^4 & & 0 \\ & D_i k_n^4 & \\ 0 & & \ddots \end{bmatrix}, \mathbf{S_c} = \frac{l}{2}\begin{bmatrix} s_c'' & & 0 \\ & s_c'' & \\ 0 & & \ddots \end{bmatrix}$$

and with the $N \times J$ mode shape matrix $\mathbf{\Phi} = \begin{bmatrix} \Phi_{11} & \Phi_{12} & \Phi_{1j} \\ \Phi_{21} & \Phi_{22} & \cdots \\ \Phi_{n1} & \vdots & \ddots \end{bmatrix}$.

The mass matrix and vectors are known as

$$\mathbf{M} = \begin{bmatrix} \mathbf{M_1} - i\frac{\rho_0 c_0 l}{2\omega \cos\theta} & 0 \\ 0 & \mathbf{M_2} - i\frac{\rho_0 c_0 l}{2\omega \cos\theta} \end{bmatrix} \text{ with } \mathbf{M_i} = \frac{l}{2} \begin{bmatrix} m''_{i,1} & & 0 \\ & m''_{i,n} & \\ 0 & & \ddots \end{bmatrix},$$

and $\mathbf{q} = \begin{pmatrix} \mathbf{q_1} \\ \mathbf{q_2} \end{pmatrix}$, $\mathbf{Q} = \begin{pmatrix} \mathbf{Q}_n \\ \mathbf{0} \end{pmatrix}$ which include the vectors of length N for the generalized amplitudes $\mathbf{q_1}$, $\mathbf{q_2}$ and the generalized pressure force vector $\mathbf{Q}_n$, see Equation 4.46.

4.3.3 Discrete cavity spring and discrete vibration absorbers

Advanced investigations on discrete two-sided internal vibration absorbers may concentrate on the total area occupied by the absorbers. Local resilient layers can be used as absorber springs. Thus, across the panel area the cavity of the double panel structure is divided into sections for the cross section of the implemented two-sided vibration absorbers (”Absorber Footprint”) and sections where the two panels are simply connected by the cavity spring. More understanding of the area used for the internal vibration absorbers and its influence on the absorber effect is expected by the analysis of the spatial ratio of the areas with attached discrete vibration absorbers to the areas with discrete cavity springs. For this purpose the beam model of Equation 4.67 is extended for the double panel partition with I discrete cavity springs and J discrete two-sided vibration absorbers using the stiffness matrix as follows

$$\mathbf{K} = \begin{bmatrix} \mathbf{K_1} + s_c'\mathbf{\Psi}\mathbf{\Psi}^\mathbf{T} + R_1\mathbf{\Phi}\mathbf{\Phi}^\mathbf{T} & -s_c'\mathbf{\Psi}\mathbf{\Psi}^\mathbf{T} - R_2\mathbf{\Phi}\mathbf{\Phi}^\mathbf{T} \\ -s_c'\mathbf{\Psi}\mathbf{\Psi}^\mathbf{T} - R_2\mathbf{\Phi}\mathbf{\Phi}^\mathbf{T} & \mathbf{K_2} + s_c'\mathbf{\Psi}\mathbf{\Psi}^\mathbf{T} + R_3\mathbf{\Phi}\mathbf{\Phi}^\mathbf{T} \end{bmatrix},$$

with the $N \times N$ diagonal matrix

$$\mathbf{K_i} = \frac{l}{2} \begin{bmatrix} D_i k_1^4 & & 0 \\ & D_i k_n^4 & \\ 0 & & \ddots \end{bmatrix},$$

with the $N \times I$ mode shape matrix $\mathbf{\Psi} = \begin{bmatrix} \Phi_{11} & \Phi_{12} & \Phi_{1i} \\ \Phi_{21} & \Phi_{22} & \cdots \\ \Phi_{n1} & \vdots & \ddots \end{bmatrix}$,

and with the $N \times J$ mode shape matrix $\mathbf{\Phi} = \begin{bmatrix} \Phi_{11} & \Phi_{12} & \Phi_{1j} \\ \Phi_{21} & \Phi_{22} & \cdots \\ \Phi_{n1} & \vdots & \ddots \end{bmatrix}$.

Using the formulations of the beam model, results for the sound transmission loss of the double panel host structure with two-sided internal vibration absorbers are presented in the parameter study in chapter 6.

Chapter 5

Plate model

In order to investigate the sound transmission characteristic of double panel partitions with internal vibration absorbers more precisely, the previous beam model is extended to a two-dimensional plate model. By this means the number and position of internal vibration absorbers are investigated on finite double panel constructions in two dimensions.

The model consists of two elastic plates with a resilient cavity layer in between. The finite plates and cavity layer are considered as a coupled mechanical acoustical system. As for the beam model, the classical thin plate theory, the acoustic wave equations and the simply supported boundary conditions were used. The main input variables for the model are the properties of the constituent single panels, the distance between the panels and the properties of the cavity spring. The model considers no interpanel connections between the plates of the double panel partition.

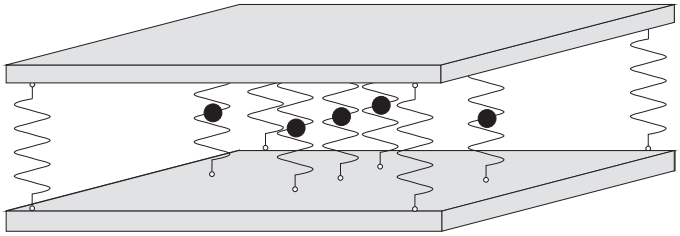

Figure 5.1: Two-dimensional illustration of a double panel partition with internal vibration absorbers.

Since the beam model and the plate model were both derived by using the modal expansion method (section 4.1), in the following the analysis of the plate model is described in less detail.

The plate model formulations for the internal one-sided vibration absorber are presented in the Appendix.

5.1 Host double panel partition

The host double panel partition consists of two simply supported plates of length a, width b and uniform thickness h. For harmonic motion with time dependence $e^{i\omega t}$ the transverse displacement of a plate can be written as

$$w(x, y, t) = \hat{w} e^{i\omega t}. \tag{5.1}$$

For a single plate with pressure load p, Kirchhoff's theory for thin plates (Equation 4.1) gives the equation of motion as

$$D\nabla^4 w(x, y) - \omega^2 m'' w(x, y) = p(x, y) \tag{5.2}$$

where D is the complex plate bending stiffness, Equation 4.2.

Using the modal expansion method, the flexural displacement of a single

plate is given by

$$w(x,y) = \sum_{n=1}^{\infty} \sum_{m=1}^{\infty} q_{nm} \Phi_{nm}(x,y). \tag{5.3}$$

The mode shape function Φ_{nm} for a simply supported single plate is written as

$$\Phi_{nm}(x,y) = \sin \frac{n\pi}{a} x \sin \frac{m\pi}{b} y. \tag{5.4}$$

Therefore, substitution of $w(x,y)$ and $\Phi_{nm}(x,y)$ into Equation 5.2 and solving the partial differentiation

$$\nabla^4 = \frac{\partial^4}{\partial x^4} + \frac{2\partial^4}{\partial x^2 \partial y^2} + \frac{\partial^4}{\partial y^4} \tag{5.5}$$

leads to the modal wave number for the single panels of the host structure

$$k_{nm}^2 = \left(\frac{n\pi}{a}\right)^2 + \left(\frac{m\pi}{b}\right)^2, \tag{5.6}$$

see also Equation 4.11.

Since the plate model is based on the modal expansion method, depending on the maximum frequency ω_{max}, a certain number of modes need to be considered in order to achieve a sufficient estimation of the structural response of the host double panel structure. This number of modes involves the generated combinations of the mode counters along the x-direction and the y-direction of the panels. Dependent on the dimensions of the panels the mode numbers N and M represent the highest mode generated along the x and y-direction. The total number of panel mode combinations generated below ω_{max} is obtained for a panel with the area A by [72]

$$\frac{k_b^2 A}{4\pi} \tag{5.7}$$

where the bending wave number of a plate is given by $k_b = \sqrt[4]{\frac{\omega_{max}^2 m''}{B}}$.

5.1.1 Continuous cavity spring

Figure 5.2 shows the double panel host structure with a continuous cavity spring and an incident pressure p_1.

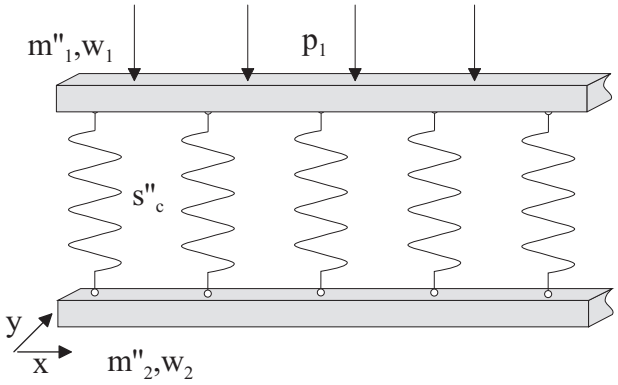

Figure 5.2: Plate model of a double panel partition.

If across the panel the incident pressure load is a constant pressure $\hat{p}_1$, the equations of motion of the host double panel partition is obtained from the plate model as follows

$$\begin{aligned} D_1\nabla^4 w_1(x,y) - \omega^2\rho_1 h_1 w_1(x,y) + s_c''(w_1(x,y) - w_2(x,y)) &= \hat{p}_1 \\ D_2\nabla^4 w_2(x,y) - \omega^2\rho_2 h_2 w_2(x,y) + s_c''(w_2(x,y) - w_1(x,y)) &= 0. \end{aligned} \tag{5.8}$$

Thus, the modal formulation for the equations of motion can be written as

$$\begin{aligned} &D_1 \sum_{n=1}^{N}\sum_{m=1}^{M} k_{nm}^4 q_{1,nm}\Phi_{nm}(x,y) - \omega^2 m_1'' \sum_{n=1}^{N}\sum_{m=1}^{M} q_{1,nm}\Phi_{nm}(x,y) \\ &\quad + s_c''\left(\sum_{n=1}^{N}\sum_{m=1}^{M} q_{1,nm}\Phi_{nm}(x,y) - \sum_{n=1}^{N}\sum_{m=1}^{M} q_{2,nm}\Phi_{nm}(x,y)\right) = \hat{p}_1 \\ &D_2 \sum_{n=1}^{N}\sum_{m=1}^{M} k_{nm}^4 q_{2,nm}\Phi_{nm}(x,y) - \omega^2 m_2'' \sum_{n=1}^{N}\sum_{m=1}^{M} q_{2,nm}\Phi_{nm}(x,y) \\ &\quad + s_c''\left(\sum_{n=1}^{N}\sum_{m=1}^{M} q_{2,nm}\Phi_{nm}(x,y) - \sum_{n=1}^{N}\sum_{m=1}^{M} q_{1,nm}\Phi_{nm}(x,y)\right) = 0. \end{aligned} \tag{5.9}$$

Multiplying by $\Phi_{rq}(x,y) = \sin\frac{r\pi}{a}x \sin\frac{q\pi}{b}y$, integrating over the surface area A and using the following orthogonality condition

$$\int_0^a \int_0^b \Phi_{nm}(x,y)\Phi_{rq}(x,y)\,\mathrm{dxdy} = \left\{ \begin{array}{cccc} 0 & n \neq r & \text{or} & m \neq q \\ \frac{A}{4} & n = r & \text{and} & m = q \end{array} \right\} \tag{5.10}$$

leads to the matrix formulation for the double panel structure with continuous spring. Thus, the matrix formulation for the host double panel partition is obtained by the plate model as

$$\left(-\omega^2 \mathbf{M}_{nm} + \mathbf{K}_{nm}\right) \mathbf{q}_{nm} = \mathbf{Q}_{nm} \tag{5.11}$$

where the mass matrix $\mathbf{M}_{nm}$ and the stiffness matrix $\mathbf{K}_{nm}$ are given by

$$\mathbf{M}_{nm} = \frac{A}{4}\begin{bmatrix} m_1'' & 0 \\ 0 & m_2'' \end{bmatrix}, \mathbf{K}_{nm} = \frac{A}{4}\begin{bmatrix} D_1 k_{nm}^4 + s_c'' & -s_c'' \\ -s_c'' & D_2 k_{nm}^4 + s_c'' \end{bmatrix}$$

and the generalized amplitude vector $\mathbf{q}_{nm}$ and force vector $\mathbf{Q}_{nm}$ are

$$\mathbf{q}_{nm} = \begin{bmatrix} q_{1,nm} \\ q_{2,nm} \end{bmatrix}, \mathbf{Q}_{nm} = \begin{bmatrix} Q_{nm} \\ 0 \end{bmatrix}.$$

For the constant pressure load $\hat{p}_1$ the generalized force can be written as

$$Q_{nm} = \int_0^a \int_0^b \hat{p}_1 \Phi_{nm}(x,y)\,\mathrm{dxdy} = \frac{\hat{p}_1 A}{nm\pi^2}(1-\cos n\pi)(1-\cos m\pi). \tag{5.12}$$

In the case that both n and m are odd numbers the solution of the integral can be simplified to

$$Q_{nm} = \frac{4\hat{p}_1 A}{nm\pi^2}. \tag{5.13}$$

Otherwise the generalized pressure force Q_{nm} is zero.

5.1.2 Fluid loads

If the fluid loads at both sides of the partition are taken into account, for an normally incident plane wave pressure load p_0 with constant amplitude $\hat{p}_0$ across the panel the mass matrix $\mathbf{M}_{nm}$ and the generalized force vector $\mathbf{Q}_{nm}$ in Equation 5.11 have to be modified using the results of section 3.1.1. Thus, assuming for normal sound incidence the radiation efficiency $\sigma = 1$ leads for the mass matrix $\mathbf{M}_{nm}$ and the generalized force vector $\mathbf{Q}_{nm}$ to (see Equation 3.11)

$$\mathbf{M}_{nm} = \frac{A}{4}\begin{bmatrix} m_1'' - i\frac{\rho_0 c_0}{\omega} & 0 \\ 0 & m_2'' - i\frac{\rho_0 c_0}{\omega} \end{bmatrix} \qquad \mathbf{Q}_{nm} = \begin{bmatrix} \frac{8\hat{p}_0 A}{nm\pi^2} \\ 0 \end{bmatrix}. \tag{5.14}$$

For oblique sound incidence the pressure field incident at the surface of the partition is given by

$$p(x,y) = \hat{p}_0 e^{i(-k_x x - k_y y)}. \tag{5.15}$$

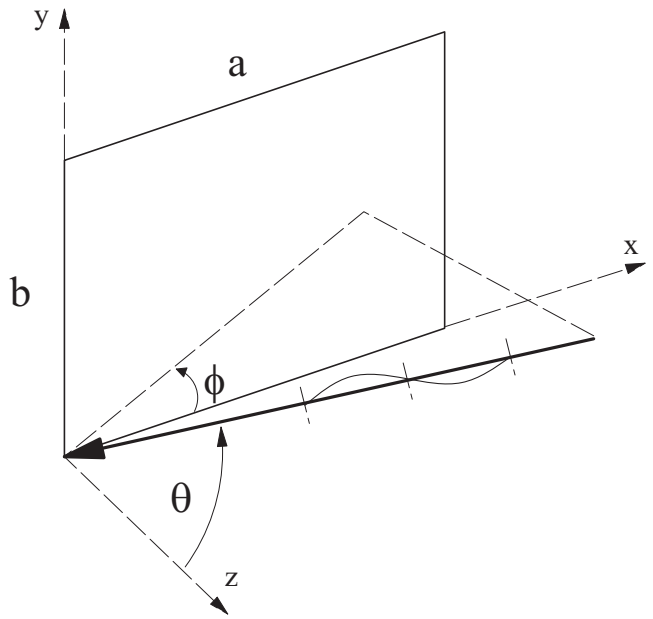

Figure 5.3: Sound field impinging on the plate.

For the two-dimensional plate model, the sound incidence is defined by the two angles θ and ϕ as illustrated in Figure 5.3. With $k_p = k_0 \sin\theta$ being the wave number of the wavefront convecting over the plate at the direction ϕ, the trace wave numbers in x and y direction are $k_x = k_p \cos\phi$ and $k_y = k_p \sin\phi$.

Above, the modal expansion method was applied by multiplying with $\Phi_{rq}(x,y)$, integrating over the surface area A and using the orthogonality condition (Equation 5.10). Thus, the generalized pressure force at oblique sound incidence is given by

$$Q_{nm} = 2 \int_0^a \int_0^b \hat{p}_0 e^{i(-k_x x - k_y y)} \Phi_{nm}(x,y)\, \mathrm{dxdy}. \tag{5.16}$$

Using Equation 4.29 the solution of the integral yields

$$Q_{nm} = 2\hat{p}_0 A j_x j_y \tag{5.17}$$

where

$$\begin{aligned} j_x(n,k_n,k_x) &= \frac{1}{n\pi\left(1-\left(\frac{k_x}{k_n}\right)^2\right)}\left(1-(-1)^n e^{\left(-in\pi\frac{k_x}{k_n}\right)}\right) \\ j_y(m,k_m,k_y) &= \frac{1}{m\pi\left(1-\left(\frac{k_y}{k_m}\right)^2\right)}\left(1-(-1)^n e^{\left(-im\pi\frac{k_y}{k_m}\right)}\right) \end{aligned}$$

which is valid for $k_x \neq k_n$ and $k_y \neq k_n$. For more information about this critical condition see section 4.1.2.

Concerning the fluid loads at both sides of the partition, the double panel partition with continuous cavity spring and plane wave pressure load at oblique incidence is described by the substitution of the generalized pressure force Q_{nm} (Equation 5.17) and the following mass matrix M_{nm} into

Equation 5.11.

$$\mathbf{M}_{nm} = \frac{A}{4}\begin{bmatrix} m_1'' - i\frac{\rho_0 c_0}{\omega\cos\theta} & 0 \\ 0 & m_2'' - i\frac{\rho_0 c_0}{\omega\cos\theta} \end{bmatrix} \tag{5.18}$$

5.1.3 Discrete cavity springs

For a normally incident sound pressure load p_0, Figure 5.4 illustrates the input parameters for the plate model when the cavity spring consists of equally distributed discrete cavity springs.

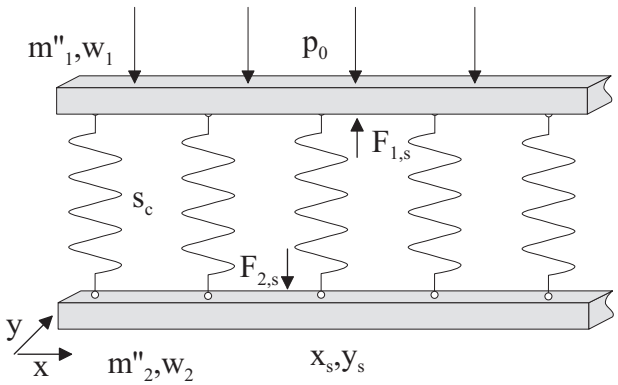

Figure 5.4: Plate model of a double panel partition with discrete cavity springs at incident plane wave pressure.

The harmonic point force at position x_s, y_s is described by

$$F(x_s, y_s, t) = \hat{F}e^{i\omega t}\delta(x - x_s)\delta(y - y_s). \tag{5.19}$$

With reference to the analysis in section 4.1.3, the generalized force Q_{nm} corresponding to the point force $F(x_s, y_s, t)$ is obtained as

$$Q_{nm}(t) = \int_0^a \int_0^b F(x_s, y_s, t)\Phi_{rq}(x, y)\,\mathrm{dxdy} = \hat{F}e^{i\omega t}\Phi_{rq}(x_s, y_s) \tag{5.20}$$

with the mode shape function $\Phi_{rq}(x,y) = \sin\frac{r\pi}{a}x \sin\frac{q\pi}{b}y$.

Thus, the generalized coupling force acting on the panels of the double panel partition is given by

$$Q_{nm,s}(t) = s_c(w_1(x_s,y_s) - w_2(x_s,y_s))e^{i\omega t}\Phi_{rq}(x_s,y_s). \tag{5.21}$$

By substitution of the transverse displacement

$$w(x_s,y_s,t) = \sum_{n=1}^{N}\sum_{m=1}^{M} q_{nm}(t)\Phi_{nm}(x_s,y_s) \tag{5.22}$$

the analysis of the modal expansion method yields the generalized coupling force

$$Q_{nm,s} = s_c\left(\sum_{n=1}^{N}\sum_{m=1}^{M}\Phi_{nm}(x_s,y_s)\Phi_{rq}(x_s,y_s)(q_{1,nm} - q_{2,nm})\right). \tag{5.23}$$

For J springs distributed throughout the panels, the generalized force Q_{nm} is obtained as

$$Q_{nm}(t) = \sum_{j=1}^{J}\hat{F}_j e^{i\omega t}\Phi_{rq}(x_j,y_j) \tag{5.24}$$

which yields for the generalized coupling force

$$Q_{nm,s} = s_c\sum_{j=1}^{J}\left(\sum_{n=1}^{N}\sum_{m=1}^{M}\Phi_{nm}(x_j,y_j)\Phi_{rq}(x_j,y_j)(q_{1,nm} - q_{2,nm})\right). \tag{5.25}$$

The host double panel partition with J discrete cavity springs at positions x_j, y_j is described for all angles of incidence by the matrix formulation as

$$\left(-\omega^2\mathbf{M} + \mathbf{K}\right)\mathbf{q} = \mathbf{Q} \tag{5.26}$$

with the mass matrix $\mathbf{M} = \begin{bmatrix} \mathbf{M_1} - i\frac{\rho_0 c_0 A}{4\omega\cos\theta} & 0 \\ 0 & \mathbf{M_2} - i\frac{\rho_0 c_0 A}{4\omega\cos\theta} \end{bmatrix}$

where the diagonal matrix $\mathbf{M_i} = \frac{A}{4}\begin{bmatrix} m''_{i,nm} & 0 \\ 0 & \ddots \end{bmatrix}$,

with the stiffness matrix $\mathbf{K} = \begin{bmatrix} \mathbf{K_1} + s_c\mathbf{\Phi}\mathbf{\Phi}^\mathbf{T} & -s_c\mathbf{\Phi}\mathbf{\Phi}^\mathbf{T} \\ -s_c\mathbf{\Phi}\mathbf{\Phi}^\mathbf{T} & \mathbf{K_2} + s_c\mathbf{\Phi}\mathbf{\Phi}^\mathbf{T} \end{bmatrix}$

where the diagonal matrix $\mathbf{K_i} = \frac{A}{4}\begin{bmatrix} D_i k_{nm}^4 & 0 \\ 0 & \ddots \end{bmatrix}$,

and with the mode shape matrix $\mathbf{\Phi} = \begin{bmatrix} \Phi_{nm,j} & \cdots \\ \vdots & \ddots \end{bmatrix}$.

The vector $\mathbf{q} = \begin{pmatrix} \mathbf{q_1} \\ \mathbf{q_2} \end{pmatrix}$ includes the vectors for the generalized amplitudes $\mathbf{q_i} = \begin{pmatrix} q_{i,nm} \\ \vdots \end{pmatrix}$, and the vector $\mathbf{Q} = \begin{pmatrix} \mathbf{Q}_{nm} \\ \mathbf{0} \end{pmatrix}$ consists of the generalized pressure force $\mathbf{Q}_{nm} = \begin{pmatrix} Q_{nm} \\ \vdots \end{pmatrix}$, with Q_{nm} given by Equation 5.17.

For normal sound incidence, the generalized pressure force is written as in Equation 5.14.

5.1.4 Sound reduction index

For the plate model, the incident power of a plane wave pressure at arbitrary angle of incidence θ is given by

$$P_i(\theta) = \frac{|p_0|^2 A}{2\rho_0 c_0} \cos\theta. \tag{5.27}$$

The radiated sound power of the double panel partition described by the generalized coordinate q_2 can be written as

$$P_{rad}(\theta) = \frac{\sigma \rho_0 c_0}{2} \int_0^a \int_0^b |\omega \sum_{n=1}^{N} \sum_{m=1}^{M} q_{2,nm}(\theta) \Phi_{nm}(x,y)|^2 \, \mathrm{dxdy}. \tag{5.28}$$

Using the orthogonality condition (Equation 5.10) yields

$$P_{rad}(\theta) = \frac{\rho_0 c_0 \omega^2 A}{8} \sum_{n=1}^{N} \sum_{m=1}^{M} |q_{2,nm}(\theta)|^2 \sigma_{nm}. \tag{5.29}$$

The sound power radiation efficiency σ_{nm} for each mode of the panels is described by an integral formulation provided by Wallace [76], see also Figure 4.5.

$$\sigma_{nm} = \frac{64 k_0^2 ab}{n^2 m^2 \pi^6} \int_0^{\pi/2} \int_0^{\pi/2} \left[\frac{\begin{matrix}\cos \\ \sin\end{matrix}\left(\frac{\alpha}{2}\right) \begin{matrix}\cos \\ \sin\end{matrix}\left(\frac{\beta}{2}\right)}{\left(\left(\frac{\alpha}{m\pi}\right)^2 - 1\right)\left(\left(\frac{\beta}{n\pi}\right)^2 - 1\right)} \right]^2 \sin\xi \mathrm{d}\xi \mathrm{d}\varphi \tag{5.30}$$

The $\cos(\alpha/2)$ function is used when m is an odd integer and the $\sin(\alpha/2)$ is used when m is an even integer. Similarly the $\cos(\beta/2)$ function is used when n is an odd integer and the $\sin(\beta/2)$ when n is an even integer. The variables α and β in Equation 5.30 are written as

$$\begin{aligned} \alpha &= k_0 a \sin\xi \cos\varphi \\ \beta &= k_0 b \sin\xi \sin\varphi. \end{aligned} \tag{5.31}$$

Therefore, for plane wave sound the sound transmission coefficient (Equation 3.12) for normal sound incidence is given by

$$\tau = \frac{\rho_0^2 c_0^2 \omega^2}{4|p_0^2|} \sum_{n=1}^{N} \sum_{m=1}^{M} |q_{2,nm}|^2 \sigma_{nm}. \tag{5.32}$$

The sound transmission coefficient for oblique sound incidence can be written as

$$\tau(\theta, \phi) = \frac{\rho_0^2 c_0^2 \omega^2}{4|p_0^2| \cos\theta} \sum_{n=1}^{N} \sum_{m=1}^{M} |q_{2,nm}(\theta, \phi)|^2 \sigma_{nm}. \tag{5.33}$$

For an incident diffuse field the sound transmission coefficient is obtained using the weighting function of Pierce [9] for panels

$$\tau_{diff} = \frac{\int_0^{2\pi} \int_0^{\pi/2} \tau(\theta, \phi) \sin\theta \cos\theta \, \mathrm{d}\theta \mathrm{d}\phi}{\int_0^{2\pi} \int_0^{\pi/2} \sin\theta \cos\theta \, \mathrm{d}\theta \mathrm{d}\phi} = \frac{1}{\pi} \int_0^{2\pi} \int_0^{\pi/2} \tau(\theta, \phi) \cos\theta \sin\theta \, \mathrm{d}\theta \mathrm{d}\phi. \tag{5.34}$$

The sound transmission loss of the host double panel partition with the dimensions 1 x $1m$ was calculated using the plate model. As for the beam model, 1 mm steel panels with a mass per unit area of 7.8 kg/m^2 were selected for the double panel partition. For the 20 mm air cavity of the construction, the MAM-resonance appears at 215 Hz. A damping factor η=0.01 was used for the panels and the air gap.

For normal sound incidence, Figure 5.5 presents the sound reduction index of the host double panel partition for the frequencies of major interest below 1000 Hz. The sound reduction index shows the same general aspects as already discussed for the beam model, see section 4.1.4. In fact, Figure 4.7 for the beam model and Figure 5.5 for the plate model show similar results. Depending on the frequency range considered, the numbers of modes used for these calculations were calculated by Equation 4.21 for the beam model calculation (e.g. min. 20 modes for frequencies up to 1000

Hz) and by Equation 5.7 for the plate model calculation (this study used in general 500 modes for frequencies up to 1000 Hz).

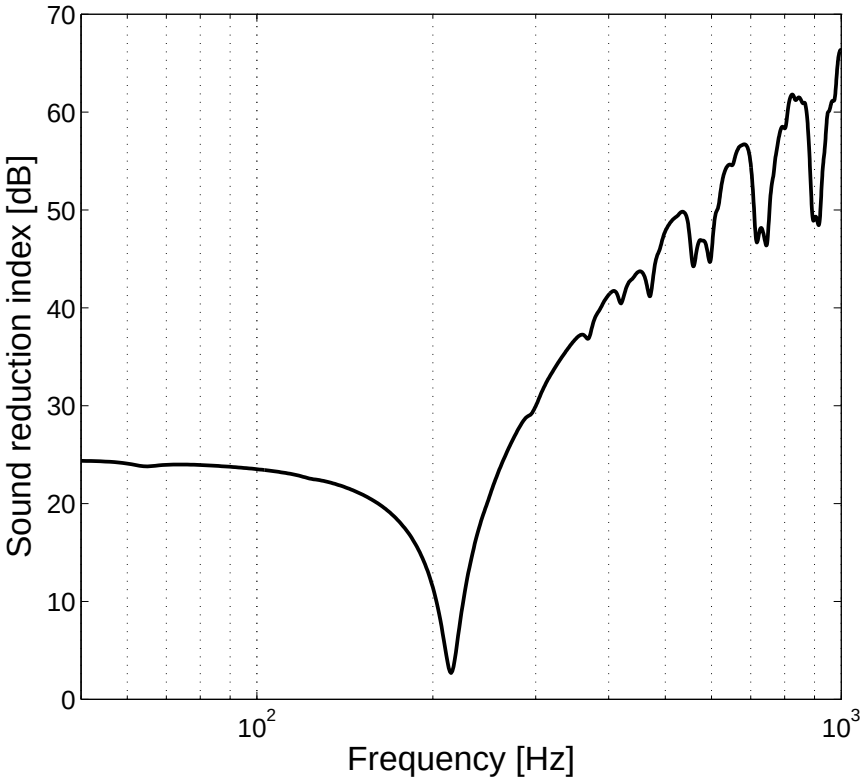

Figure 5.5: Sound reduction index of the host double panel partition at normal sound incidence, using the plate model.

In Figure 5.5 beyond the MAM-resonance the sound reduction index drops at frequencies related to individual flexural modes of the equal panels. For example, the mode n=1, m=11 cause the dip in the sound reduction at 300.3 Hz. Since the investigated host double panel partition has equal length and width the mode n=11, m=1 also occurs at 300.3 Hz. Further pa-

nel modes which cause the deterioration in the sound reduction shown in Figure 5.5 are:

n / m	Hz	n / m	Hz
1 / 13	419,3	13 / 1	419,3
1 / 15	557,4	15 / 1	557,4
1 / 17	715,3	17 / 1	715,3
1 / 19	892,9	19 / 1	892,9

For the calculation of the diffuse field sound transmission loss, the numerical routine for each frequency needs to be computed for a sufficient number of angles θ and ϕ. The entire research for this thesis was carried out on a laptop computer system with a 1.4 GHz processor. In fact, a calculation for the beam model for a frequency range up to 20000 Hz requires approximately one week time. Since the Matlab student edition was the only available numerical software package for this work, a faster calculation routine using e.g. three dimensional matrices was impossible due to the limitations of the student edition. On the other hand, at this stage of the project the major interest was to present the fundamental concepts and principles of internal vibration absorbers. In the following parameter study in chapter 6, this aim was achieved by beam model calculations for a frequency range up to 20000 Hz and plate model calculations up to 1000 Hz. In this thesis calculations were carried out for normal sound incidence using the beam and plate model. For oblique sound incidence, calculations were only performed for the beam model.

5.2 Two-sided vibration absorber

5.2.1 Continuous vibration absorber

For the continuous two-sided vibration absorber, the coupling forces due to the two-sided vibration absorber are described using the coefficients R_1 to R_3 of Equation 4.64. Figure 5.6 presents the plate model of the double panel partition with continuous two-sided vibration absorber.

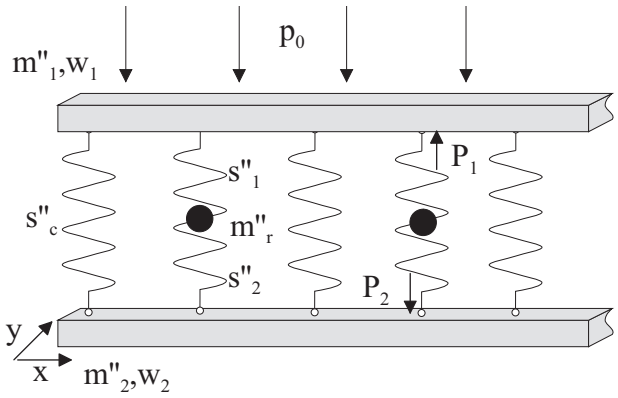

Figure 5.6: Plate model of a double panel partition with continuous cavity spring and continuous two-sided vibration absorber for an incoming plane wave pressure load.

The matrix formulation of the plate model for the double panel partition with continuous cavity spring and continuous two-sided vibration absorber is obtained as

$$\left(-\omega^2\mathbf{M}_{nm} + \mathbf{K}_{nm}\right)\mathbf{q}_{nm} = \mathbf{Q}_{nm} \tag{5.35}$$

where

$$\mathbf{M}_{nm} = \frac{A}{4}\begin{bmatrix} m_1'' - i\frac{\rho_0 c_0}{\omega\cos\theta} & 0 \\ 0 & m_2'' - i\frac{\rho_0 c_0}{\omega\cos\theta} \end{bmatrix},$$

$$\mathbf{q}_{nm} = \begin{bmatrix} q_{1,nm} \\ q_{2,nm} \end{bmatrix}, \mathbf{Q}_{nm} = \begin{bmatrix} Q_{nm} \\ 0 \end{bmatrix}.$$

For Q_{nm} refer to Equation 5.26.

Accounting for the two-sided vibration absorbers the stiffness matrix is given by

$$\mathbf{K}_{nm} = \begin{bmatrix} D_1 k_{nm}^4 \frac{A}{4} + s_c'' \frac{A}{4} + R_1 & -s_c'' \frac{A}{4} - R_2 \\ -s_c'' \frac{A}{4} - R_2 & D_2 k_{nm}^4 \frac{A}{4} + s_c'' \frac{A}{4} + R_3 \end{bmatrix}. \tag{5.36}$$

5.2.2 Continuous cavity spring and discrete vibration absorbers [77,78]

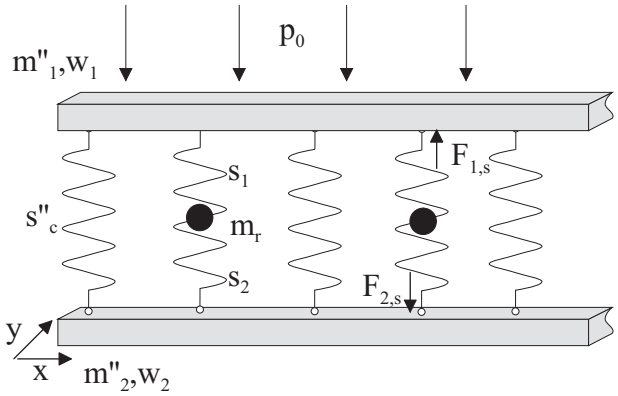

Figure 5.7: Plate model of a double panel partition with continuous cavity spring and discrete two-sided vibration absorber for an incoming plane wave pressure load.

For discrete two-sided vibration absorbers the following formulations are used

$$
\begin{aligned}
R_1 &= \frac{(\omega_{2_r}^2 - \omega^2) m_r}{1 + \dfrac{\omega_{2_r}^2}{\omega_{1_r}^2} - \dfrac{\omega^2}{\omega_{1_r}^2}} \\
R_2 &= \frac{\omega_{2_r}^2 m_r}{1 + \dfrac{\omega_{2_r}^2}{\omega_{1_r}^2} - \dfrac{\omega^2}{\omega_{1_r}^2}} \\
R_3 &= \frac{(\omega_{1_r}^2 - \omega^2) m_r}{1 + \dfrac{\omega_{1_r}^2}{\omega_{2_r}^2} - \dfrac{\omega^2}{\omega_{2_r}^2}}.
\end{aligned}
\tag{5.37}
$$

Thus, the concept of locally distributed two-sided vibration absorbers that are implemented into the cavity of a double panel partition is described by the stiffness matrix

$$
\mathbf{K} = \begin{bmatrix} \mathbf{K_1} + \mathbf{S_c} + R_1 \mathbf{\Phi}\mathbf{\Phi}^\mathbf{T} & -\mathbf{S_c} - R_2 \mathbf{\Phi}\mathbf{\Phi}^\mathbf{T} \\ -\mathbf{S_c} - R_2 \mathbf{\Phi}\mathbf{\Phi}^\mathbf{T} & \mathbf{K_2} + \mathbf{S_c} + R_3 \mathbf{\Phi}\mathbf{\Phi}^\mathbf{T} \end{bmatrix},
$$

with the diagonal matrices

$$
\mathbf{K_i} = \frac{A}{4} \begin{bmatrix} D_i k_{nm}^4 & 0 \\ 0 & \ddots \end{bmatrix}, \mathbf{S_c} = \frac{A}{4} \begin{bmatrix} s_c'' & 0 \\ 0 & \ddots \end{bmatrix}
$$

and the mode shape matrix $\mathbf{\Phi} = \begin{bmatrix} \Phi_{nm,j} & \cdots \\ \vdots & \ddots \end{bmatrix}$

substituted into Equation 5.26.

5.2.3 Discrete cavity spring and discrete vibration absorbers

For the last arrangement, when both cavity spring and two-sided vibration absorber are discrete, the matrix formulation of Equation 5.26 is written using the stiffness matrix for I cavity springs and J absorbers as follows

$$\mathbf{K} = \begin{bmatrix} \mathbf{K_1} + s_c \mathbf{\Psi}\mathbf{\Psi}^\mathbf{T} + \omega_{r1}^2 m_{r1} \mathbf{\Phi}\mathbf{\Phi}^\mathbf{T} & -s_c \mathbf{\Psi}\mathbf{\Psi}^\mathbf{T} \\ -s_c \mathbf{\Psi}\mathbf{\Psi}^\mathbf{T} & \mathbf{K_2} + s_c \mathbf{\Psi}\mathbf{\Psi}^\mathbf{T} + \omega_{r2}^2 m_{r2} \mathbf{\Phi}\mathbf{\Phi}^\mathbf{T} \end{bmatrix},$$

with the diagonal matrix

$$\mathbf{K_i} = \frac{A}{4} \begin{bmatrix} D_i k_{nm}^4 & 0 \\ 0 & \ddots \end{bmatrix}$$

and the mode shape matrices $\mathbf{\Psi} = \begin{bmatrix} \Psi_{nm,i} & \cdots \\ \vdots & \ddots \end{bmatrix}$, $\mathbf{\Phi} = \begin{bmatrix} \Phi_{nm,j} & \cdots \\ \vdots & \ddots \end{bmatrix}$.

In this chapter formulations for finite double panel partitions with internal two-sided vibration absorbers were derived. Number, distribution and resonance frequency of the internal vibration absorbers can be predesigned for a required sound transmission loss. Using the plate model, first results for the double panel host partition with different number and distribution of internal two-sided vibration absorbers are presented in the following parameter study.

Chapter 6

Parameter study

Using the derived analytical models, the concept of internal vibration absorbers was analysed for low frequency sound transmission. In particular, this thesis aimed to present an increase of the sound reduction index at the MAM-resonance. Hence, the focus of the following parameter study was on the frequency range around the MAM-resonance of the host double panel partition. In order to design internal vibration absorbers having identical resonance frequency as the MAM-resonance, a tuning approach is presented. Results for different number and distribution of two-sided vibration absorbers provide fundamental evidence for the potential of internal resonators as solution for the reduction of sound transmission at structural resonances. The calculations are carried out using the mass-spring model, the beam model for continuous and discrete absorber springs and the plate model for continuous and discrete absorber springs.

Additionally, the issue of broadening the frequency range of the resonance effect is discussed in terms of the advantages of wideband vibration absorbers.

6.1 Tuning of the internal vibration absorbers

Since the two-sided vibration absorber is connected to the host double panel structure by two springs, the resonance of the implemented vibration absorbers could not be calculated by the general mass-spring formulations of a vibration absorber. In principle, the implementation of internal vibration absorbers is based on the idea of increasing the resistance of the host structure due to the motion of a resonant system. In the ideal case, this leads to high motion of the absorber mass and zero motion of the host structure.

If the mass of the internal absorber is much smaller than the mass of the panels, the mass-spring model of the two-sided vibration absorber (section 3.3) can be simplified at resonance of the internal absorber, as shown in Figure 6.1.

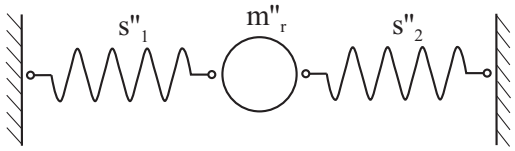

Figure 6.1: Simplified representation of the two-sided vibration absorber at resonance.

With this simplified representation the resonance frequency ω_r of the two-sided vibration absorber is determined by

$$\omega_r^2 = \frac{s_1'' + s_2''}{m_r''}. \tag{6.1}$$

By applying internal vibration absorbers, it is intended to reduce the motion of the radiating panel at a certain frequency which consequently leads to a reduced sound radiation and thus an increase in the sound transmission loss of the host structure. Taking into account the general behaviour of a vibration absorber, at resonance, the absorber mass moves out of pha-

se to the host structure. In the case of the double panel partition under investigation, this yields the following assumption. If the two-sided vibration absorber is tuned to the MAM-resonance of the host double panel partition, the radiating panel is ideally at antiresonance with zero motion and the motion of the absorber mass is out of phase to the motion of the incident panel. Using the mass-spring model, this fundamental consideration of the implementation of internal vibration absorbers is shown for the two-sided vibration absorber in Figure 6.2.

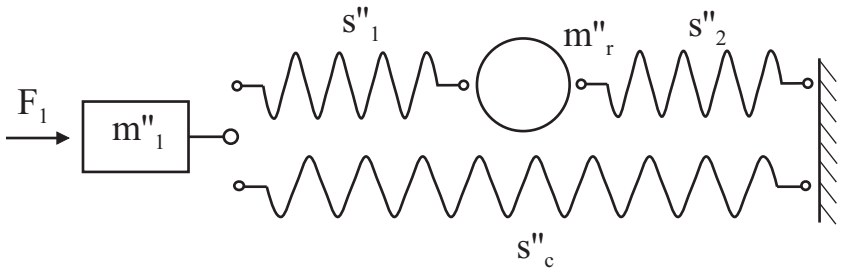

Figure 6.2: Mass spring representation of the two-sided vibration absorber at resonance.

where $\omega_r = 2\pi f_r$, and f_r represents the MAM-resonance frequency.

Thus, for an input force F_1 the resonance frequency of the two-sided vibration absorber is obtained by substituting the antiresonance condition $v_2/F_1 = 0$ into the mass-spring model as (see Appendix B)

$$\omega_r^2 = \frac{s_c''(s_1'' + s_2'') + s_1'' s_2''}{m_r'' s_c''}. \tag{6.2}$$

In the following parameter study both Equation 6.1 and Equation 6.2 were used for the tuning of the internal absorbers. The parameters of the internal absorbers were first estimated by Equation 6.1 followed by a fine tuning using the more sophisticated Equation 6.2.

6.2 Finite Element Model

The major interest of this thesis is the situation when the resonance of the two-sided vibration absorber appears at the MAM-resonance. For a better understanding of the physical principles at this specific relation between the two-sided vibration absorber and the double panel host structure, the frequency dependent behaviour of the construction was visualized by using the Finite Element software package Ansys.

The input parameters of the finite element analysis were defined referring to the previous beam model. For the panels of the double panel partition simply supported boundary conditions were assigned. The cavity layer was defined as flexible only in the vertical axis using plane strain elements. Plane strain elements were also used for the panels of the host structure. Each internal absorber was modelled by a mass and two spring elements. Figure 6.3 shows schematically the structural model for the double panel partition with one two-sided vibration absorber per unit length.

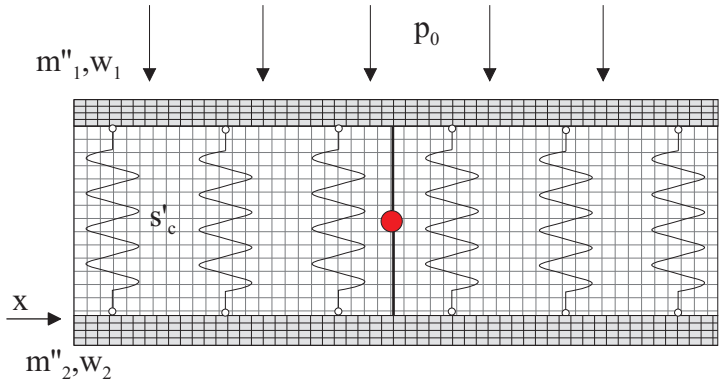

Figure 6.3: Illustration of the finite element input mesh of the double panel partition with two-sided vibration absorber.

For the 1 *m* long host double panel structure the following input parameters were assigned using Plane 82 elements:

Input-Mesh	
Length l=1 m	100 divisions
1 mm steel panels	2 divisions
20 mm air gap	25 divisions
Structural damping	0.01

For the two-sided vibration absorber the springs are represented by two Combin14 elements and the absorber mass is represented by one 2D Mass21 element.

Applying a unit line force Figure 6.4 presents the calculated real part of the transverse displacement of the double panel host structure at 215 Hz. As before, the double panel host structure is constructed with a 20 mm air cavity and 1 mm steel panels. Each panel has a mass per unit area of 7.8 kg/m^2. Therefore, the MAM-resonance appeared at 215 Hz. Throughout the structure, nine two-sided vibration absorbers per unit length with a total mass of 1 kg were attached. Each absorber was tuned to the MAM-resonance assigning $\omega_{r1}/(2\pi) = 100\ Hz$ and $\omega_{r2}/(2\pi) = 185\ Hz$ as defined on page 64. The calculation was performed for a panel and air gap damping of η=0.01. For these parameters Equation 6.2 yields for $\frac{\omega_r}{2\pi} = f_r = 214.76Hz$ as the resonance frequency of the two-sided vibration absorber.

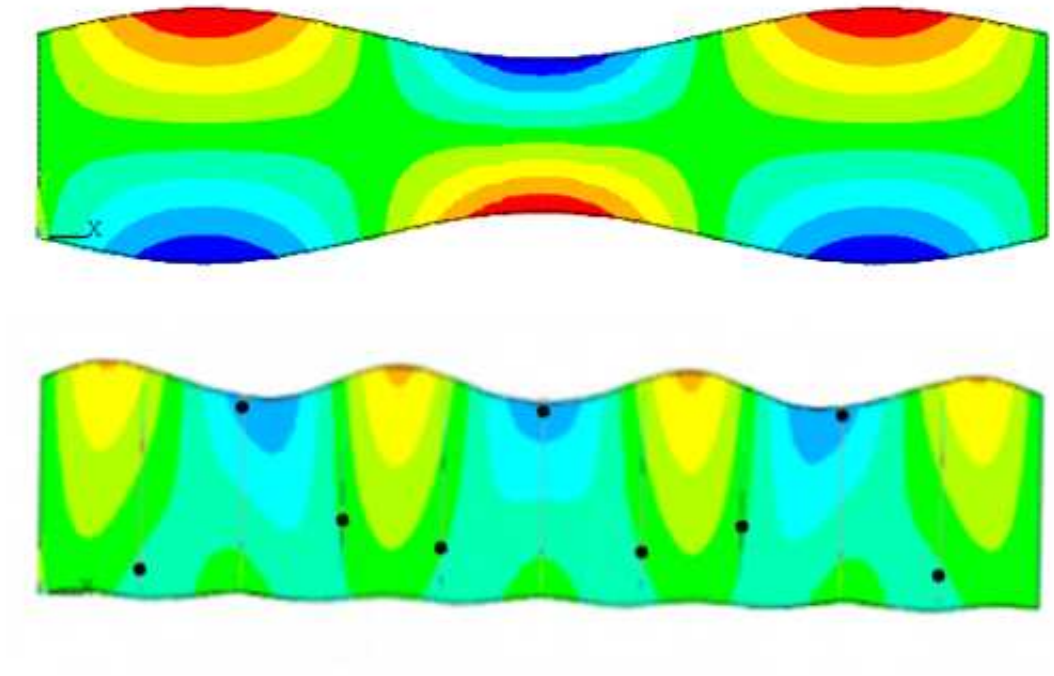

Figure 6.4: Real part of the forced response of the transverse displacement at 215 Hz without (upper figure) and with absorbers (lower figure). The absorbers masses are represented by the black dots.

This result reveals the desired reduced motion of the radiating panel (lower panel) caused by the internal vibration absorbers. According to the finite element mesh (Figure 6.3), the equilibrium point of the absorber mass is located at the vertical centre of the construction. Therefore, the finite element analysis shows that the absorber mass is moving in the opposite direction to the incident panel which leads to the expected reduction in the transverse displacement of the radiating panel and respectively in the sound transmission.

6.3 Absorber effect around MAM-resonance

In order to verify this effect of the two-sided vibration absorbers by the derived models, the resonance of the vibration absorber was assigned to various frequencies across a frequency range around the MAM-resonance. For the host double panel partition with the MAM-resonance at 215 Hz, Figure 6.5 presents the sound reduction index of a frequency range from 150 to 280 Hz calculated by the mass-spring model. The total additional mass of the internal vibration absorbers was kept constant at a value of 1 kg per unit area. It was assumed that both springs of the two-sided vibration absorber have identical spring stiffness s_1'' and s_2''.

Figure 6.5 reveals that only away from the MAM-resonance an absorber effect can be identified. Even if the two-sided vibration absorber was tuned (section 6.1) to the MAM-resonance at 215 Hz, an absorber effect was not detected in the sound reduction index of the double panel host structure.

The same result is observed in Figure 6.6, when the resonances of the vibration absorbers were chosen within a smaller frequency range around the MAM-resonance. It can be seen, that for the symmetric double panel partition consisting of panels with equal properties, the effect of a two-sided vibration absorber with both springs having equal spring stiffness vanishes towards the MAM-resonance. In the case of equal absorber springs, at the MAM-resonance frequency the absorber mass is at rest at its equilibrium position. The two panels of the structure move almost unaffected in opposite direction as without internal absorbers, see also Figure 6.4.

Using the mass-spring model for the two-sided vibration absorber (section 3.3), this structural behaviour of the symmetric construction ($m_1'' = m_2''$ and $s_1'' = s_2''$) is analytically determined by the eigenvalue solution of the

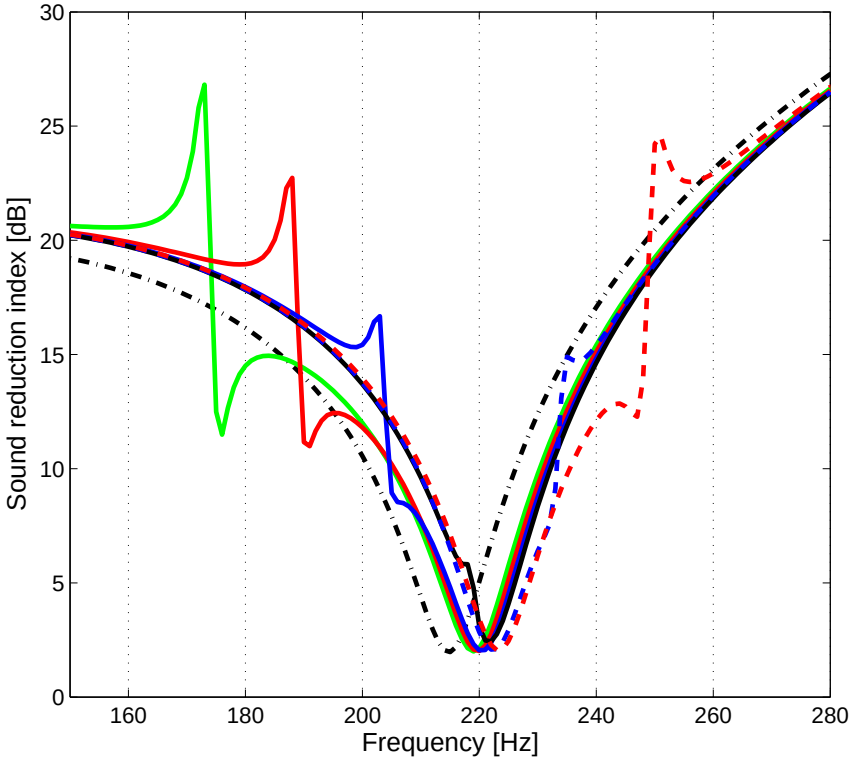

Figure 6.5: Resonator effect across the MAM-resonance frequency range calculated by the mass-spring model. (-·-) host double panel partition $m_1'' = m_2''$; absorber resonance if $s_1'' = s_2''$: (–) 173 Hz (–) 188 Hz (–) 203 Hz (–) 215 Hz (- -) 234 Hz (- -) 242 Hz

following equation (see also Equation 3.20).

$$-\omega^2 \begin{bmatrix} m_1'' & 0 & 0 \\ 0 & m_r'' & 0 \\ 0 & 0 & m_1'' \end{bmatrix} + \begin{bmatrix} s_c'' + s_1'' & -s_1'' & -s_c'' \\ -s_1'' & 2s_1'' & -s_1'' \\ -s_c'' & -s_1'' & s_1'' + s_c'' \end{bmatrix} = 0 \qquad (6.3)$$

Computing the eigenvectors and eigenvalues reveals the natural frequency of the structure at 221 Hz with the mode shape $\begin{pmatrix} -1 \\ 0 \\ 1 \end{pmatrix}$, e.g. for the

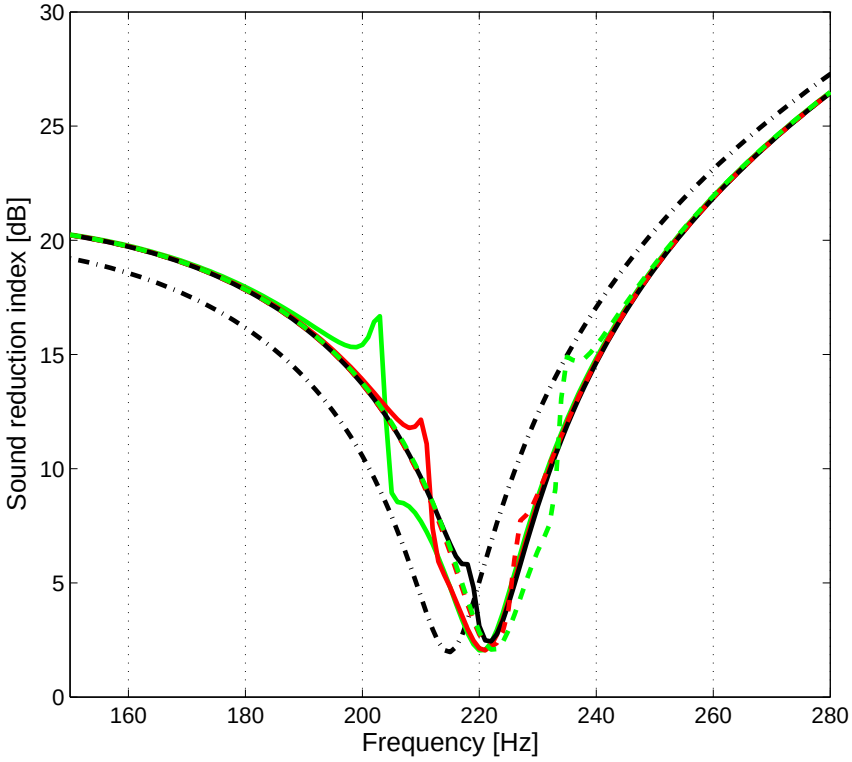

Figure 6.6: Resonator effect adjacent to the MAM-resonance calculated by the mass-spring model.(-·-) host double panel partition $m_1'' = m_2''$; absorber resonance if $s_1'' = s_2''$: (–) 203 Hz (–) 211 Hz (–) 215 Hz (- -) 226 Hz (- -) 234 Hz

internal absorber with a resonance of 215 Hz (see Figure 6.6). This result shows analytically the two panels of the structure moving in opposite direction and the absorber mass being at rest.

On the other hand, with increasing frequency distance to the MAM-resonance, the characteristic of the typical absorber effect is obtained. The sound reduction characteristic shows a resonance peak which is accompanied by a dip, e.g. shown in Figure 6.6.

6.4 Asymmetry and Reciprocity

The MAM-resonance can be influenced by the two-sided vibration absorber introducing asymmetry into the structure. In this case, the internal vibration absorber causes the expected effect, that a resonance dip in the sound reduction characteristic is split into two dips with the absorber peak at the tuned frequency (Equation 6.2) in between. One possibility to insert asymmetry into the construction can be achieved by assigning different spring stiffness to the two absorber springs. Figure 6.7 shows the sound reduction index of different spring ratios $\frac{s_1''}{s_2''}$ of a two-sided vibration absorber attached to the host double panel construction with 1 mm steel panels. Low damping with $\eta = 0.01$ was applied to the double panel structure and the absorbers. For each presented spring ratio, various absorber resonances across the MAM-resonance are found. A rising absorber effect is evident if the spring stiffness of the two internal absorber springs are increasingly divergent.

For different mass ratios m_1''/m_2'' Figure 6.8 shows the sound reduction index of the host double panel structure without internal absorbers. These double panel structures were studied with attached two-sided vibration absorbers consisting of a total absorber mass of 1 kg/m^2 and absorber springs with equal stiffness. The internal absorbers were tuned (see section 6.1) to the MAM-resonance of the individual structures with different mass ratios. Figure 6.9 presents the calculated sound reduction index using the mass-spring model.

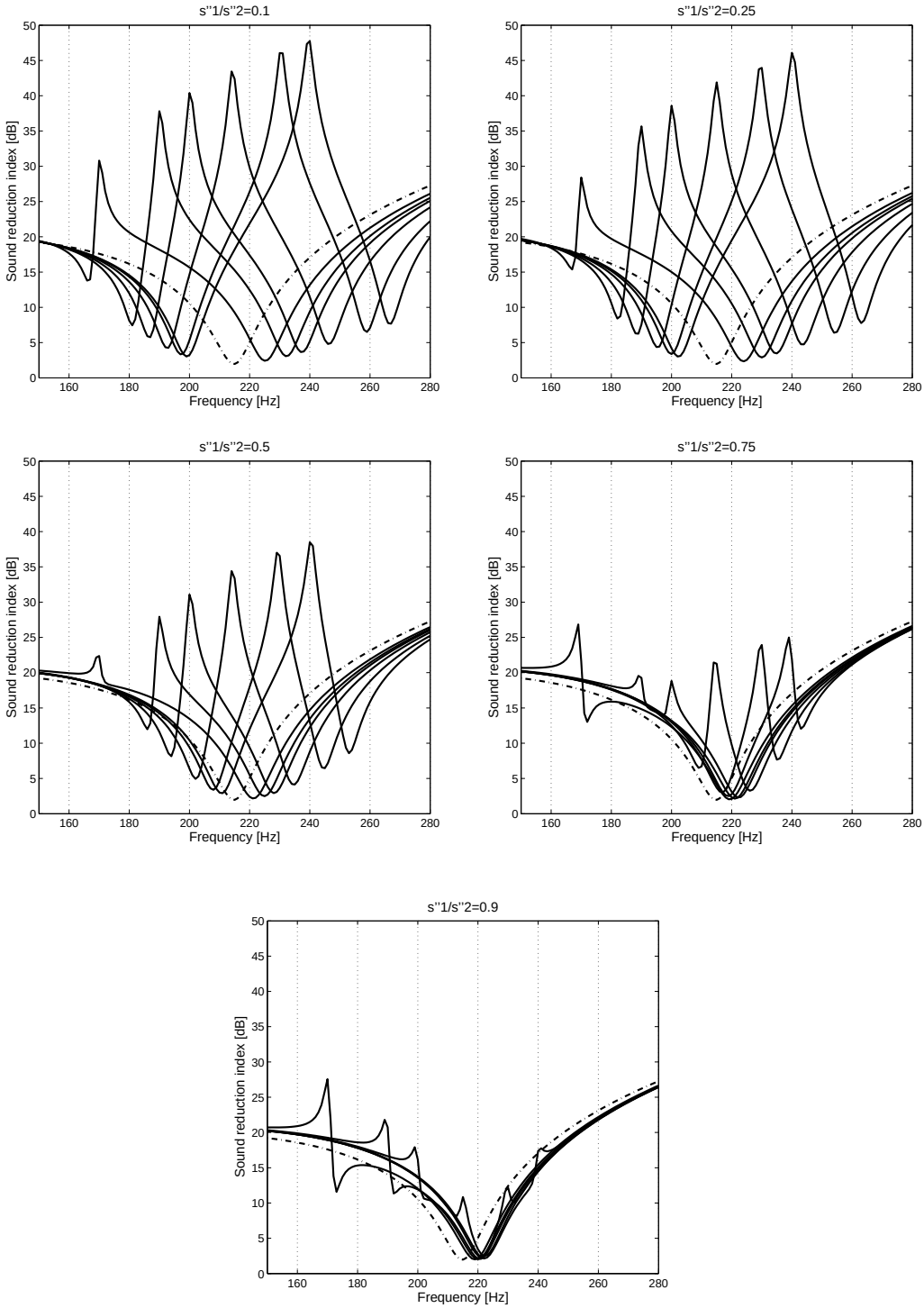

Figure 6.7: Mass-spring model: Sound reduction index across the MAM for different spring ratios and m_1''=m_2''. (- -) without; (–) with absorber

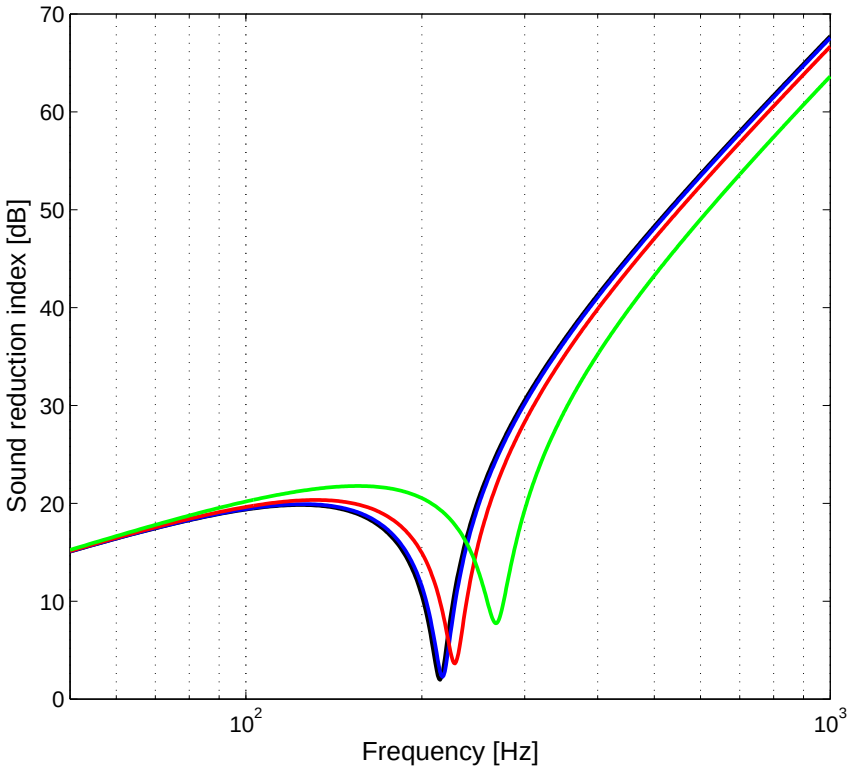

Figure 6.8: Sound reduction index of the double panel structure without internal absorbers dependent on the mass ratio of the panels. (–) host double panel partition $m_1'' = m_2''$; (–) m_1''/m_2''=0.75; (–) m_1''/m_2''=0.5; (–) m_1''/m_2''=0.25

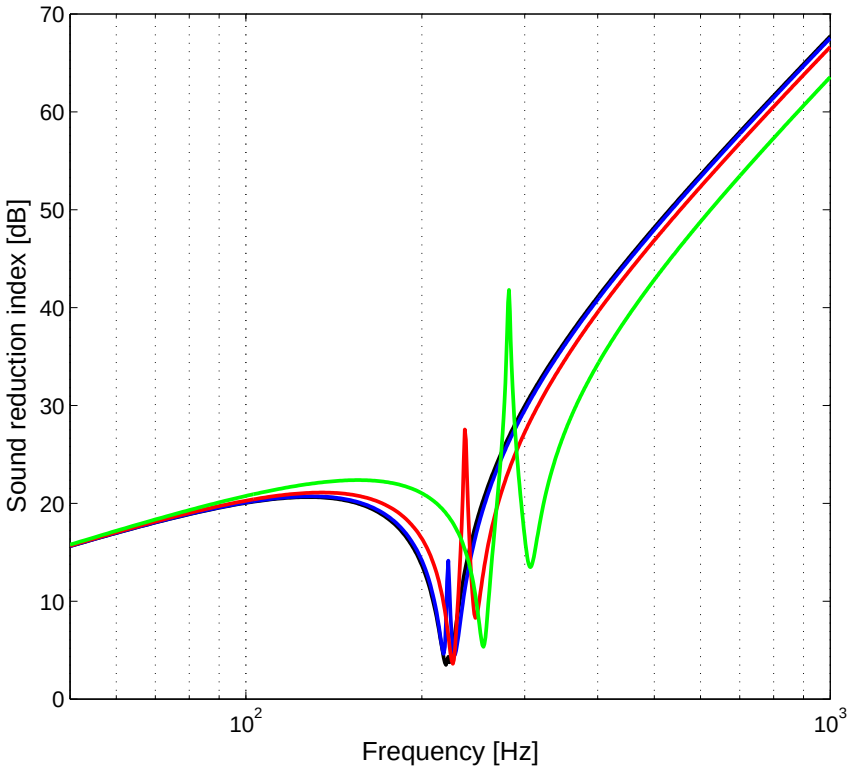

Figure 6.9: Sound reduction index of the double panel structure with different mass ratio of the panels and attached internal absorbers (s_1''=s_2'') calculated by the mass-spring model. (–) host double panel partition m_1''=m_2''; (–) m_1''/m_2''=0.75; (–) m_1''/m_2''=0.5; (–) m_1''/m_2''=0.25

For two-sided vibration absorbers with different absorber springs an increased absorber effect was observed for a higher degree of asymmetry. Figure 6.9 shows, that this result is also true for two-sided vibration absorbers with equal springs, if an increased asymmetry is achieved by an increased mass difference of the two panels of the double panel structure.

The absorber effect due to asymmetry in the structure is even increased if additionally to the different mass of the two panels (Figure 6.9) the two ab-

sorber springs have different spring stiffness. For the mass ratio $\frac{m_1''}{m_2''} = 0.5$ and the spring ratio $\frac{s_1''}{s_2''} = 2$ Figure 6.10 reveals this increase of the absorber effect.

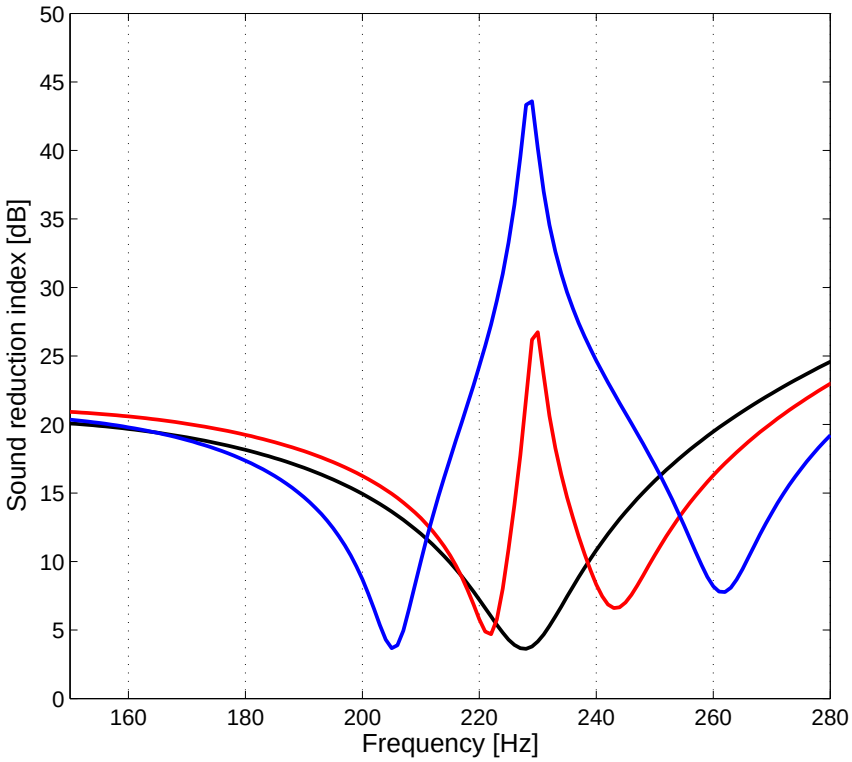

Figure 6.10: Sound reduction index for the double panel partition with both asymmetric panel masses m_1''/m_2''=0.5 and asymmetric absorber springs calculated by the mass-spring model. (–) without internal absorber;(–) $s_1'' = s_2''$; (–) $s_1''/s_2'' = 2$

If two-sided internal absorbers are implemented into a double panel construction in order to achieve an increased sound reduction at the MAM-resonance, an asymmetry in the structure is required. However, higher absorber effect are achieved if mass ratio and spring ratio are different. This can be concluded by comparing the sound transmission index of the

double panel partition shown in Figure 6.11 and Figure 6.12. Using the mass-spring model, Figure 6.11 shows the sound reduction index for the double panel partitions with asymmetric configurations $\frac{m_1''}{m_2''} = 2$, $\frac{s_1''}{s_2''} = 0.5$ and $\frac{m_1''}{m_2''} = 0.5$, $\frac{s_1''}{s_2''} = 2$, when the total mass of the two panels was kept constant at $15.6\frac{kg}{m^2}$ and the total absorber mass was $1\frac{kg}{m^2}$.

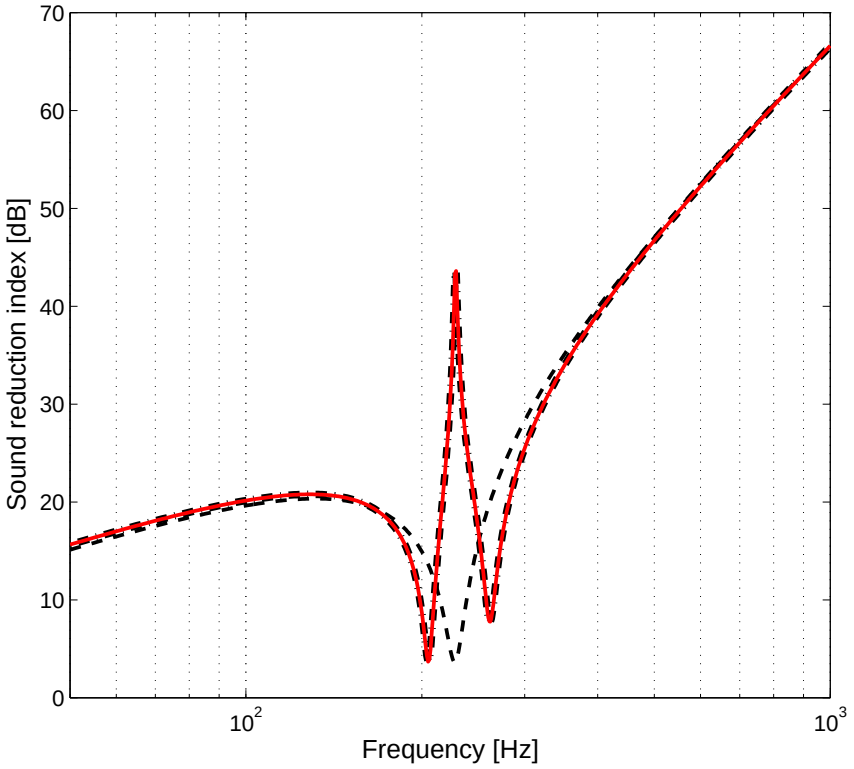

Figure 6.11: Sound reduction index for the double panel partition with asymmetric panel masses and asymmetric absorber springs calculated by the mass-spring model. (- -) double panel partition m_1''/m_2''=0.5 or m_1''/m_2''=2 without internal absorber; (-·-) double panel partition m_1''/m_2''=2 with asymmetric absorbers $\frac{s_1''}{s_2''}$= 0.5; (–) double panel partition m_1''/m_2''=0.5 with asymmetric absorbers $\frac{s_1''}{s_2''}$=2

It can be observed that these two results, which are identical, correspond to sound transmission through the same panel configuration in opposite directions.

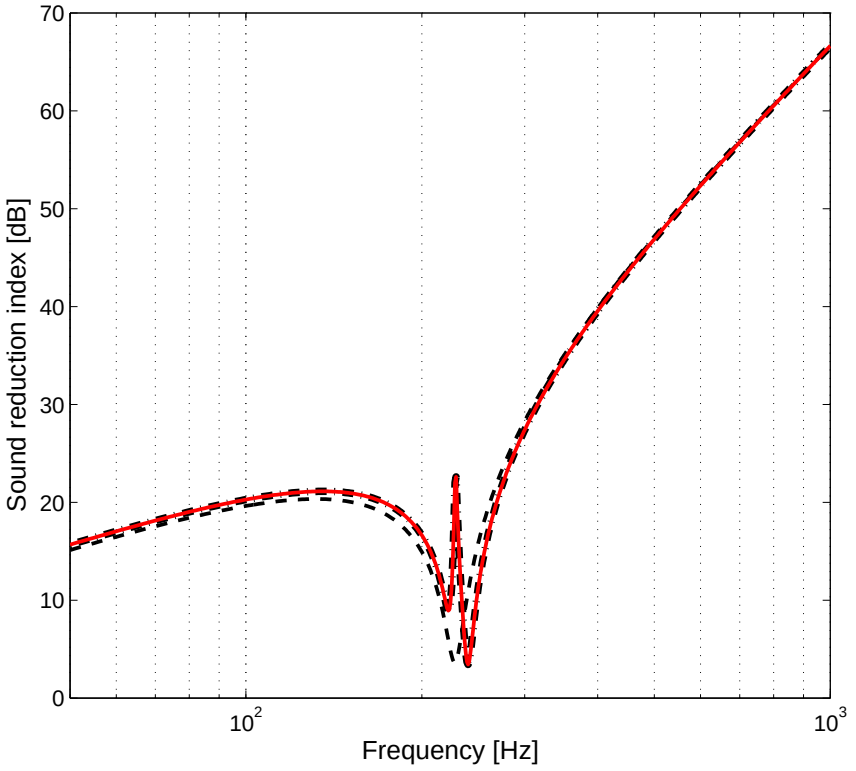

Figure 6.12: Sound reduction index for the double panel partition with equal asymmetric mass and spring ratios calculated by the mass-spring model. (- -) double panel partition m_1''/m_2''=0.5 or m_1''/m_2''=2 without internal absorber; (-·-) double panel partition m_1''/m_2''=0.5 with asymmetric absorbers $\frac{s_1''}{s_2''}$= 0.5; (–) double panel partition m_1''/m_2''=2 with asymmetric absorbers $\frac{s_1''}{s_2''}$=2

Identical results for the sound transmission through the double panel partition with internal absorbers were also obtained in Figure 6.12 for the double panel panel configurations $\frac{m_1''}{m_2''} = 0.5$, $\frac{s_1''}{s_2''} = 0.5$ and $\frac{m_1''}{m_2''} = 2$, $\frac{s_1''}{s_2''} = 2$. As

for the previous calculations shown in Figure 6.11, the total mass of the two panels was $15.6\frac{kg}{m^2}$ and the total absorber mass was $1\frac{kg}{m^2}$.

In fact, the sound reduction index is independent from the direction in which sound is transmitted through the structure [33]. This reciprocity principle of sound transmission was observed in Figure 6.11 and Figure 6.12.

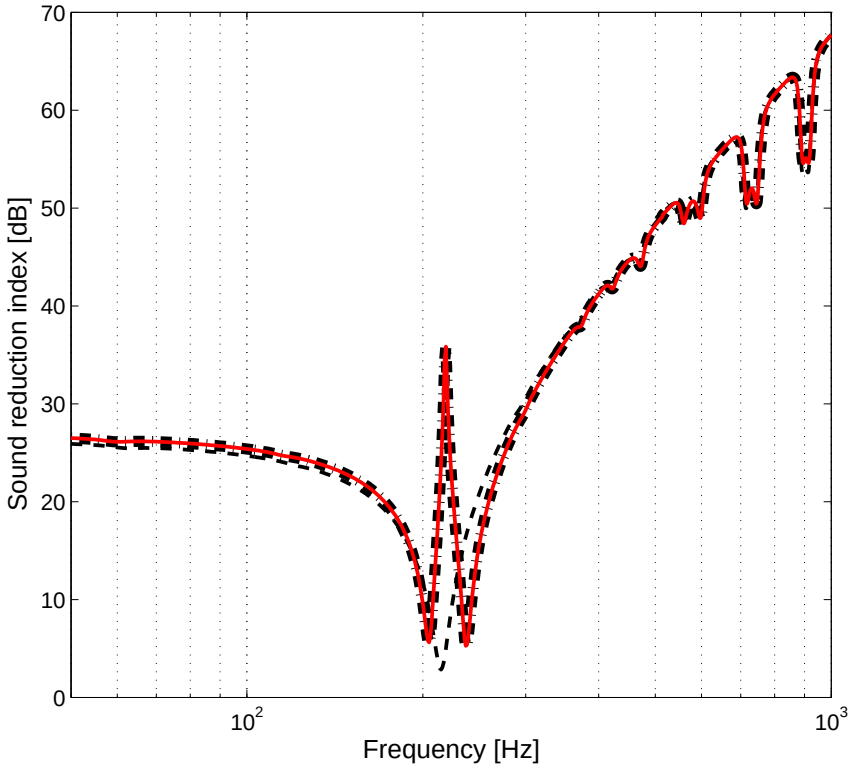

Figure 6.13: Reciprocal sound reduction index of the host double panel partition with m_1''=m_2''=$7.8\frac{kg}{m^2}$ and continuous two-sided vibration absorber using the beam model. (- -) host double panel partition;(-·-) sound transmission with asymmetric absorbers $\frac{s_1''}{s_2''} = 0.25$; (–) opposite sound transmission with asymmetric absorbers $\frac{s_1''}{s_2''} = 4$.

Additionally, Figure 6.13 shows the reciprocity principle for the sound transmission through the double panel host structure (page 62) with continuous two-sided vibration absorbers using the beam model (see section 4.3.1). The internal absorbers with the total mass of $1\frac{kg}{m^2}$ were tuned to the MAM-resonance with spring stiffness $\frac{s_1''}{s_2''} = 0.25$ and $\frac{s_1''}{s_2''} = 4$ ($\frac{s_2}{s_1} = 0.25$).

So far, the analysis above revealed a tuning approach for the two-sided vibration absorber. If the absorber is designed in order to increase the sound reduction at the MAM-resonance, a significant asymmetry in the structure is required. In this case, the increase of the sound transmission loss due to the internal absorbers is dependent on the degree of asymmetry achieved by different spring or panel properties.

Consequently, for a highly asymmetric double panel construction with two-sided vibration absorbers the implemented absorber systems can be considered as a one-sided vibration absorber system (section 4.2). In fact, the presented results for a double panel partition with implemented two-sided vibration absorbers and high asymmetry (see Figure 6.7 for $\frac{s_1''}{s_2''} = 0.1$) revealed a similar significant increase in the sound transmission loss at the MAM-resonance as a one-sided vibration absorber (Figure 4.10).

In conclusion, if both one-sided vibration absorbers and two-sided vibration absorbers are tuned with their resonance to the MAM-resonance, both can be considered as a powerful measure for increasing the sound transmission loss of a double panel lightweight construction. However, the two-sided vibration absorber achieves the increased sound transmission loss with hardly any mentioned constructional issues that are expected for the one-sided vibration absorber. This was an important reason, why this work was mainly devoted to the investigation of the two-sided vibration absorber.

6.5 Discussion of analytical models

Results of the previous section have shown, that the two-sided vibration absorber can be applied to lightweight double panel partitions in order to achieve a significant increase of the sound transmission index at the MAM-resonance. Taking the required structural asymmetry into account and using the presented tuning approach, the following parameter studies present results of the sound transmission index for the host double panel partition with various two-sided vibration absorbers using all three previously derived analytical models.

The host double panel partition for the following calculations consists of 1 mm steel panels having a mass per unit area of 7.8 kg/m^2 and a 20 mm air cavity, as defined in section 4.1.4. Hence, the MAM-resonance appears at 215 Hz. Using the mass-spring model, the sound reduction index was calculated first for two-sided vibration absorbers with a spring ratio $\frac{s_1''}{s_2''}$ of 0.5 and a total absorber mass of 1 kg/m^2. Structure and absorber had a damping factor of $\eta = 0.01$. Figure 6.14 shows the comparison of the sound reduction index for the double panel partition with and without two-sided vibration absorber.

In general, the effectiveness of a standard vibration absorber depends upon two parameters, namely its mass and internal damping. If the damping is increased then the vibration absorber is less effective, but its bandwidth increases. This effect of an increased damping is shown in Figure 6.15. Using the same host structure as for the calculation of Figure 6.14, both springs of the two-sided vibration absorber had now a damping loss factor of $\eta = 0.3$ while the panels were still calculated with the damping factor $\eta = 0.01$.

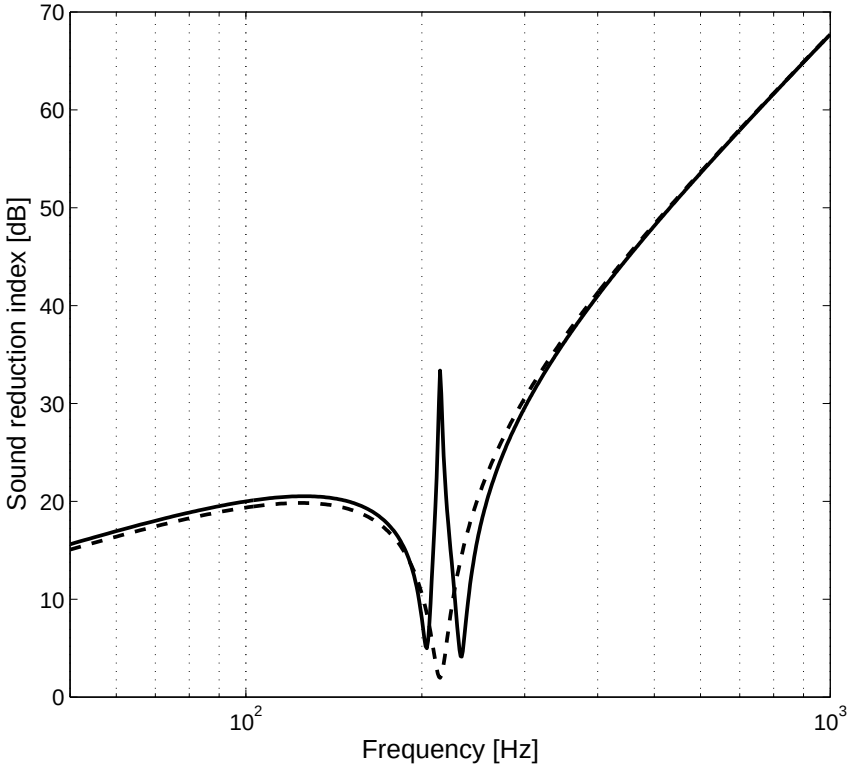

Figure 6.14: Sound reduction index of the host double panel partition with two-sided vibration absorber ($\frac{s_1''}{s_2''}$=0.5) for normal sound incidence calculated by the mass-spring model. (- -) without; (–) with absorber

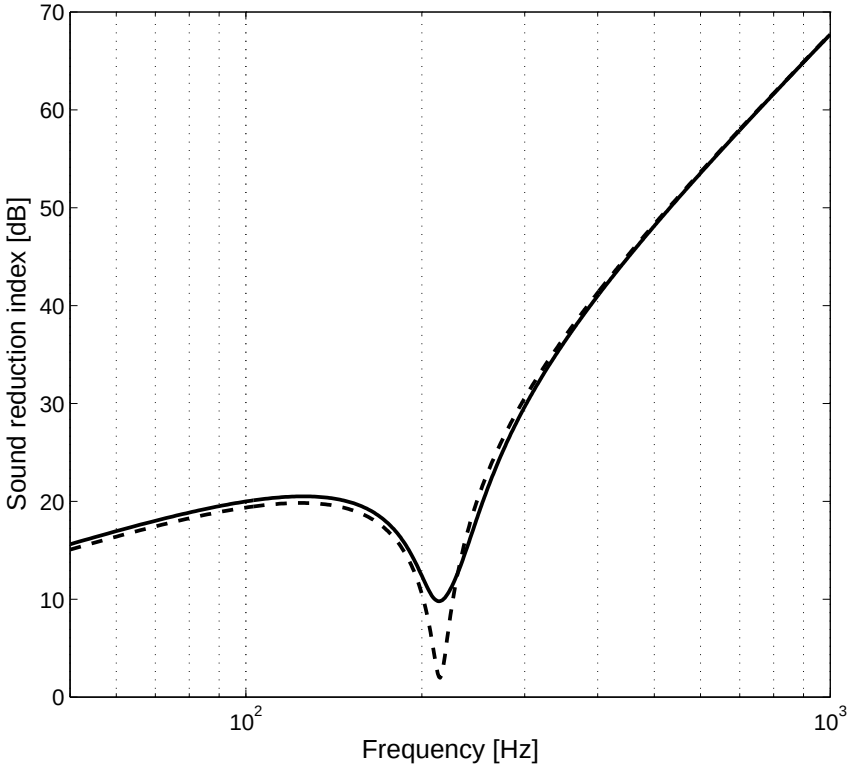

Figure 6.15: Sound reduction index of the host double panel partition with highly damped (η=0.3) two-sided vibration absorber ($\frac{s_1''}{s_2''}$=0.5) for normal sound incidence calculated by the mass-spring model. (- -) without; (–) with absorber

Additionally, Figure 6.16 shows the results of the sound transmission index for the intermediate damping loss factors of the vibration absorbers $\eta = 0.1$ and $\eta = 0.03$ in relation to the results of Figure 6.14. For this project it can be concluded, using two-sided vibration absorbers the sound transmission through the host structure under investigation can be reduced at the MAM-resonance by a minimum of approximately 8 dB. In the case of highly damped two-sided vibration absorbers, the MAM-resonance is even not split into two dips adjacent to the absorber resonance peak. Thus, highly damped two-sided vibration absorbers are a promising but limited

measure for reducing the MAM-resonance effect.

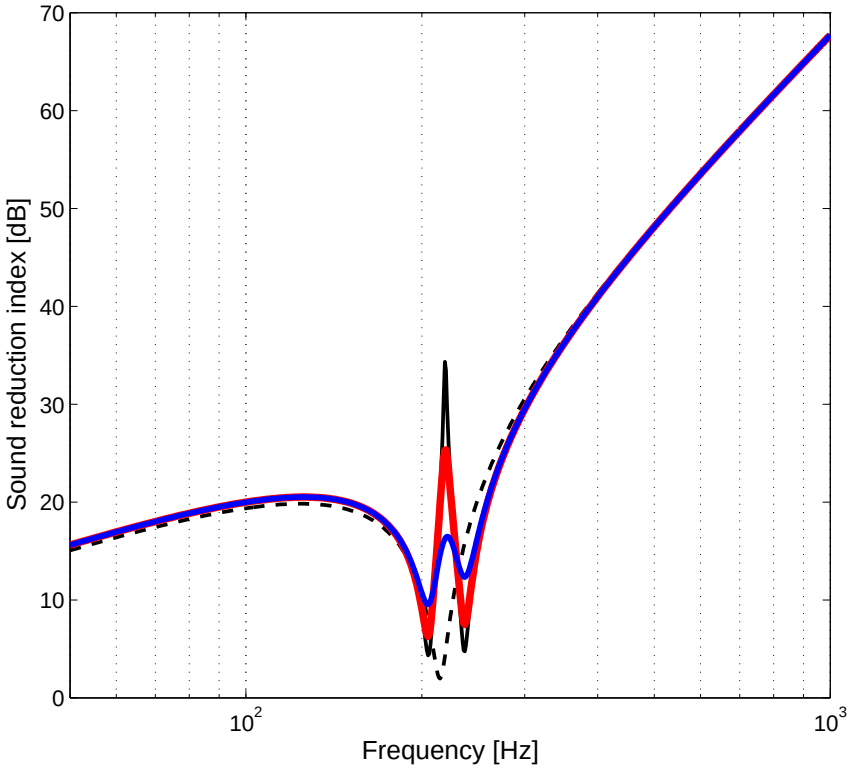

Figure 6.16: Sound reduction index of the host double panel partition with two-sided vibration absorber ($\frac{s_1''}{s_2''}$=0.5) for normal sound incidence calculated by the mass-spring model. The damping factors $\eta = 0.01$, $\eta = 0.03$ and $\eta = 0.1$ were assigned to the absorbers. (- -) without absorber; (-) η=0.01;(-) η=0.03;(-) η=0.1;

Next, for a 1 m long beam, a comparison of the sound reduction index with and without two-sided vibration absorber was calculated using the beam model. The internal absorbers were considered to be attached at discrete positions along the beams. Hence, the sound reduction index for the double panel structure with internal absorbers was calculated using the beam-model for continuous cavity spring and discrete vibrations absorbers (Equation 4.67).

For the beams and absorber springs the damping loss factor $\eta = 0.01$ was assigned. In this case, nine vibration absorbers with $\frac{s_1'}{s_2'} = 0.5$ and the total mass per unit length of 1 kg/m were equally spaced across the length of the structure. The calculated result is presented in Figure 6.17. It can be seen, that at normal sound incidence the peak due to the internal absorber appears at the tuned frequency at 215 Hz. For the chosen arrangement of nine absorbers per unit length, the sound reduction characteristic at frequencies above and below the MAM-resonance remained unchanged.

The beam model provides the possibility of fast computation of normal and oblique sound fields impinging on the structure. For this reason, in this thesis the influence of the two-sided vibration absorber on the sound reduction index was studied for normal and diffuse field sound incidence using the beam model. In Figure 6.18, the diffuse sound reduction index for the double panel partition with two-sided vibration absorbers is compared to the plain host double panel partition. It can be seen, that besides the typical absorber peak at 215 Hz, the internal absorbers have no further effect on the sound transmission behaviour of the host partition. The sound reduction index of the structure at higher frequencies and in particular at the coincidence frequency did not change.

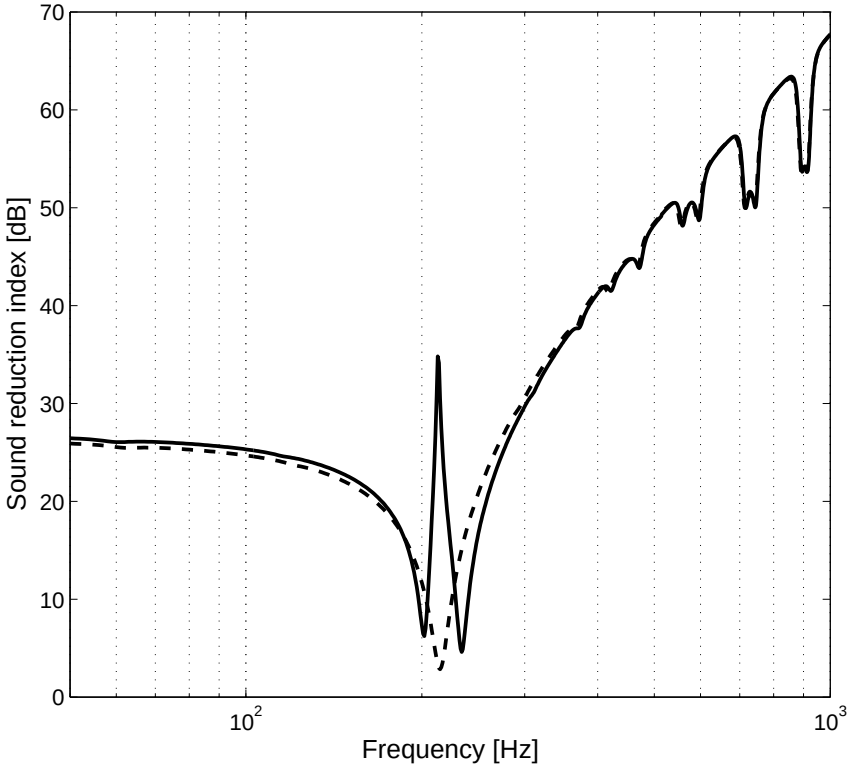

Figure 6.17: Sound reduction index of the host double panel partition with 9 equally spaced two-sided vibration absorbers ($\frac{s_1'}{s_2'}$=0.5) for normal sound incidence calculated by the beam model. (- -) without; (–) with absorber

Since the attached internal absorbers have low mass compared to the mass of the panels, this result complies with the general theory of a vibration absorber. The design of the implemented absorbers should not include too heavy absorber masses, since for high absorber masses the panels can be pinned at the positions of the internal absorbers [32]. The ripples above 600 Hz are due to the radiation of higher order modes at resonance. At the resonance frequencies of higher order modes, the sound reduction index is reduced below the dominating characteristic of the first fundamental panel mode at 2.5 Hz. Above 12000 Hz, the critical frequency of the steel

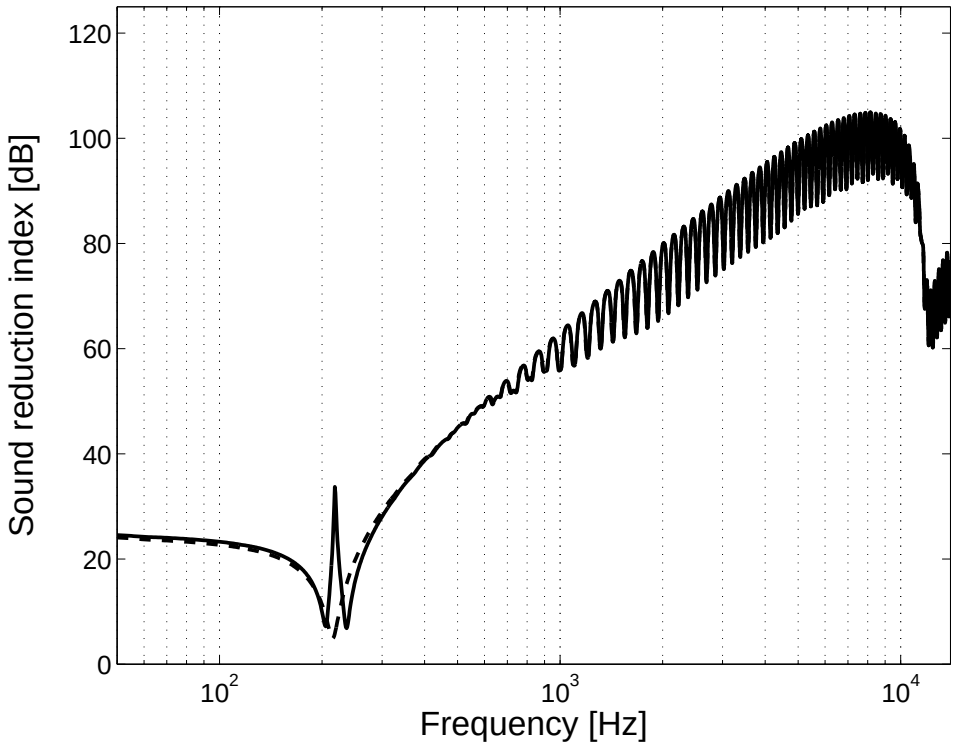

Figure 6.18: Sound reduction index of the host double panel partition with 9 equally spaced two-sided vibration absorbers ($\frac{s'_1}{s'_2}$=0.5) for diffuse sound incidence using the beam model. (- -) without; (–) with absorber

panels is evident but is not affected by the assigned absorber distribution.

The sound reduction index of the double panel partition with nine absorber systems was compared for normal sound incidence with diffuse sound incidence. This comparison is illustrated in Figure 6.19. At higher frequencies the sound reduction index for diffuse sound incidence shows the reduced characteristic as discussed in section 4.1.4. The differences in the sound reduction index for diffuse and normal sound incidence was not changed by the implementation of the two-sided vibration absorbers, see also Figure 4.7.

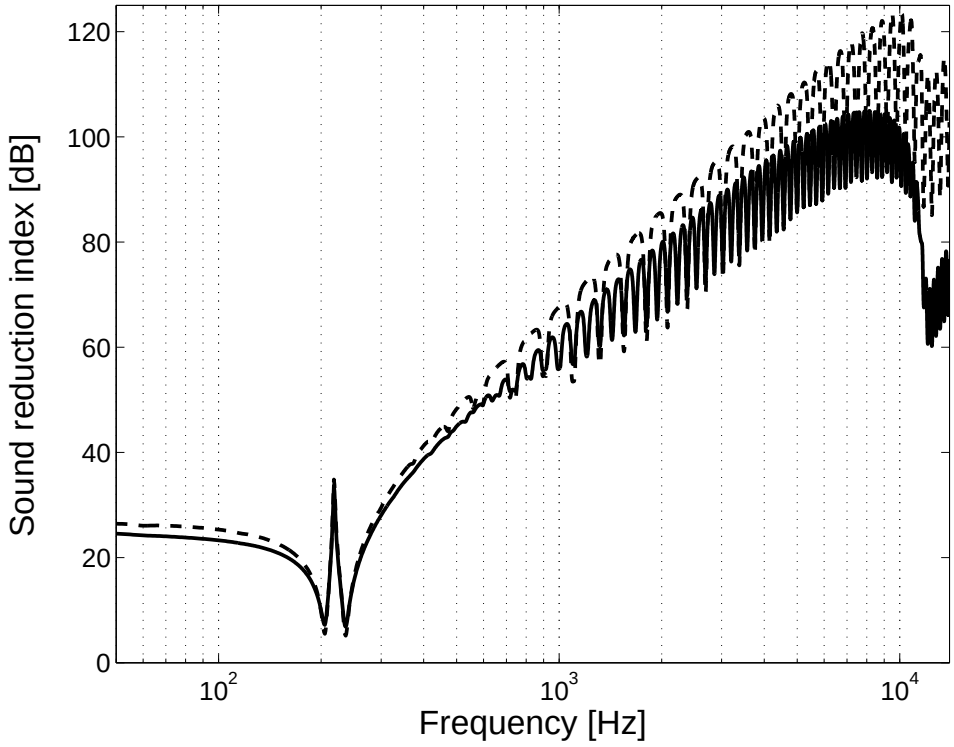

Figure 6.19: Comparison of the sound reduction index of the host double-panel partition with 9 equally spaced two-sided vibration absorbers ($\frac{s_1'}{s_2'}$=0.5) for normal and diffuse sound incidence using the beam model. (- -) normal sound incidence; (—) diffuse sound incidence

As a consequence, if the two-sided vibration absorber is tuned to the MAM-resonance, the internal absorber has negligible influence to the sound transmission at frequencies below and beyond the MAM-resonance frequency. Additionally, the behaviour of the internal vibration absorber is not changed by diffuse sound incidence.

The issue of number and position of the internal absorbers was studied for the first time using the plate model (section 5.2.2). With reference to the results for the mass and beam model presented above, the host double panel partition remained unchanged. The two-sided vibration absorbers

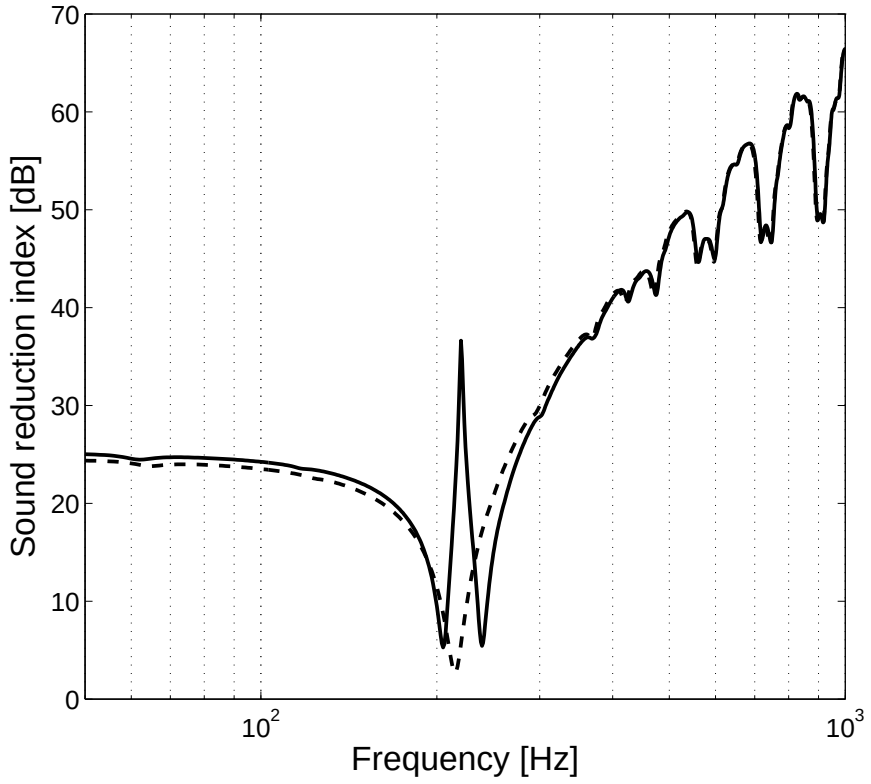

Figure 6.20: Sound reduction index of the host double panel partition with 140 two-sided vibration absorbers ($\frac{s_1}{s_2}$=0.5) for normal sound incidence using the plate model. (- -) without internal absorbers;(—) with 140 internal absorbers

had in total the mass of 1 kg per unit area and were tuned to the MAM-resonance using the spring ratio $\frac{s_1}{s_2} = 0.5$. As input for the plate model the double panel partition had the dimensions $1m$ x $1m$. The fundamental mode of the individual panels appears at 4.9 Hz. For normal sound incidence Figure 6.20 shows the calculated sound transmission index for the host double panel partition with 140 two-sided vibration absorbers. The absorbers were distributed throughout the panel area using a net of 10 equally spaced absorbers along the length times 14 equally spaced absorbers along the width of the panel. At the MAM-resonance, the plate model showed the expected absorber effect, which was already obtained by the

beam model, see Figure 6.17.

This is only true for a rather high density of attached vibration absorbers. The purpose of the plate model becomes more obvious when the number of absorbers is reduced to 35, shown in Figure 6.21.

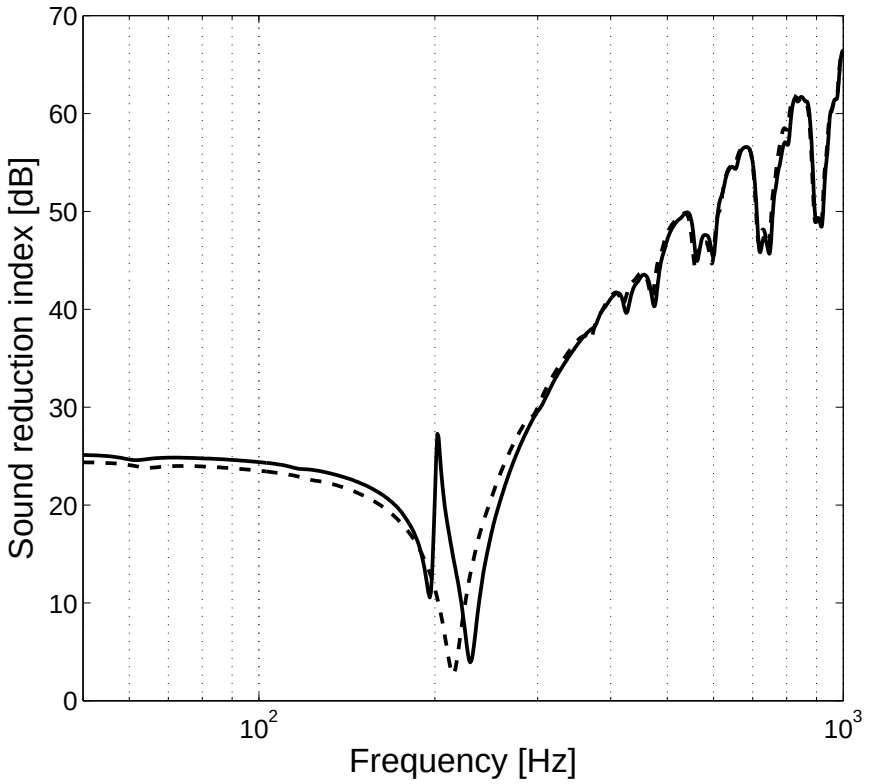

Figure 6.21: Sound reduction index of the host double panel partition with 35 two-sided vibration absorbers ($\frac{s_1}{s_2}$=0.5) for normal sound incidence using the plate model. (- -) without internal absorbers; (—) with 35 internal absorbers

This time the net of absorbers throughout the panel area was decided as 5 equally spaced absorbers along the length times 7 equally spaced ab-

sorbers along the width. The 35 two-sided vibration absorbers were again tuned to the MAM-frequency and the overall mass of the absorbers was kept at 1 kg/m^2. It can be seen, that due to the reduced number of vibration absorbers the resonance peak appears at a slightly lower frequency and is reduced in its amplitude. This effect is even increased, if only 25 equally distributed (5 x 5) two-sided vibration absorbers are implemented, see Figure 6.22.

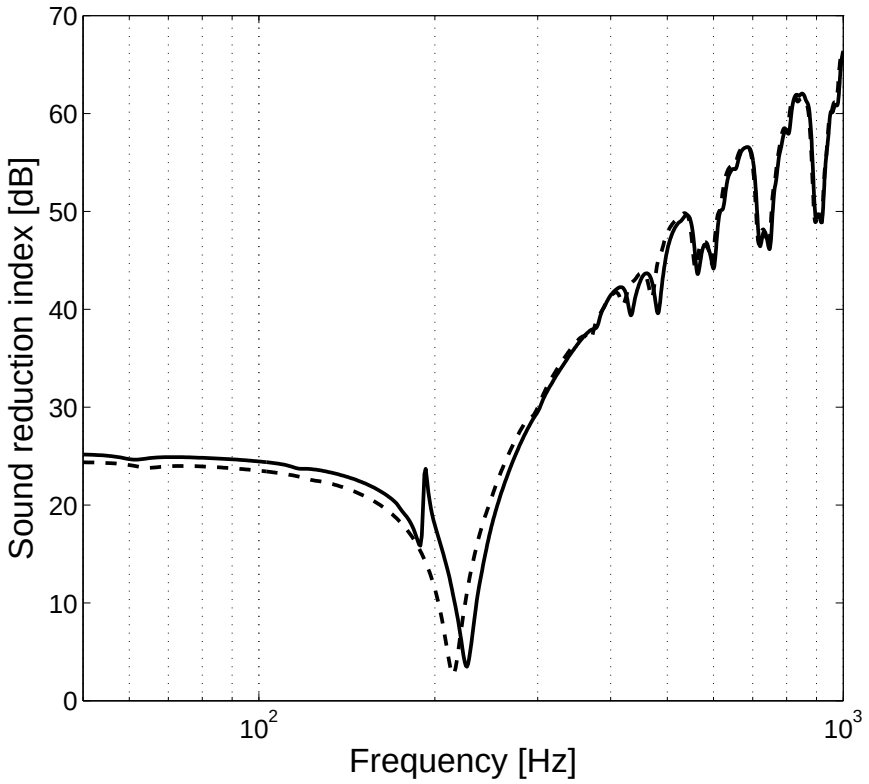

Figure 6.22: Sound reduction index of the host double panel partition with 25 two-sided vibration absorbers ($\frac{s_1}{s_2}$=0.5) for normal sound incidence using the plate model. (- -) without internal absorbers; (—) with 25 internal absorbers

It is assumed, a low number of vibration absorbers distributed across the area of the construction reduce only an insufficient number of lower order modes in their transverse amplitudes at 215 Hz. Accordingly, the overall transverse response of the radiating panel at the MAM-resonance remains almost unaffected. But this is only one possible explanation. The shift in the frequency of the absorber peak for a smaller number of absorbers can be an indication that a lower number of absorbers require a different absorber tuning. However, using Equation 6.2 for various absorber resonance frequencies across the MAM-resonance did not improve the result for 35 attached two-sided absorbers. On the other hand, any kind of relation between the number and tuning of the absorbers was not considered for the tuning approach of section 6.1. Therefore, an answer to this question needs to be investigated by further studies. With the results above for locally distributed internal absorbers this study has shown the expected influence due to a different number of locally attached absorbers. For further research on efficient distributions of the internal absorbers, this study provides the two dimensional plate model.

6.6 Wideband two-sided vibration absorber

The previous calculations showed the relation of amplitude and frequency bandwidth for the efficiency of lightweight two-sided vibration absorbers. In general, a vibration absorber is effective only over a relatively narrow frequency range. Increasing the damping will broaden the bandwidth of the absorber effect at the expense of a rapidly reduced resonance amplitude. Recently, another solution for a broadened effective bandwidth was

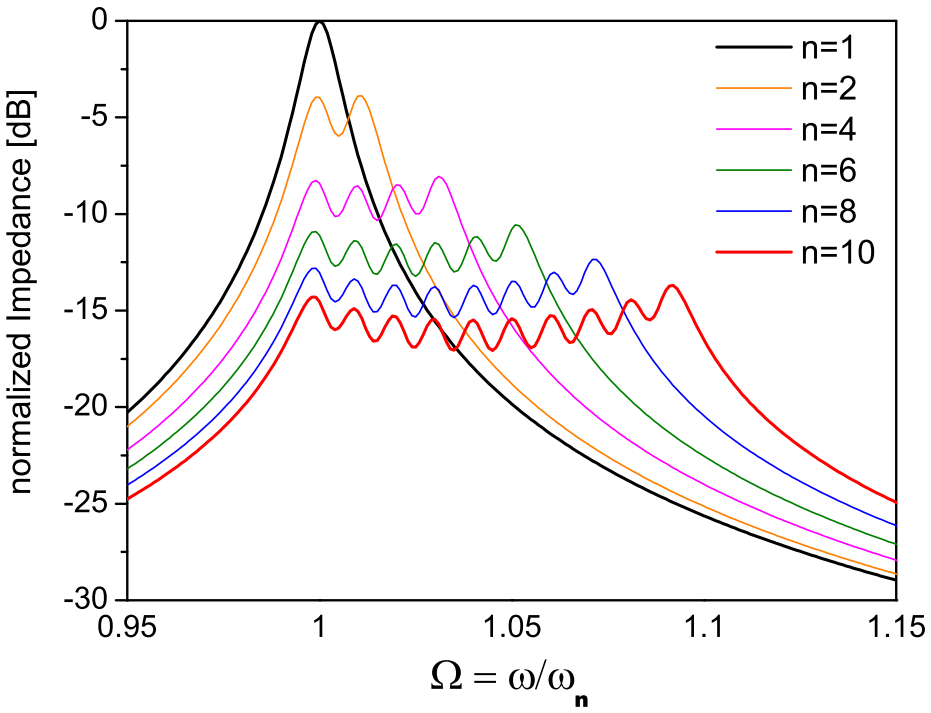

Figure 6.23: Normalized absorber resonance frequency for an array of 1-10 absorbers.

presented, which is called wideband vibration absorber. A wideband vibration absorber consists of an array of absorbers that are all tuned to slightly different resonance frequencies. The absorbers were attached at the same point of a flexible structure [79,80]. Based on the formulations of

Brennan [81], Figure 6.23 illustrates the dependence of the absorber resonance on the number of absorbers.

The origin of the idea of wideband vibration absorbers was found by an investigation of Heckl [82], who investigated the propagation of bending waves over a plate with one beam or with a periodic array of beams attached. Heckl showed that the damping of a beam was considerably increased over a wide frequency range by the attachment of many small cantilevered strips of various lengths. Strasberg and Feit [83] derived a simple expression for this kind of structures. The model considers the vibration damping induced in a large main structure by a multitude of small substructures attached to it, when each substructure is dissipating vibratory power at its frequencies of resonance. Most of the wideband vibration absorbers studied were composed of multiple sprung masses. Maidanik and Becker investigated wideband vibration absorbers using more elaborate satellite oscillator systems. They presented a linear impedance analysis [84] and an energy analysis [85].

Besides the wideband vibration neutralizer of Brennan [81], the idea of a wideband vibration absorber was subject of practical applications for example for the reduction of noise from a railway track [86] or even as sound absorber [87].

An array of two-sided vibration absorbers with multiple tuning frequencies can be also implemented into the cavity of a double panel structure. Furthermore, the idea of internal vibration absorbers possessed always a spatial aspect. Instead of attaching several multiple absorbers at the same points of the structure, it is suggested to achieve the effect of a wideband vibration absorber by distributing the absorbers with slightly different resonance frequency across the double panel structure. In order to achieve an equivalent wideband absorber effect, the single absorber systems of the wideband absorber have to be attached to locations with equal dynamic characteristic. Accordingly, at the MAM-resonance this approach depends

on the modes that are excited at the frequency of the MAM-resonance.

Using the mass-spring model for 4 differently tuned two-sided vibration absorbers (see section 6.1) with a damping loss factor η=0.01, Figure 6.24 presents the expected wideband absorber effect at the MAM-resonance. The total mass of the absorbers was kept constant with the previously used 1 kg/m^2. With the spring ratio $\frac{s_1}{s_2} = 0.5$ the absorbers were tuned to the four frequencies 205 Hz, 215 Hz, 225 Hz and 235 Hz.

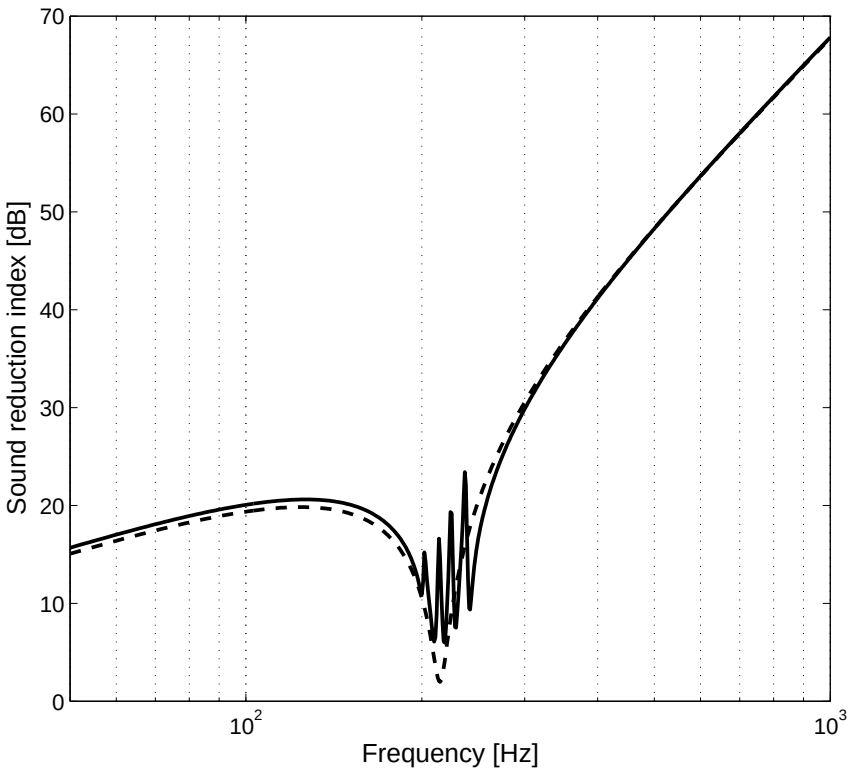

Figure 6.24: Wideband absorber effect at the MAM-resonance for 4 different two-sided vibration absorbers.(- -) without; (–) with absorber

In comparison to the absorber effect due to internal absorbers that are only tuned to an equal frequency, the wide band absorber achieves better results of a broader frequency range. For example, the minimums in Figure 6.24 are about 2 dB higher than for the narrow band absorbers in Figure 6.14.

Even if these improvements look rather low, for specific conditions at low frequencies such improvements can actually provide the required sound transmission loss that makes the application of a lightweight structure possible. For this reason, further research on complex distributions should either use the wideband vibration absorber attached at single points of the structure or realize the discussed spatial solution. However, this requires more information about the vibrational modes involved in the generation of the MAM-resonance and the corresponding influence of the two-sided vibration absorbers.

Chapter 7

Measurement

One essential aim of this thesis was to find experimental evidence for the existence of the absorber effect at low frequencies in the sound reduction index of double panel partitions. As mentioned in section 2.3, earlier measurements on double panel structures with mass inclusions did not show any effect in the sound transmission loss. These measurements were carried out in typical sound transmission laboratories which turned out to be just one step too early.

Therefore, at this early stage of the research on internal vibration absorbers, the experimental work of this thesis focused on fundamental results. Therefore, a precise experimental representation of the derived analytical models was not considered. Instead, the main efforts were spent on the first successful experimental generation of the absorber effect at the MAM-resonance. Accordingly, it was considered as sufficient to prove the existence of the absorber effect by comparing the measured radiated sound power level for a double panel structure with and without internal absorbers. It was also decided to start experimental investigations with samples based on a smaller scale instead of measuring realistic double panel partitions with the size of typical room dimensions. Thus, the use of the available sound transmission laboratories was not intended.

The following measurement was performed in a semi-anechoic chamber where the double panel structure was mounted into an opening of the room floor. The opening had the dimensions of 0.5 x 0.5 m. At 2.5 cm below the surface of the floor, each dimension is reduced by 1 cm. Regarding the required simply supported boundary conditions, Figure 7.1 shows a sketch of the double panel structure mounted into the opening. While the lower panel could be rested straight on the bottom frame of the opening the upper panel had to be rested on four wooden bars having the dimensions 0.5 x 0.5 x 2 cm. The four wooden bars were temporally fastened at the upper edge of the opening.

For the suggested suspension the maximum thickness of the structure was limited to the 2.5 cm between the lower suspension and the surface of the room floor. Only if the structure is mounted flat with the floor surface, a simply supported boundary condition with a sufficiently sound proof frame could be achieved at the boundaries of the upper panel.

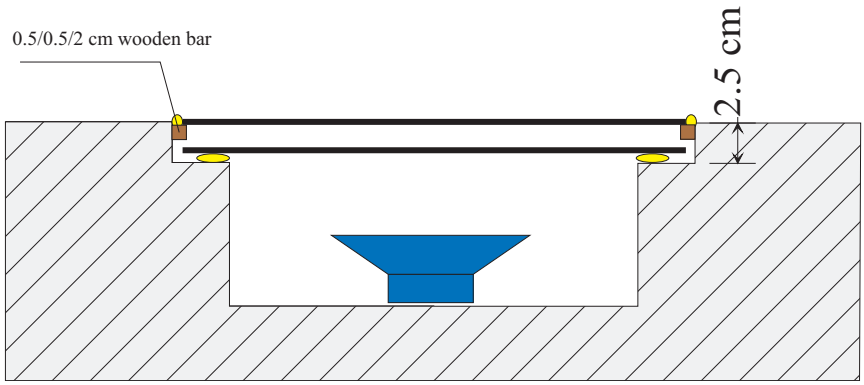

Figure 7.1: Sketch of mounted sample.

The double panel structure consisted of 1 mm thick steel panels with a mass per unit area of 7.8 kg/m^2. The cavity was suggested to be a 23 mm thick air cavity with no structural connections and a MAM-resonance at about 200 Hz. For such a thin cavity layer of only 23 mm and a corresponding MAM-resonance in the intended low frequency range, difficul-

ties were encountered for the selection of an appropriate absorber spring material. Using the tuning approach, for the two springs of the two-sided vibration absorber a resilient material (yellow Sylomer) with a Young's modulus E = 0.35 N/mm^2 and a damping loss factor η=0.23 was found. The previously discovered necessary asymmetry was realized by the absorber springs. The first spring had a layer thickness of 4 mm and the second spring a thickness of 10 mm. The cross sectional area of the two-sided vibration absorber with the dimensions 25 x 12 mm was 3 cm^2. For this area the 1 cm thick steel absorber mass had a weight of 25 g.

Figure 7.2: Open sample of double panel structure with two-sided vibration absorber.

An array of 63 equally spaced two-sided vibration absorbers (total mass 1.575 kg) were implemented in rows of 9 x 7 absorbers as shown in Figure 7.2 for the mounted sample.

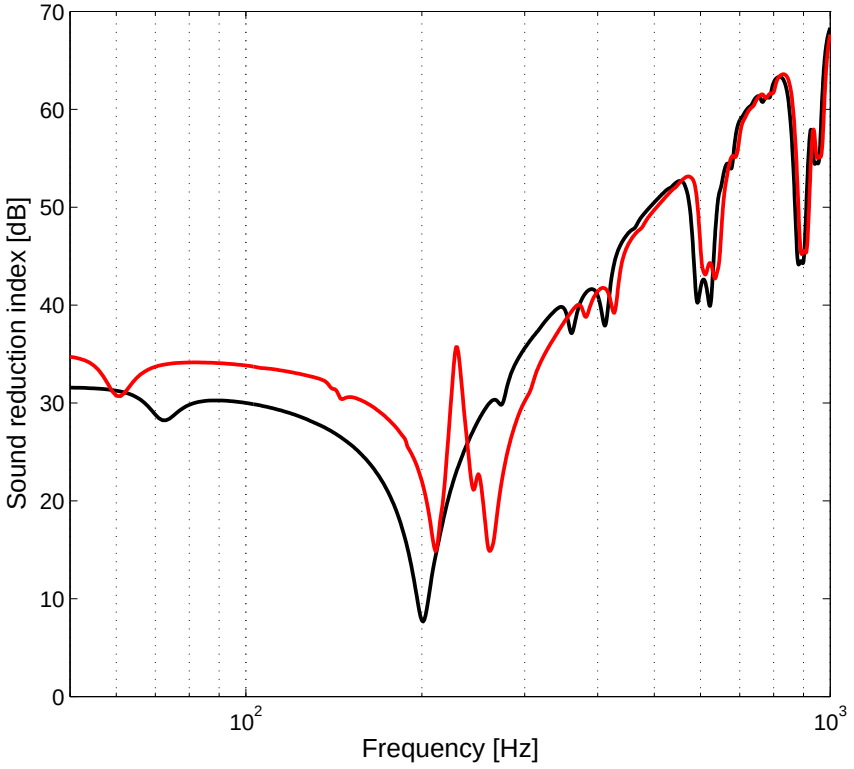

Figure 7.3: Plate model prediction of the measurement sample with lightly damped absorbers. (–) without absorbers; (–) with absorbers

Prior to the measurement, the sound reduction index was predicted using the plate model. Different to the actual two-sided vibration absorbers the tuning approach was first carried out for lightly damped absorbers with the low damping loss factor η=0.01. The predicted sound reduction index for the final configuration with lightly damped absorbers is shown in Figure 7.3.

In a second step, the sound reduction index was then predicted for the actual damping of the internal vibration absorbers, see Figure 7.4.

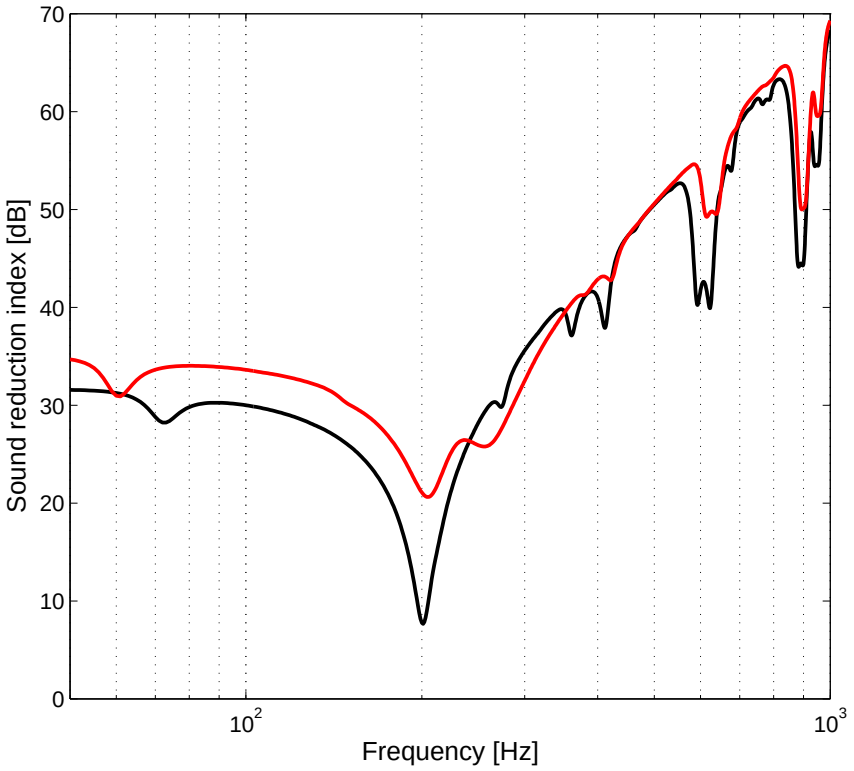

Figure 7.4: Plate model prediction of the actual measurement sample.
(–) without absorbers; (–) with absorbers

As far as the preparation of the measurement is concerned, both estimations revealed the necessary information for a first successful experimental detection of the absorber effect. However, due to the restrictions in the measurement set-up, material selection and the corresponding configuration of the internal vibration absorbers, the implementation of the two-sided vibration absorbers increased the total mass of the double panel structure by the mentioned amount of 1.575 kg. Since this is a mass increase to the sample structure of about 40 %, the calculated sound reduction

index of the double panel sample with implemented internal vibration absorber presented in Figure 7.3 and Figure 7.4 reveal an expected increase at low frequencies.

Figure 7.3 and Figure 7.4 illustrate an absorber effect in the sound reduction index next to the MAM-resonance. The amplitude was considered as sufficient for the detection of an influence on the radiated sound power. Consequently, the selected number of internal absorbers and the resulting absorber density was also assumed to be sufficient.

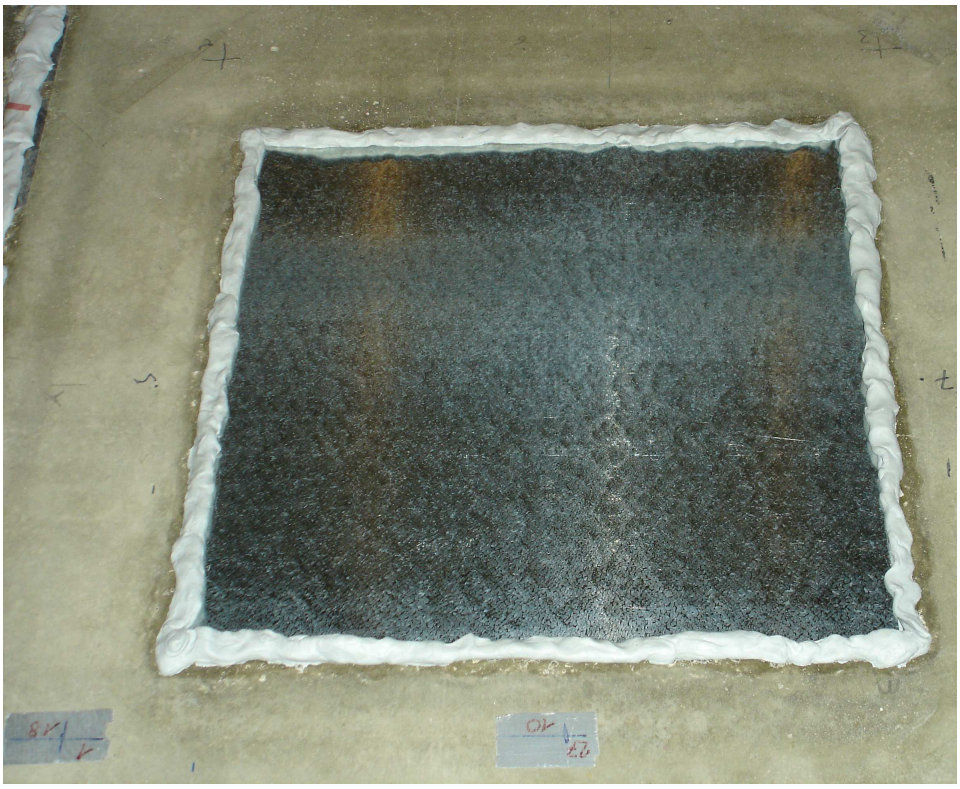

Figure 7.5: Closed measurement set-up.

The sound power measurements in the semi-anechoic chamber were carried out following the standard procedure of DIN EN ISO 3744 [88]. Above

the sample, the sound pressure was measured on a hemisphere with a radius of 2 m. The comparison of the measured sound power radiated by the sample with and without internal vibration absorbers is presented in Figure 7.6

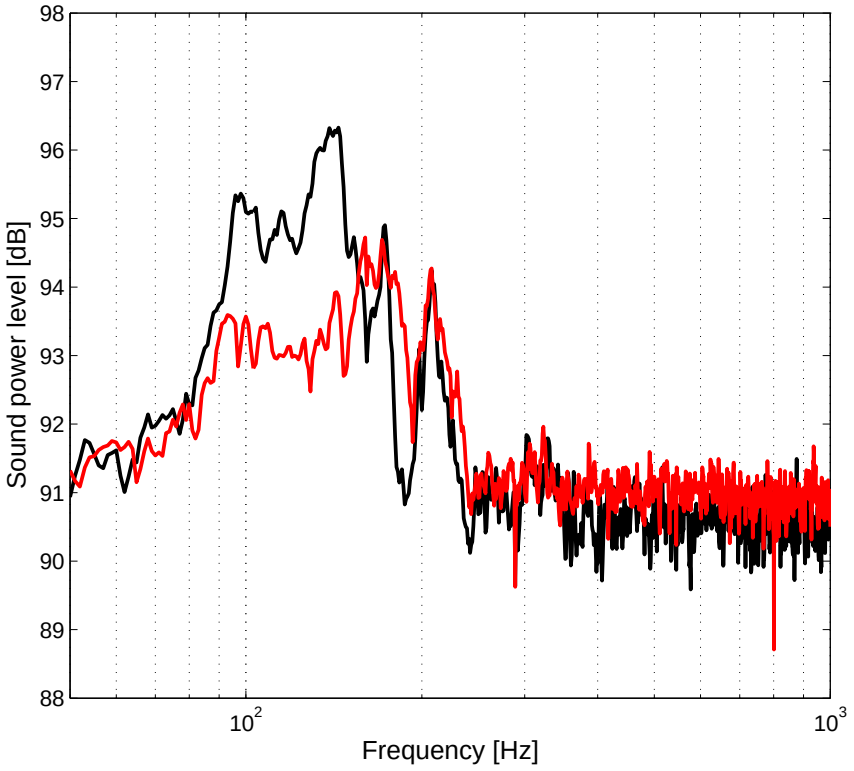

Figure 7.6: Comparison of the measured radiated sound power with and without implemented two-sided vibration absorbers. (–) without internal absorbers; (–) with the 63 internal absorbers

It can be seen that the implementation of two-sided vibration absorbers reduced the transmitted sound through the double panel structure at the MAM-resonance. Above, the tuning of the internal vibration absorbers used for the measurement was presented. With regards to this tuning of the absorbers it is assumed, that the reduction of the transmitted sound power in the frequency range between 90 and 150 Hz can be assigned to

the implemented two-sided vibration absorbers.

A complex issue in the measurement set-up was the edge of the upper panel of the structure which was mounted at the level of the floor surface (Figure 7.5). A significant amount of sound proof material was placed between the edge of the structure and the boundary of the opening. This was necessary to achieve a sufficient sound insulation and avoid the sound from escaping directly from the cavity without being transmitted through the upper panel. Unfortunately the sound proof material increased the total mass of the host structure and definitively the damping of the upper radiating panel. Therefore, the MAM-resonance of the host structure appeared in the frequency range from 90 Hz to approximately 150 Hz instead of the predicted 200 Hz.

With the measurement of the sound power and the difficulties in the measurement set-up a detailed analysis throughout the measured frequency range was impossible. The main conclusion is drawn from the comparison of the measured sound power at the frequency area where the two characteristics differ significantly. Except for the frequency range between 90 and 150 Hz the two sound power characteristics can be considered as identical. Since the structures of the two measurements were kept absolutely identical besides the implementation of the internal absorbers, the differences between the two sound power characteristics can be related to the internal absorbers. Although the two-sided vibration absorbers were originally tuned to a MAM-resonance frequency at 200 Hz, the internal absorbers still achieved a significant reduction of the actual MAM-resonance at the frequency range between 90 and 150 Hz. However, since the absorber resonance was tuned to a higher frequency, the absorbers were not excited at resonance but the remaining effect was still sufficient to assume the expected indication for a promising absorber effect.

Furthermore, due to constructional difficulties in the manual production of the layers for the absorber springs, the absorbers may differ in their

resonance frequencies and consequently spread over a broader frequency range. In this case, the resonance effect is reduced in the amplitude and appears over a broader frequency range. Therefore, the obtained results were also interpreted taking this constructional issues into account.

Unfortunately a resilient material with less damping factor that would have been suitable as absorber spring was not available. Such a spring material could have revealed a sharp absorber effect within a narrow frequency range.

Chapter 8

Summary and Outlook

This thesis analysed the implementation of internal vibration absorbers into double panel structures. Due to economical and environmental reasons many engineering areas have an increased demand for multi-layer lightweight constructions. Such multi-layer lightweight constructions generally provide sufficient sound transmission loss at higher frequencies but at low frequencies the sound transmission loss characteristic deteriorates significantly at the commonly known MAM-resonance.

Using internal vibration absorbers lightweight structures combine the benefits at higher frequencies with the frequency dependent effect of locally distributed internal resonators. At the beginning of this thesis a comprehensive literature research about fundamental and recent studies on sound transmission through partitions and the related research on smart materials was provided. The essential investigations over the last decades established the basis for innovative solutions regarding troublesome frequencies. In order to increase the sound transmission index at specific frequencies, several resonant concepts like Helmholtz-resonators, resonant sonic materials or vibration absorbers were applied on lightweight constructions. All of these studies have in common that they investigated these solutions only for high frequencies. Yet, there are no investigations taking lower frequencies and finite structures into account.

Based on the research of embedded masses, this study on internal vibration absorbers was initiated with a focus on the low frequency range and finite structures. Hence, this thesis investigated the implementation of vibration absorbers into the cavity of a double panel partition. Special interest was given to the MAM-resonance of the double panel partition. Considering the classical mass-spring attachment of vibration absorbers to panels, in the case of a double panel partition the internal vibration absorbers were attached to either of the two panels or to both panels.

However, this thesis focused on a so called two-sided vibration absorber. Regarding the research on sonic materials, the two-sided vibration absorber is attached to both panels of a double panel partition. Similar to embedded masses, the two-sided vibration absorber can simply be integrated into the resilient cavity material already at the factory. Hence, this thesis is different to earlier publications on mass inclusions, which only considered the typical system of a vibration absorber with one absorber mass attached to the structure by one spring, e.g. [54, 55, 66, 67, 89].

With the focus on low frequencies, this thesis is the first fundamental study on the novel implementation of internal vibration absorbers into the cavity of finite double panel structures. The intention of the thesis was therefore to establish a fundamental analysis of the effect of internal vibration absorbers. Using this analysis, the thesis had the major objective to find first experimental evidence for an increase of the sound transmission loss at the MAM-resonance due to the resonance of internal vibration absorbers.

Three analytical models were derived. With these models various assemblies of internal vibration absorbers were investigated by their influence on the sound reduction index of the double panel partition. For this purpose the models computed the transverse displacement of the structure and the corresponding sound radiation.

First, the significant physical principles of the implemented internal vibration absorbers were analysed by a mass-spring model. The mass-spring model considered the panels of the double panel host partition as lumped masses without flexural characteristics. The panels and the air gap were described as a coupled mechanical acoustical system. In order to take the modal behaviour of the two panels of the host structure into account, a one-dimensional beam model has been derived for the analysis of the transverse displacement of the double panel partitions with internal vibration absorbers. Based on the modal expansion method, the beam model is entirely modal considering the contribution of each mode over the frequency band of interest. By this means, the effect of internal vibration absorbers on the structure can be determined for different locations and numbers. As a third analytical model, a two-dimensional plate model was derived for the estimation of the effect of internal vibration absorbers distributed across a finite structure. Thus, by the plate model a comprehensive study on various two-dimensional distributions of internal absorbers can be carried out. Actually, it is possible to study the efficiency of internal vibration absorbers without extensive experimental efforts.

The results presented for a double panel partition with internal vibration absorbers revealed the sound reduction index of the double panel host partition is unchanged apart from close to the tuned absorber resonance. With a specific tuning approach the absorber effect was successfully tuned to the MAM-resonance. Depending on the damping and a required asymmetry in the structure, the application of internal vibration absorbers achieved a promising increase in the sound reduction index. In particular for a reduced sound transmission at the MAM-resonance, the internal vibration absorber is considered as a very efficient solution with all the benefits of passive vibration control. The higher the degree of asymmetry in the construction the higher the effect of the internal two-sided vibration absorber at the MAM-resonance.

The absorbers were exceptionally tuned to low frequencies which revealed an unaffected characteristic at the coincidence. There was also no difference between the effects for normal and diffuse sound incidence detected. Hence, it was concluded that the internal vibration absorbers can be easily combined with existing sound reduction solutions for higher frequencies, such as for the limitation of the coincidence effect.

Since the plate model requires high computational effort only a few results were presented for the verification of the model and the discussion on the number of internal absorbers. These results obtained the expected dependency on the number of the internal absorbers. The internal absorbers were attached at specific locations. Finally, the promising numerical results were extended by experimental evidence for a two-sided vibration absorber tuned to the MAM-resonance. The measurements were carried out in a semi-anechoic chamber. For the intended low-scale measurement set-up, the tuning approach of this thesis revealed difficulties in the material selection. The material selection is expected to be easier for larger samples. Hence, a comprehensive material survey can provide the foundation for measurements in ordinary sound transmission laboratories.

This thesis revealed essential analytical formulations, the principle of the mechanism and the potential of a frequency dependent increase of the sound reduction index of double panel partitions by the implementation of internal vibration absorbers. Based on these results, following investigations should focus on efficient and practical configurations of internal vibration absorbers. The sound transmission loss of intended measurement samples should still be predicted using the analysis of this thesis prior to any measurements in order to keep the experimental efforts on a low scale.

Subsequent analytical research on internal vibration absorbers requires an increased access to computational resources. This will make the plate model a very powerful analytical tool for the investigation of the distribution of implemented internal absorbers. The study on distributions should con-

centrate on the number and locations of the absorbers. Afterwards, attention can be given to an efficient design of each individual internal absorber.

All these further considerations should always find a frequency dependent increase in the sound transmission loss of the structure without a significant mass penalty due to the additional absorber masses. It is suggested to analyse distributions based on periodic, stochastic or pseudo-random distributions. In particular, pseudo-random maximum-length sequences are already successfully used in room acoustics for sound absorbers and diffusors.

This thesis also discussed the application of wideband vibration absorbers which should be continued. It is also expected to find interesting synergies with vibration control approaches that are studied in the area of active vibration control.

To sum up, once more it may be pointed out the fundamental character of the study presented in this thesis. The application of internal vibration absorbers implemented into the cavity of double panel constructions was studied for finite structures and low frequencies. The study established fundamental formulations for the prediction of the effect due to the attached internal vibration absorbers. Finally, this thesis accomplished a measurement of internal two-sided absorbers. It is concluded that using the provided analysis subsequent research on internal vibration absorbers can concentrate on specific commercial applications. The presented results revealed a promising influence of internal vibration absorbers on the sound reduction characteristic of double panel partitions. Particularly the two-sided vibration absorbers can be successfully implemented into the market as novel material for sound control.

Appendix A

Plate model:One-sided vibration absorber

A.1 Continuous vibration absorber

Using the angular resonance frequencies of the vibration absorbers $\omega_{r1}^2 = \frac{s_1''}{m_{r1}''}$ and $\omega_{r2}^2 = \frac{s_2''}{m_{r2}''}$, the continuous one-sided vibration absorbers are implemented into the plate model by Equation 4.57. Therefore, the matrix formulation describing the double panel partition with continuous cavity spring and continuously distributed internal vibration absorbers is obtained by the plate model as

$$\left(-\omega^2 \mathbf{M}_{nm} + \mathbf{K}_{nm}\right) \mathbf{q}_{nm} = \mathbf{Q}_{nm} \tag{A.1}$$

where for oblique incidence

$$\mathbf{M}_{nm} = \frac{A}{4} \begin{bmatrix} m_1'' - i\frac{\rho_0 c_0}{\omega \cos\theta} & 0 \\ 0 & m_2'' - i\frac{\rho_0 c_0}{\omega \cos\theta} \end{bmatrix},$$

$$\mathbf{q}_{nm} = \begin{bmatrix} q_{1,nm} \\ q_{2,nm} \end{bmatrix}, \mathbf{Q}_{nm} = \begin{bmatrix} Q_{nm} \\ 0 \end{bmatrix}.$$

The generalized pressure force Q_{nm} was derived in Equation 5.17.

The stiffness matrix $\mathbf{K}_{nm}$ in Equation A.1 is given by

$$\mathbf{K}_{nm} = \begin{bmatrix} D_1 k_{nm}^4 \frac{A}{4} + s_c'' \frac{A}{4} + \frac{\omega_{r1}^2 m_{r1}''}{1-\frac{\omega_{r1}^2}{\omega^2}} & -s_c'' \frac{A}{4} \\ -s_c'' \frac{A}{4} & D_2 k_{nm}^4 \frac{A}{4} + s_c'' \frac{A}{4} + \frac{\omega_{r2}^2 m_{r2}''}{1-\frac{\omega_{r2}^2}{\omega^2}} \end{bmatrix}.$$

A.1.1 Continuous cavity spring and discrete vibration absorbers

The plate model for the double panel partition with locally distributed one-sided internal vibration absorbers is shown in Figure A.2.

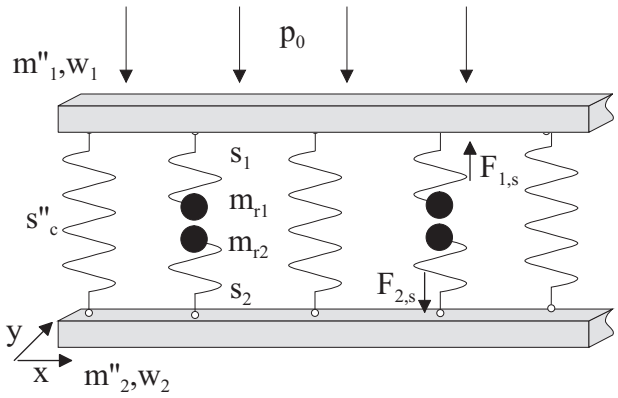

Figure A.2: Plate model of a double panel partition with continuous cavity spring and discrete one-sided vibration absorbers.

For J internal one-sided vibration absorbers attached at the positions x_s, y_s the plate model of the double panel host partition is obtained as

$$\left(-\omega^2\mathbf{M}+\mathbf{K}\right)\mathbf{q}=\mathbf{Q} \tag{A.2}$$

where the stiffness matrix is written as

$$\mathbf{K}=\begin{bmatrix} \mathbf{K_1}+\mathbf{S_c}+\frac{\omega_{r1}^2 m_{r1}}{1-\frac{\omega_{r1}^2}{\omega^2}}\mathbf{\Phi}\mathbf{\Phi}^\mathbf{T} & -\mathbf{S_c} \\ -\mathbf{S_c} & \mathbf{K_2}+\mathbf{S_c}+\frac{\omega_{r2}^2 m_{r2}}{1-\frac{\omega_{r2}^2}{\omega^2}}\mathbf{\Phi}\mathbf{\Phi}^\mathbf{T} \end{bmatrix},$$

with the diagonal matrices

$$\mathbf{K_i}=\frac{A}{4}\begin{bmatrix} D_i k_{nm}^4 & 0 \\ 0 & \ddots \end{bmatrix}, \mathbf{S_c}=\frac{A}{4}\begin{bmatrix} s_c'' & 0 \\ 0 & \ddots \end{bmatrix}$$

and the mode shape matrix $\mathbf{\Phi}=\begin{bmatrix} \Phi_{nm,j} & \cdots \\ \vdots & \ddots \end{bmatrix}$.

The mass matrix is given by

$$\mathbf{M}=\begin{bmatrix} \mathbf{M_1}-i\frac{\rho_0 c_0 A}{4\omega\cos\theta} & 0 \\ 0 & \mathbf{M_2}-i\frac{\rho_0 c_0 A}{4\omega\cos\theta} \end{bmatrix} \text{ with } \mathbf{M_i}=\frac{A}{4}\begin{bmatrix} m_{i,nm}'' & 0 \\ 0 & \ddots \end{bmatrix}.$$

The vectors are $\mathbf{q}=\begin{pmatrix}\mathbf{q_1}\\ \mathbf{q_2}\end{pmatrix}$ and $\mathbf{Q}=\begin{pmatrix}\mathbf{Q}_{nm}\\ \mathbf{0}\end{pmatrix}$ which include vectors for the generalized amplitudes $\mathbf{q_1}$, $\mathbf{q_2}$ and for the generalized pressure force $\mathbf{Q}_{nm}$, see Equation 5.26.

Appendix B

Derivation of Equation 6.2

The mass-spring model for the host double panel structure with two-sided vibration absorber as shown in Figure 3.9 is described by the following equations of motion (see Equation 3.20).

$$i\omega_r(m_1'' - i\frac{\rho_0 c_0}{\omega_r})v_1 + \frac{1}{i\omega_r}(s_c'' + s_1'')v_1 - \frac{1}{i\omega_r}s_1''v_r - \frac{1}{i\omega_r}s_c''v_2 = F_1 \quad \text{(B.1a)}$$

$$i\omega_r m_r''v_r - \frac{1}{i\omega_r}s_1''v_1 + \frac{1}{i\omega_r}(s_1'' + s_2'')v_r - \frac{1}{i\omega_r}s_2''v_2 = 0 \quad \text{(B.1b)}$$

$$i\omega_r(m_2'' - i\frac{\rho_0 c_0}{\omega_r})v_2 - \frac{1}{i\omega_r}s_c''v_1 - \frac{1}{i\omega_r}s_2''v_r + \frac{1}{i\omega_r}(s_2'' + s_c'')v_2 = 0 \quad \text{(B.1c)}$$

Solving Equation B.1b and Equation B.1c for v_1 and v_r yields

$$v_1 = \frac{\frac{\omega_r^4 m_r''(m_2'' - i\frac{\rho_0 c_0}{\omega_r})}{s_1'' s_2''}v_2 - \frac{\omega_r^2 m_r'' s_c''}{s_1''^2}v_2 - \frac{\omega_r^2 m_r''}{s_1''}v_2 - \frac{\omega_r^2 m_r'' s_c''}{s_1'' s_2''}v_2}{1 - \frac{\omega_r^2 s_c'' m_r''}{s_1'' s_2''} + \frac{s_c''}{s_2''} + \frac{s_c''}{s_1''}} \quad \text{(B.2a)}$$

$$v_r = \frac{-\frac{\omega_r^2(m_2'' - i\frac{\rho_0 c_0}{\omega_r})}{s_2''}v_2 + \frac{s_c''}{s_1''}v_2 + v_2 + \frac{s_c''}{s_2''}v_2}{1 - \frac{\omega_r^2 s_c'' m_r''}{s_1'' s_2''} + \frac{s_c''}{s_2''} + \frac{s_c''}{s_1''}} \quad \text{(B.2b)}$$

Substitution of Equation B.2a and Equation B.2b for v_1 and v_r into Equation B.1a leads for $\frac{v_2}{F_1} = 0$ to

$$\frac{v_2}{F_1} = 0 = 1 - \frac{\omega_r^2 s_c'' m_r''}{s_1'' s_2''} + \frac{s_c''}{s_2''} + \frac{s_c''}{s_1''} \tag{B.3}$$

Thus, the tuning equation Equation 6.2 is given by

$$\omega_r^2 = \frac{s_c''(s_1'' + s_2'') + s_1'' s_2''}{m_r'' s_c''}. \tag{B.4}$$

References

[1] **Cremer, L.**, *Theorie der Schalldämmung dünner Wände bei schrägem Einfall*, Akustische Zeitschrift, Vol. 7, pp. 81–104, 1942.

[2] **Fahy, F.**, Sound and structural vibration: Radiation, Transmission and Response, Academic Press, London, 1987, pp. 69; 156; 166; 173.

[3] **London, A.**, *Transmission of reverberant sound through single walls*, Journal of the National Bureau of Standards, Vol. 42, pp. 605–615, 1949.

[4] **Sewell, E.**, *Transmission of reverberant sound through a single-leaf partition surrounded by an infinite rigid baffle*, Journal of Sound and Vibration, Vol. 12, pp. 21–32, 1970.

[5] **Beranek, L. L.** and **Work, G. A.**, *Sound transmission through multiple structures containing flexible blankets*, J. Acoust. Soc. Am., Vol. 21, pp. 419–428, 1949.

[6] **London, A.**, *Transmission of reverberant sound through double walls*, J. Acoust. Soc. Am., Vol. 22, pp. 270–279, 1950.

[7] **Mulholland, K. A., Parbrook, H.** and **Cummings, A.**, *The transmission loss of double panels*, Journal of Sound and Vibration, Vol. 6, pp. 324–334, 1967.

[8] **Cummings, A.** and **Mulholland, K. A.**, *The transmission loss of finite sized double panels in a random incidence sound field*, Journal of Sound and Vibration, Vol. 8, pp. 126–133, 1968.

[9] **Pierce, A. D.**, Acoustics, An introcution to its physical principles and applications, Acoustical Society of America, New York, 3rd edn., 1994, p. 279.

[10] **White, P.** and **Powell, A.**, *Transmission of random sound and vibration through a rectangular double wall*, J. Acoust. Soc. Am., Vol. 40, pp. 821–832, 1966.

[11] **Crocker, M. J.** and **Price, A. J.**, *Sound transmission using statistical energy analysis*, Journal of Sound and Vibration, Vol. 9, pp. 469–486, 1969.

[12] **Price, A. J.** and **Crocker, M. J.**, *Sound transmission through double panels using SEA*, J. Acoust. Soc. Am., Vol. 47, pp. 683–693, 1970.

[13] **Elmallawany, A.**, *Criticism of statistical energy analysis for the calculation of sound insolation - part 2: double partitions*, Applied Acoustics, Vol. 13, pp. 33–41, 1980.

[14] **Steel, J. A.** and **Craik, R. J. M.**, *Statistical energy analysis of structure-borne sound transmission by finite element methods*, Journal of Sound and Vibration, Vol. 178, No. 4, pp. 553–561, 1994.

[15] **Craik, R. J. M., Nightingale, T. R. T.** and **Steel, J. A.**, *Sound transmission through a double leaf partition with edge flanking*, J. Acoust. Soc. Am., Vol. 101, No. 2, pp. 964–969, 1997.

[16] **Craik, R. J. M.** and **Smith, R. S.**, *Sound transmission through double leaf lightweight partitions Part I: airborne sound*, Applied Acoustics, Vol. 61, pp. 223–245, 2000.

[17] **Gösele, K.**, *Zur Berechnung der Luftschalldämmung von doppelschaligen Bauteilen*, Acustica, Vol. 45, pp. 218–227, 1980.

[18] **Fahy, F.**, Foundations of engineering acoustics, Academic Press, New York, 2001, pp. 337; 149-153; 324-328.

[19] **Bolton, J. S., Shiau, N. M.** and **Kang, Y. J.**, *Sound transmission through multi-panel structures lined with elastic porous materials*, Journal of Sound and Vibration, Vol. 191, No. 3, pp. 317–347, 1996.

[20] **Biot, M. A.**, *Theory of propagation of elastic waves in a fluid-saturated porous solid. I. Low-frequency range. II. Higher frequency range*, J. Acoust. Soc. Am., Vol. 28, pp. 168–191, 1956.

[21] **Allard, J. F., Depollier, C.** and **Lauriks, W.**, *Measurement and prediction of surface impedance at oblique incidence of a plastic foam of high flow resistivity*, Journal of Sound and Vibration, Vol. 132, No. 1, pp. 51–60, 1989.

[22] **Skelton, E. A.** and **James, J. H.**, *Acoustics of anisotropic planar layered media*, Journal of Sound and Vibration, Vol. 152, No. 1, pp. 157–174, 1992.

[23] **Maysenhölder, W.**, *LAYERS - ein Werkzeug zur Untersuchung der Schalldämmung von Platten aus homogenen anisotropen Schichten*, IBP-Mitteilung 26, 420, Fraunhofer-Institute of Building Physics, 1999.

[24] **Au, A.** and **Byrne, K.**, *On the insertion loss produced by plane acoustic lagging structures*, J. Acoust. Soc. Am., Vol. 82, pp. 1325–1333, 1987.

[25] **Ver, I.**, *Interaction of sound waves with solid structures*, *Vibration Control Engineering (eds.)*, edited by Beranek, L. and Ver, I., John Wiley and Sons Inc., New York, 1992.

[26] **Möser, M.**, *Eine Theorie zur Schalldämmung von Doppelwänden unter Berücksichtigung der Randeinspannung*, Fortschrittsberichte der VDI Zeitschriften, Reihe 4: Bauingenieurwes., 1983.

[27] **Mehra, S.**, Berechnung der Luftschalldämmung von einschaligen Trennbauteilen endlicher Abmessung, Phd dissertation, University of Stuttgart, 1995.

[28] **Petyt, M.** and **Jones, C.**, *Numerical methods in acoustics*, *Advanced applications in acoustics, noise and vibration*, edited by Fahy, F. and Walker, J., p. 53ff, SPON Press, London, 2004.

[29] **Osipov, A., Mees, P.** and **Vermeir, G.**, *Low-frequency airborne sound transmission through single partitions in buildings*, Applied Acoustics, Vol. 52, No. 3/4, pp. 273–288, 1997.

[30] **Maluski, S.** and **Gibbs, B.**, *Application of a finite-element model to low frequency sound insulation in dwellings*, J. Acoust. Soc. Am., Vol. 108, No. 4, pp. 1741–1751, 2000.

[31] **Sgard, F., Atalla, N.** and **Nicolas, J.**, *A numerical model for the low frequency diffuse field sound transmission loss of double wall sound barriers with elastic porous linings*, J. Acoust. Soc. Am., Vol. 108, No. 6, pp. 2865–2872, 2000.

[32] **Mead, D. J.**, Passive vibration control, Wiley, New York, 2000, pp. 35ff; 237; 369; 268.

[33] **Fahy, F.** and **Walker, J.**, Fundamentals of noise and vibration, SPON Press, London, 1998, pp. 282; 283; 288.

[34] **Enger, J.** and **Vigran, T. E.**, *Transmission loss of double partitions containing resonant absorbers*, Proceeding of The Institute of Acoustics, Vol. 7, No. 2, pp. 125–128, 1985.

[35] **Mason, J. M.** and **Fahy, F. J.**, *The use of acoustically tuned resonators to improve the sound transmission loss of double-panel partitions*, Journal of Sound and Vibration, Vol. 124, No. 2, pp. 367–379, 1988.

[36] **Prydz, R. A. et al.**, *Transmission loss of a multilayer panel with internal tuned helmholtz-resonators*, J. Acoust. Soc. Am., Vol. 87, No. 4, pp. 1597–1602, 1990.

[37] **Munjal, M. L.**, *Response of a multi-layered infinite plate to an oblique plane wave by means of transfer matrices*, Journal of Sound and Vibration, Vol. 162, No. 2, pp. 333–343, 1993.

[38] **Mao, Q.** and **Pietrzko, S.**, *Control of sound transmission through double wall partitions using optimally tuned helmholtz resonators*, Acta Acustica united with Acustica, Vol. 91, pp. 723–731, 2005.

[39] **Estève, S. J.** and **Johnson, M. E.**, *Adaptive helmholtz resonators and passive vibration absorbers for cylinder interior noise control*, Journal of Sound and Vibration, Vol. 288, pp. 1105–1130, 2005.

[40] **Ladner, P., Mazoyer, T.** and **Périsse, J.**, *Acoustic splitter development based on hollow spheres materials for aircraft engine application*, *Proceedings of Euronoise*, p. ID: 431, Naples, 2003.

[41] **Iwao, K., Asahara, Y., Yamazaki, I.** and **Yashiro, H.**, *Study of the sound insulation panel with ventilation holes*, JSME Journal, Vol. 40, No. 4, pp. 616–622, 1997.

[42] **Iwao, K., Shimpo, Y., Yashiro, H.** and **Nishikawa, S.**, *Aplication of a sound insulation panel with ventilation holes to the engine under-cover*, JSAE Review, Vol. 19, pp. 243–249, 1998.

[43] **Rayleigh, J. W. S.**, *On the remarkable phenomenon of crystalline reflexion described by Prof. Stokes*, Phil. Mag., Vol. 26, pp. 256–265, 1888.

[44] **Liu, Z. et al.**, *Locally resonant sonic materials*, Science, Vol. 289, pp. 1734–1736, 2000.

[45] **Ho, K. M., Yang, Z., Zhang, X. X.** and **Sheng, P.**, *Measurements of sound transmission through panels of locally resonant materials between impedance tubes*, Applied Acoustics, Vol. 66, pp. 751–765, 2005.

[46] **Maysenhölder, W.**, *Transmission loss of inhomogeneous plates with local resonators: Methods of theoretical modeling*, *Forum Acousticum*, Sevilla, 2002.

[47] **Maysenhölder, W.**, *Sound transmission through periodically inhomogeneous plates: Generalizations of Cremer's thin plate theory*, Acustica, Vol. 84, pp. 668–680, 1998.

[48] **Maysenhölder, W.**, *HYPERAKUS - ein Werkzeug zur Untersuchung der Schalldämmung von periodisch strukturierten Wänden*, IBP-Mitteilung 25, 330, Fraunhofer-Institute of Building Physics, 1998.

[49] **Chen, S., Tang, T.** and **Wang, Z.**, *The mechanical models of the local resonance phenomenon in one-dimensional phononic crystals*, Acta Acustica united with Acustica, Vol. 93, pp. 31–36, 2007.

[50] **Maysenhölder, W.**, *Transmission loss of plates with internal resonators modelled by harmonic oscillators with frequency dependent complex mass and spring stiffness*, *Euronoise*, Naples, 2003.

[51] **Viktorova, R. N.** and **Tyutekin, V. V.**, *Physical foundation for synthesis of sound absorbers using complex-density composites*, Acoustical Physics, Vol. 44, No. 3, pp. 275–280, 1998.

[52] **Krynkin, S. V.** and **Tyutekin, V. V.**, *Optimization of the parameters of sound-absorbing materials made on the basis of rubberlike media with heavy inclusions*, Acoustical Physics, Vol. 48, No. 4, pp. 458–466, 2002.

[53] **Xiao, W., Zeng, G.** and **Cheng, Y.**, *Flexural vibration band gaps in a thin plate containing a periodic array of hemmed discs*, Applied Acoustics, Vol. 69, pp. 255–261, 2008.

[54] **Kidner, M., Fuller, C.** and **Gardner, B.**, *Increase in transmission loss of single panels by addition of mass inclusions to a poro-elastic layer: Experimental investigation*, Journal of Sound and Vibration, Vol. 294, pp. 466–472, 2006.

[55] **Idrisi, K., Johnson, M., Toso, A.** and **Carneal, J.**, *Increase in transmission loss of a double panel system by addition of mass inclusions to a poro-elastic layer: A comparison between theory and experiment*, Journal of Sound and Vibration, Vol. 323, pp. 51–66, 2009.

[56] **Weith, W.** and **Petersson, B.**, *Wave propagation in periodic microstructure-composite*, *Proc. 11th International Congress of Sound and Vibration*, pp. 3637–3644, St. Petersburg, 2004.

[57] **Weith, W.** and **Petersson, B.**, *Bending wave propagation in plates with embedded resonant inserts*, *Proc. IX International Conference on Recent Advances in Structureal Dynamics*, Southampton, 2006, no. 104.

[58] **Weith, W.** and **Petersson, B.**, *Körperschall-Reduktion in periodischen Mikrostruktur-Kompositen*, *DAGA Conference*, München, 2005.

[59] **Weith, W.** and **Petersson, B.**, *Manipulation von Biegewellen in Platten mit anti-resonanten Mikro-Struktur-Kompositen*, *DAGA Conference*, Braunschweig, 2006.

[60] **Hettler, S.**, Acoustical behaviour of inhomogeneous structures and plates, Master's thesis, University of Southampton, 2003.

[61] **Ormondroyd, J.** and **Den Hartog, J. P.**, *Theory of the dynamic vibration absorber*, Tans. ASME, Vol. 50, pp. 9–22, 1928.

[62] **Brennan, M. J.** and **Dayou, J.**, *Global control of vibration using a tunable vibration neutralizer*, Journal of Sound and Vibration, Vol. 232, No. 3, pp. 585–600, 2000.

[63] **Dayou, J.** and **Brennan, M. J.**, *Global control of structural vibration using multiple-tuned tunable vibration neutralizers*, Journal of Sound and Vibration, Vol. 258, No. 2, pp. 345–357, 2002.

[64] **Efimtsov, B. M.** and **Lazarev, L. A.**, *Sound transmission of panels with resonant elements*, Acoustical Physics, Vol. 47, No. 3, pp. 291–296, 2001.

[65] **Efimtsov, B. M.** and **Lazarev, L. A.**, *Analysis of the sound transmission loss of panels with resonant systems on the basis of equivalent representations*, Acoustical Physics, Vol. 51, No. 3, pp. 300–305, 2005.

[66] **Huang, Y. M.** and **Fuller, C. R.**, *The effects of dynamic absorbers on the forced vibration of a cylindrical shell and its coupled interior sound field*, Journal of Sound and Vibration, Vol. 200, pp. 401–418, 1997.

[67] **Efimtsov, B. M.** and **Lazarev, L. A.**, *Acoustic field in a closed layered shell with resonant systems*, Acoustical Physics, Vol. 52, No. 1, pp. 43–49, 2006.

[68] **Gösele, K.**, *Verbesserung des Schallschutzes von Holzbauteilen durch Schwingungstilger ("akustische Blutegel")*, Bauphysik, Vol. 24, No. 2, pp. 93–101, 2002.

[69] **Cremer, L.**, *Theorie des Klopfschalles bei Decken mit schwimmendem Estrich*, Acustica, Vol. 2, pp. 167–178, 1952.

[70] **Kropp, W.** and **Rebillard, E.**, *On the air-borne sound insulation of double wall constructions*, Acustica, Vol. 85, pp. 707–720, 1999.

[71] **Vaicaitis, R.**, *Study of noise transmission through double wall aircraft windows*, NASA Contractor Report, Vol. 172182, 1983.

[72] **Cremer, L., Heckl, M.** and **Ungar, E. E.**, Structure-borne sound, Springer-Verlag, Berlin, 1988.

[73] **Wallace, C.**, *Radiation resistance of a baffled beam*, J. Acoust. Soc. Am., Vol. 51, pp. 936–945, 1970.

[74] **Hettler, S., Leistner, P.** and **Thompson, D.**, *A modal approach to lightweight partitions with internal resonators*, *Forum Acousticum*, Budapest, 2005.

[75] **Hettler, S.**, *Akustische Modellierung von Leichtbauteilen mit internen Resonatoren*, *DAGA Conference*, Munich, 2005.

[76] **Wallace, C. E.**, *Radiation resistance of a rectangular panel*, J. Acoust. Soc. Am., Vol. 51, pp. 946–952, 1972.

[77] **Hettler, S.** and **Thompson, D.**, *Vibroacoustic behaviour of double panel structures with spatially distributed neutralizers*, *Ninth international conference on recent advances in structural dynamics*, Southampton, 2006.

[78] **Hettler, S.** and **Leistner, P.**, *Vibroakustisches Verhalten von Doppelwandstrukturen mit räumlich verteilten resonatoren*, *DAGA Conference*, Stuttgart, 2007.

[79] **Maidanik, G.** and **Becker, K. J.**, *Characterization of multiple-sprung masses for wideband noise control*, J. Acoust. Soc. Am., Vol. 106, No. 6, pp. 3109–3118, 1999.

[80] **Maidanik, G.** and **Becker, K. J.**, *Criteria for designing multiple-sprung masses for wideband noise control*, J. Acoust. Soc. Am., Vol. 106, No. 6, pp. 3119–3127, 1999.

[81] **Brennan, M. J.**, *Characteristics of a wideband vibration neutralizer*, Noise Control Eng. J., Vol. 45, No. 5, pp. 201–207, 1997.

[82] **Heckl, M.**, *Wave propagation on beam plate systems*, J. Acoust. Soc. Am., Vol. 33, No. 5, pp. 640–651, 1961.

[83] **Strasberg, M.** and **Feit, D.**, *Vibration damping of large structures induced by attached small resonant structures*, J. Acoust. Soc. Am., Vol. 99, No. 1, pp. 335–344, 1996.

[84] **Maidanik, G.** and **Becker, K. J.**, *Dependence of the induced loss factor on the coupling forms and coupling strenghts: linear analysis*, Journal of Sound and Vibration, Vol. 266, pp. 15–32, 2003.

[85] **Maidanik, G.** and **Becker, K. J.**, *Dependence of the induced loss factor on the coupling forms and coupling strenghts: energy analysis*, Journal of Sound and Vibration, Vol. 266, pp. 33–48, 2003.

[86] **Thompson, D. J.**, *A continuous damped vibration absorber to reduce broad-band wave propagation in beams*, Journal of Sound and Vibration, Vol. 311, pp. 824–842, 2008.

[87] **Tyutekin, V. V.**, *Computer simulation of a sound absorber synthesized from mechanical resonators*, Acoustical Physics, Vol. 43, No. 5, pp. 589–595, 1997.

[88] **DIN EN ISO 3744:2006-07**, *Acoustics - Determination of sound power levels and sound energy levels of noise sources using sound pressure - Engineering method for an essentially free field over a reflecting plane*.

[89] **Idrisi, K., Johnson, M. E., Theurich, D.** and **Carneal, J. P.**, *A study on the characteristic behavior of mass inclusions added to a poro-elastic layer.*, Journal of Sound and Vibration, Vol. 329, pp. 4136–4148, 2010.